NASA Contractor Report 172470

Operational Fitness of Box Truss Antennas in Response to Dynamic Slewing

E. Bachtell, S. S. Bettadapur, W. A. Schartel,
L. A. Karanian

Martin Marietta Aerospace
Denver Aerospace
P.O. Box 179
Denver, CO 80201

Contract NAS1-17551
January 1985

National Aeronautics and
Space Administration

Langley Research Center
Hampton, Virginia 23665

NASA Contractor Report 172470

Operational Fitness of Box Truss Antennas in Response to Dynamic Slewing

E. Bachtell, S. S. Bettadapur, W. A. Schartel, L. A. Karanian

Martin Marietta Aerospace
Denver Aerospace
P.O. Box 179
Denver, CO 80201

Contract NAS1-17551
January 1985

NASA
National Aeronautics and
Space Administration

Langley Research Center
Hampton, Virginia 23665

N85-19012#

FOREWORD

This report was prepared by Martin Marietta Denver Aerospace under Contract NAS1-17551. This report covers the results of Task 2. The contract was administered by the Langley Research Center of the National Aeronautics and Space Administration. The Task 2 study was performed from February 1984 to October 1984 and the NASA-LaRC Project Manager was Mr. U. M. Lovelace.

GLOSSARY

α	Angular Acceleration
β	Antenna Surface Pitch
θ	Antenna Surface Roll
ψ	Antenna Surface Yaw
B	Bandwidth
BDF	Beam Deviation factor
BE	Beam Efficiency
BWFN	Beam Width First Null
ΔBWFN	Change from BWFN
CM	Center of Mass
D	Antenna Diameter
	Dissipation Function
EOS	Earth Orbiting Spacecraft
dB	Decibles
F	Focal Length
ΔF	Combined Change in Focal Length of Surface and Feed
FEER	Fast Eigenvalve Extraction Routine
F(r)	Aperture Illumination Function
g	Acceleration Due to Gravity
G	Antenna Gain
ΔG	Change in Gain
GHz	Gigahertz
Hz	Hertz
ϕ	Instantenous Slew Angle
I_{sp}	Specific Impulse
I_t	Total Mass Impulse
I_{xp}	Mass Moment of Inertial About Principal X-Axis
I_{yp}	Mass moment of inertia about principal y-axis.
I_{zp}	Mass moment of inertia about principal z-axis.
J_0(ur)	Bessel function of the first kind of order zero.
J_1(ur)	Bessel function of the first kind of order one.
K	Degrees Kelvin
kg	Kilograms
km	Kilometers
L	Moment Arm
m	Maximum Phase Deviation
	Meters
	Mass of Fuel

m_T	Total Fuel Mass
N	Newtons Number of Complete Maneuvers
NASA	National Aeronautics and Space Administration
θ	Angle the spacecraft rotates toward orbit plane.
ω_o	Radial Frequency
PACOSS	Passive and Active Control of Space Structures
PPT	Pulse Plasma Thruster
θ_F	Scan Angle of Feed
θ_S	Scan Angle of Surface
θ_T	Combined Scan Angle
ϕ_T	Total Slew Angle
RF	Radio Frequency
rms	Root Mean Squared
rms_{dyn}	rms of the Surface Error Due To Dynamics Only
rms_{sys}	Average Total rms Surface Error
s	Seconds
SAR	Synthetic Aperture Radar
t	Integration Time Time that EOS can remain in out-of-plane position.
T	System Kinetic Energy Torque
ΔT	Minimum Detectable Change in T_A
T_A	Antenna Temperature
T_{ggxp}	Gravity Gradient Torque
T_H	Thrust
T_{sys}	Effective Temperature of Receivers/Electronic Noise Temperature of Receivers
t_T	Total Slew Time
U	System Potential Energy
V_R	Output Voltage
λ	Wavelength
X(t)	Generalized External Force
q_i	Generalized displacements in independent coord.

TABLE OF CONTENTS

LIST OF FIGURES

LIST OF TABLES

1.0 INTRODUCTION

The Box Truss Analysis and Technology Development task contract was commissioned by NASA to further the understanding and technical definition of the box truss concept and its application to antenna missions. As part of the contract, Task 2--Dynamic Analysis, was selected to conduct a parametric analysis of the Earth Observations Spacecraft (EOS), as defined in NASA CR-3689, slewing capability along with associated system changes or subsystem weight, and complexity impacts. Many missions are enhanced by the capability to slew the antenna spacecraft to point toward targets not located at the spacecraft nadir. Varying slew rates, settling times, maneuver frequencies, and attitude hold times provide the data required to establish applicability to a wide range of potential missions.

1.1 SLEWING AS A SOLUTION

A slewing capability for a large radiometer satellite offer a variety of advantages and will increase the capability of the system. Although certain antennas, such as an array, can electronically shift the direction of the main beam, a push-broom system, e.g., EOS, must mechanically slew the entire antenna. A satellite with slewing capability increases capability with the potential for improved surface coverage and increased radiometric resolution due to increased dwell time.

A satellite that does not have pointable instruments must wait until the object of interest is at the spacecraft nadir for observation. Repeated observations are governed by orbit parameters. Slewing allows objects to be observed that are not in the current ground swath, but in adjacent areas. The revisit time can, therefore, be reduced for those objects. Slewing also permits the option of a targeting capability to be included in the operating mode of the mission profile.

An important characteristic of a radiometer system is the ability to discern small changes in the microwave signal. This ability can be improved if the system has a long time to "dwell" on the object. Slewing could also be used to compensate for the forward spacecraft motion, dwell on an object for a longer period of time, and improve the radiometric sensitivity.

1.2 EOS BACKGROUND

The EOS study, NASA Contract NAS1-16756, emphasized the selection and analysis of complementary sets of sensors for Earth, oceanic, and atmospheric observation, and the development of the EOS spacecraft design in some detail. EOS was to operate in low-Earth orbit, be deployable as a fully operational satellite from the Shuttle orbiter, and be capable of a 10-year lifetime, including two- to three-year revisit periods for resupply, maintenance, and sensor changeout. For this study, the EOS baseline configuration was used. The salient characteristics of the EOS system are summarized in Table 1 through 3.

TABLE 1 - SPACECRAFT SUMMARY

Reflector dimensions	58x116 m
Focal length	116.1 m
Spherical radius	234.8 m
Total system weight	7635 kg
Fundamental dynamic mode	1.09 Hz
Stowed envelope	4.25 m Diameter by 17.8 m Length

TABLE 2 - ORBIT PARAMETERS

Mission	Inclination, deg	Equatorial altitude, km	Crossing	Synchronous
I. Baseline	98	705	Noon	Yes
II. Land	98	705	9:30	Yes
III. Ocean	98	705	Noon or 9:30	Yes
IV. Atmospheric	60	705	None	No

TABLE 3 - GROUND GEOMETRY

Frequency, GHz	Ground resolution, km		Max No. horns	Swathwidth, km	Revisit intervals, days (w/o slew)
	Optimistic	Conservative			
1.4	2.95	14.75	58	173	16
5.5	0.88	4.5	90	350	16
10.68	0.41	2.06	88	18	16

EOS represents a major advancement in the capability, completeness and approach to Earth orbiting remote sensing platforms that use a large microwave radiometer as the "core" instrument. Figure 1 is an artist's concept of the resulting EOS.

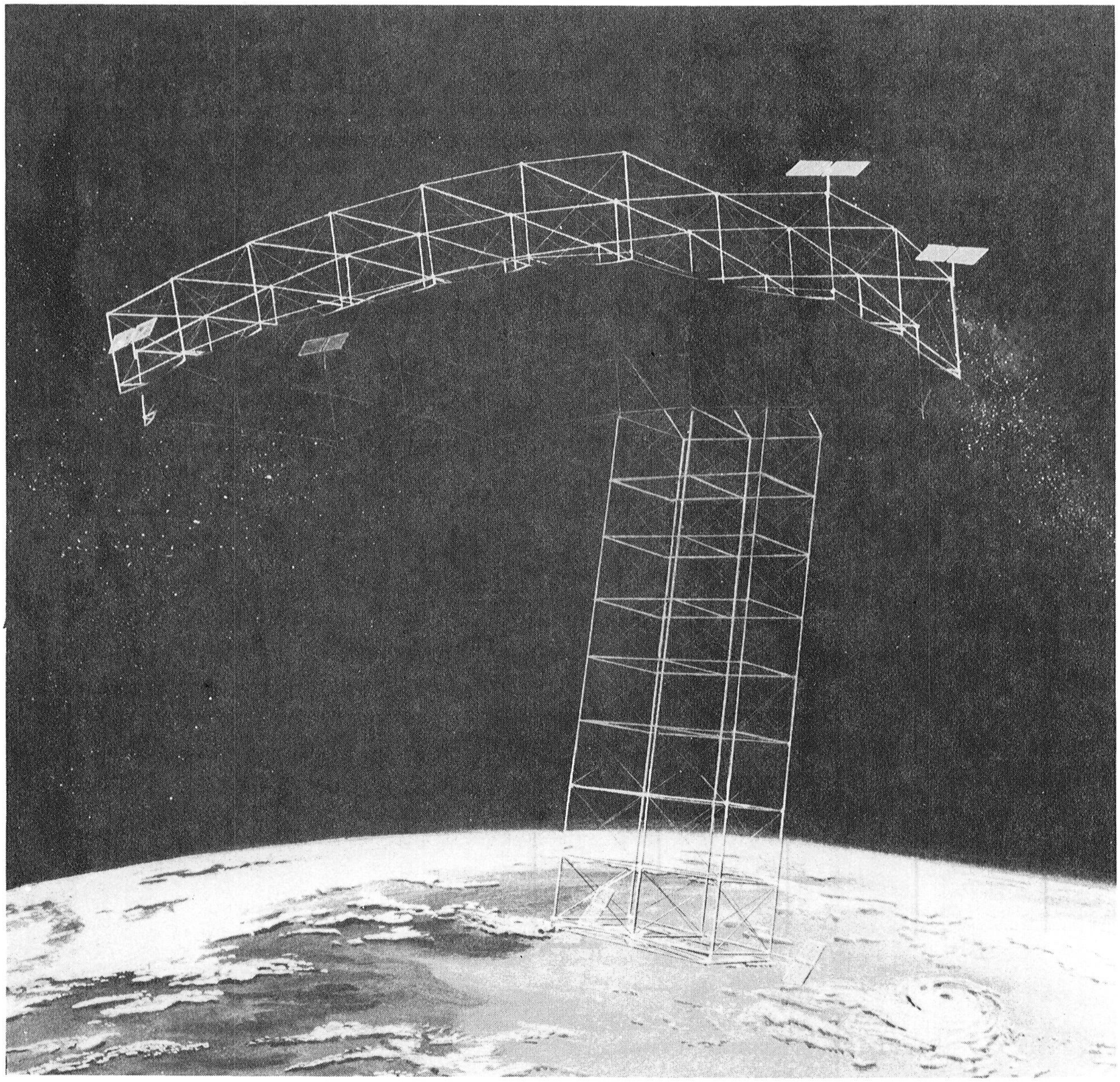

Figure 1 - Deployed EOS.

1.3 EOS ENHANCEMENTS BY SLEWING

EOS provides global resources monitoring with a microwave radiometer and ancillary sensors to augment and complement the microwave observations. These additional sensors have specific requirements for surface lighting and observation conditions. These requirements, when combined with the swath width, resolution, and packaging constraints of EOS, drove the baseline orbits to be sun synchronous. Sun-synchronous orbits restrict both operating altitude and inclination and cannot provide the two or three day revisit time desirable for global monitoring.

The baseline orbit had a 705-km altitude, 98-degree inclination, and a normal revisit time of 16 days. This orbit has an alternating or interstital ground track pattern such that adjacent swaths would be imaged with a two-day interval, (Fig. 2). A partial solution, one that improves the revisit time for selected objects to two days, can be accomplished taking advantage of the alternate pattern and a 15-degree off-nadir slew. The slew angle is determined by the 175-km swath width and 705-km orbit.

For example, a selected object is imaged on "Day 1." The adjacent swath is imaged on "Day 3," and the selected object can be reviewed with a slew maneuver. Additionally, objects in swath C can be revisited with a 1-day interval if a slew is effected to the right on "Day 1" and to the left on "Day 2".

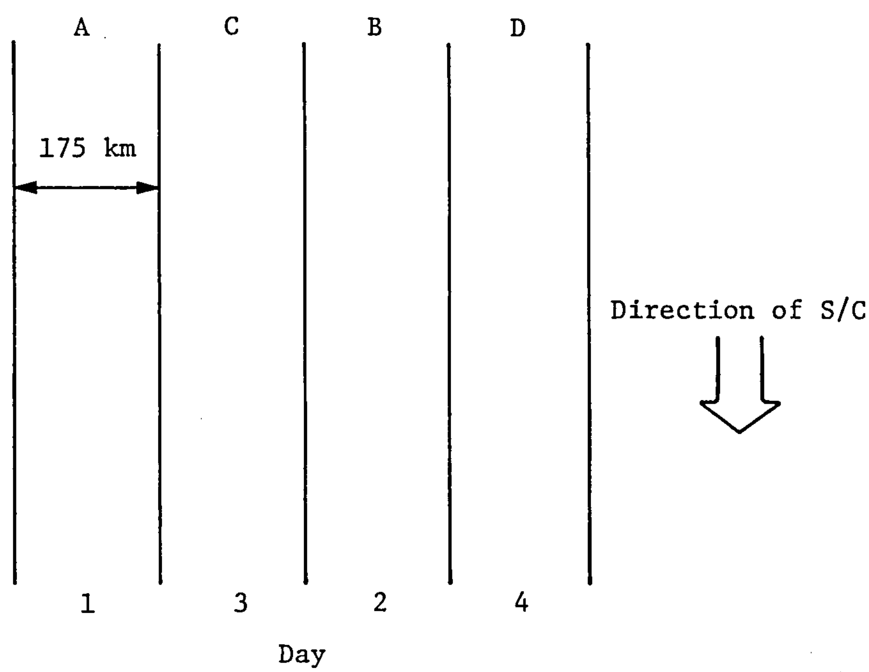

Figure 2 - Ground track.

1.4 TASK 2 RESULTS SUMMARY

Task 2, Dynamic Analysis, resulted in showing the EOS slew capability. This section is intended to highlight and summarize the data obtained on slew rates, settling times, maneuver frequency, and attitude hold requirements for a 15-degree slew.

Tables 4 through 6 summarize the parametric data.

TABLE 4 - SUMMARY OF SLEW TIMES, THRUST LEVELS AND SETTLING TIME RESULTS

Case	Slew time, s	Thrust level/ thruster, N	Damping ratio	Settling time, s
1	41.7	45	0.2	0.0
1'	41.2[a]	45	0.2	82.0[b]
2	41.7	45	1.0	0.0
2'	41.2[a]	45	1.0	32.3
3	39.5	50	1.0	0.0
4	36.1	60	0.2	250.0[b]
5	36.1	60	1.0	55.1[b]
6	36.1	60	5.0	7.7
7	25.5	120	1.0	75.6[b]
8	25.5	120	5.0	13.6

[a]Resulted in a 14.665 degree slew angle.

[b]Extrapolated results.

TABLE 5 - SUMMARY OF MANEUVER FREQUENCY RESULTS

Case	Total fuel per maneuver, kg	No. of maneuvers[a]
1	6.80	186
1	6.72	188
2	6.80	186
2	6.72	188
3	7.16	176
4	7.85	161
5	7.85	161
6	7.85	161
7	11.09	114
8	11.09	114

[a]Assumes 1265 kg of propellant available for slewing.

TABLE 6 - SUMMARY OF ATTITUDE HOLD REQUIREMENTS

Slew hold time without stationkeeping	90.2 s
Thrust required for stationkeeping	0.02 N
Fuel required per minute	0.005 kg

Slew Rates - The slew rates investigated ranged from a maximum of 41.7 seconds slew time to a minimum of 25.5 seconds. To achieve these slew rates, the thruster levels ranged from 45 N per thruster to 120 N per thruster, respectively, using a four-thruster slewing system.

These thruster levels represent the appropriate range that could easily be incorporated into EOS. Any less thrust and the slew time becomes excessive. Any more thrust and the fuel requirements and settling time become excessive while the incorporation of the thrusters onto the EOS structure becomes difficult.

Settling Times - The settling rates resulting from the various thrust level and damping ratio combinations ranged from 0.0 second for the 45 N per thruster and 1% damping case to an estimated 250.0 seconds for the 60 N per thruster and 0.2% damping case.

Note that for the 45- and 50-N cases, the slew period for a 15-degree slew resulted in the removal of the thrust force at a time when the elastic displacement of the structure was close to zero. Therefore, the deformation of the structure at the start of settling time was small enough to produce an operational environment immediately. This occurred for all 45-N cases regardless of damping.

This means the initial conditions at the beginning of settling time are strictly a function of the response frequency and the slewing period; a slewing period can be determined that will reduce the settling time to a minimum for any thrust level chosen. This also allows the structure to be built without requiring additional damping, i.e., 5% damping to reduce settling time, thus keeping the cost, weight, and complexity of the system to a minimum. The only adverse effect in choosing the proper slewing period is that the period will dictate the slew angle achieved, and, in the case of the EOS, the 15-degree slew is required to obtain a two-day revisit interval of ground targets.

Maneuver Frequency - Using a chemical thruster system to slew the EOS resulted in fuel requirements ranging from 6.8 kg of propellant to 11.1 kg of propellant for a complete maneuver. A complete maneuver is slewing EOS out 15 degrees and back again. This calculates to a total of 186 and 114 slew maneuvers, respectively, assuming 1265 kg of slew propellant is available, before resupply is required.

Attitude Hold Requirements - Because the EOS spacecraft is gravity gradient stabilized, thrust is required to hold EOS at a 15-degree slew angle if the stationing hold requirements exceeds 90.2 seconds. The length of time the EOS can remain in the out-of-plane position and still meet the pointing requirements of ± 0.08 degrees is 90.2 seconds. If station holding is required, the thrust and fuel per minute required is 0.02 N and 0.005 kg, respectively.

2.0 ANALYSIS METHODOLOGY

To conduct a parametric analysis of the EOS slewing capability, the sequence and methodology of the analysis was first determined. The sequence of analysis used to perform the parametric study is shown in Figure 3. The following sections describe the methodology of the four types of analyses used--system operational requirements analysis, rigid body analysis, dynamic transient response analysis, and system error analysis.

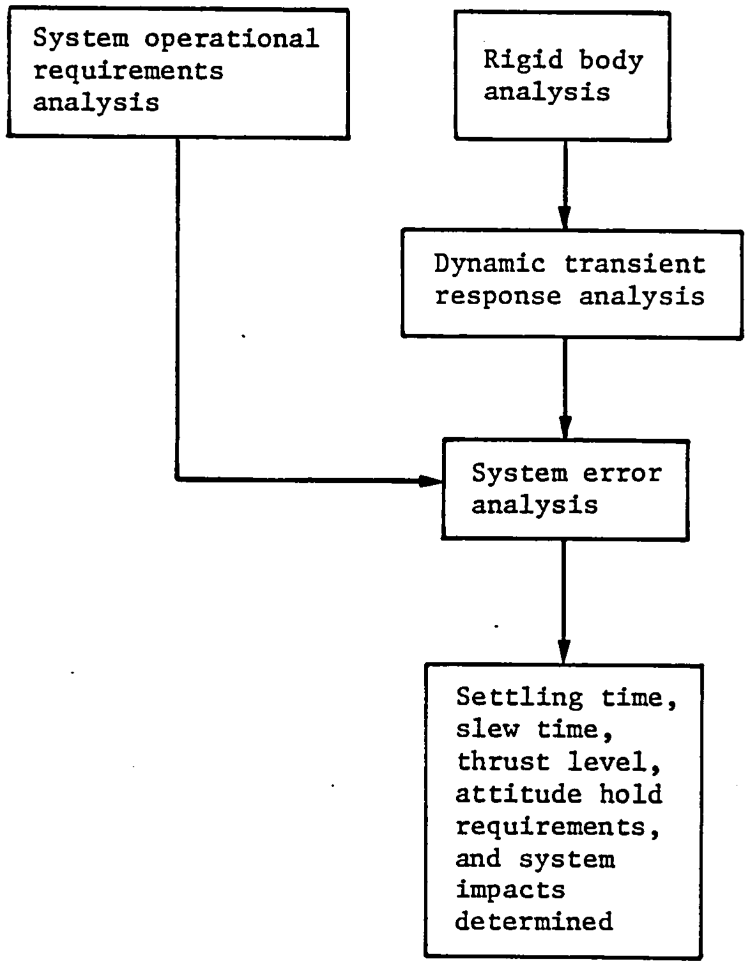

Figure 3 - Sequence of analysis to determine EOS slew capability.

Additionally, the structural damping ratios to be used in the parametrics had to be determined. The values of damping chosen where 0.2, 1 and 5%. The 0.2 and 1% damping values are the two extremes inherent in large deployable space structures. The 5% damping value is an enhanced structural damping technology development being investigated under the Passive and Active Control of Space Structures (PACOSS) program sponsored by the Air Force.

2.1 SYSTEM OPERATIONAL REQUIREMENTS ANALYSIS

The four system parameters governing operational fitness of the EOS are (1) radiometric resolution; (2) beam efficiency; (3) resolutions; and (4) image tolerance. For each parameter, the three error mechanisms that can degrade the system parameters are beam scanning, axial defocus, and surface errors.

2.1.1 Radiometric Resolution

The radiometric resolution characterizes the sensitivity of the antenna/receiver system. In such a system, the antenna collects microwave energy from the Earth's surface. This signal is amplified by a receiver to produce an output voltage V_R. A quantity known as the antenna temperature, T_A, can be recovered from V_R. The antenna temperature is the temperature that a resistor would have to be at to produce the same receiver output voltage. Thus, ΔT is the minimum detectable change in the radiometric antenna temperature T_A. For the EOS, this value, ΔT, equals 5 K. Generally, the radiometric resolution requirement, ΔT, is 1 K, the EOS uses six microwave frequencies at two polarization, enabling multiple regression analysis to reduce the final (derived) temperature determination to approximately 1 K.

The three system errors (error mechanisms) that affect this requirement are beam scanning, axial defocusing, and rms surface error. Through each of these, a ratio of difference in gain (ΔG) to the original gain is found, the sum total of which must not exceed the limit of 0.05. From the systems errors analysis, the following are obtained: (1) combined change on focal length of the feed and surface; (2) the scan angles of both the surface and feed and their combination, in both E and H planes; and (3) average rms surface error.

Axial Defocusing -

[1] $$\frac{\Delta G}{G} = (2\pi\Delta F/\lambda)^2/12$$

where

λ = wavelength = 0.028 m
ΔF = combined change in focal length of the surface and feed, m

Beam Scanning* -

[2] $$4.75(\Delta G)^4 - 26.75(\Delta G)^2 + BDF/(1.22(\lambda/D)) * \theta_T/(\lambda F^2)/(1 + 72/F^2) = 0$$

*J. Ruze: "Lateral Feed Displacement in a Parabolic." IEEE Trans Antennas Prop. Vol AP-13 No. 5, Sept. 1965, pp. 660-665.

Solve for ΔG, taking the lowest positive root.

[3] $$\frac{\Delta G}{G} = \Delta G/59.8$$

where

λ = wavelength = 0.028 m (corresponding to an operating frequency of 10.68 GHz).
D = reflector diameter = 60 m
BDF = beam deviation factor = 0.992
θ_T = combined scan angle (radians) = $2\theta_s - \theta_f$
F = focal length of reflector = 116.1 m
G = $10 * LOG(4\pi D/\lambda^2)$ = 59.8 dB

Surface Error* -

[4] $$\frac{\Delta G}{G} = 1 - e^{-\left(\frac{4\pi rms_{dyn}}{\lambda}\right)^2}$$

where

λ = wavelength = 0.028 m
rms_{dyn} = rms surface error due to dynamics, m

Equations [1] thru [4] are used to calculate $\Delta G/G$ due to axial defocusing, beam scanning and surface errors. The three individual values are then summed. The effect on the radiometric resolution (ΔT) is given by equation [5]**.

[5] $$\Delta T = T_{sys}\left[\frac{1}{Bt} + \left(\frac{\Delta G}{G}\right)^2\right]^{1/2}$$

where

T_{sys} = electrical noise temperature of the receivers = 100 K
B = bandwidth = 10% of operating frequency
t = integration time (0.33 s)
$\Delta G/G$ = sum of three individual errors

*J. Ruze: "The Effect of Aperture Errors on the Antenna Radiation Pattern." Supplemento al Nuovo Cimento, Vol 9, No. 3, 1952, pp. 364-380.

** R. H. Dicke: "The Measurement of Thermal Radiation at Microwave Frequencies." Rev Sci Instr, Vol 17, pp 268-275.

2.1.2 Beam Efficiency

The main beam efficiency (BE) is defined as the integral of power over the main beam by the integral over the complete antenna pattern. It is a measure of how much energy is collected by the main beam and the entire pattern. Generally, BE must be greater than 0.90 otherwise it becomes difficult to separate, during data reduction, power that was received from the side lobes versus power received from the main beam.

The beam efficiency test assumes both beam scanning and axial defocusing to be negligible effects. The rms surface error that is considered is a total one, i.e., it takes into account dynamics, thermal distortions, and manufacturing error. This differs from radiometric resolution in that the concern is now with total distortion rather than change in distortion. The calculated system beam efficiency must exceed 90%. The system beam efficiency is calculated through the following equation*:

[1] $$BE_{sys} = 0.97e^{-\left(\frac{4\pi rms_{sys}}{\lambda}\right)^2}$$

where rms_{sys} = average total rms surface error
λ = wavelength = 0.028m

2.1.3 Resolution

The resolution element for the radiometer system is determined by the main beam width of the antenna pattern. A related image-quality requirement stipulates that variations in the resolution element size for a multiple beam system shall not exceed 10% of the initial (error-free) system. The resolution requirement, as used in this study, was concerned with variations in the width of the main beam.

Resolution concerns itself with all three distortive aspects, rms surface error, axial defocusing, and beam scanning. The interest here is to obtain ΔBWFN (delta beam width first null). Once again, since this is a delta that is being obtained, dynamic distortion is the only concern. Δ BWFN is found through the integration of Bessel functions of the first kind and of order zero and order one. ΔBWFN cannot exceed 10% of BWFN, where BWFN equals 0.00114 radian. The ΔBWFN is given by equation [1]**

[1] $$\Delta BWFN = \frac{m^2/2 \int_0^1 F(r)\ J_0(ur) r dr}{\frac{\pi D}{\lambda} \int_0^1 F(r)\ J_1(ur) r^2 dr}$$

*R. C. Johnson and H. Jasik: Antenna Engineering Handbook. McGraw-Hill Book Company, New York, 1984, Chapter 31.

** D. K. Cheng: "Effect of Arbitrary Phase Errors on the Gain and Beam Width Characteristics of Radiation Pattern." IRE Translations Ant. Prop., 1955, p 145.

Equation [1] is approximated to be equation [2], which is reduced to equation [3].

[2] $$\Delta BWFN = \frac{m^2/2 \sum_{0}^{1} F(r)\ J_0(ur) r \Delta r}{\frac{\pi D}{\lambda} \sum_{0.1}^{1} F(r)\ J_1(ur) r^2 \Delta r}$$

where

$F(r)$ = aperture illumination function for step size $\Delta r = 0.1$.

m = maximum phase deviation, rad

$(\frac{2\pi}{\lambda})$ (rms + axial defocus + (beam scan x 116.1))

[3] $$BWFN = \frac{0.825114 * m^2}{\frac{\pi D}{\lambda}}$$

2.1.4 Image Tolerance

The EOS spacecraft operates in the push-broom mode. In this configuration, a linear feed array produces individual contiguous spots that provide the cross-track imaging, while the orbit velocity provides the along-track motion. Allowable deviations from perfect contiguity restrict gaps between individual resolution elements to the width of 1 resolution element of 0.0014 radian for EOS.

Image tolerance is the easiest of the four categories to verify. The total beam scan, Θ_T, is obtained from the system errors analysis and, after being multiplied by a beam deviation factor of 0.992, must be less than 0.0014 radian.

2.2 RIGID BODY ANALYSIS

A rigid-body analysis was conducted to determine slew times, attitude hold requirements, and system thrust levels and thruster angles. This analysis included the use of the rigid-body dynamic analysis conducted under the EOS study. The dynamic analysis identified the frequencies, mode shapes, principal inertias, and center-of-gravity location for the EOS baseline structure with slew propellant. The mass moments of inertia were used in the determination of slew time, thrust levels, and attitude hold requirements. The center-of-gravity location for the structure was necessary in the determination of the thruster angles.

2.2.1 Rigid Body NASTRAN Model

A NASTRAN finite-element technique was used to determine these modal characteristics. A total of 720 structural finite elements were used to model the spacecraft as shown in Figure 4. The surface members and the vertical members were modeled with beam elements, while the interior and exterior diagonals were represented by rod elements. Because the surface members are pinned at either end, this degree of freedom was released in the rotational direction along the axis of these pins to rigorously model the structure. The diagonal members were modeled with rod elements that have no bending stiffness, which is representative of their operational behavior. The diagonal members are pretensioned to a level high enough that they never go slack under all operating conditions. This eliminates any nonlinearities in the structure caused by slackening of the diagonal members. For this reason, the diagonal members in this analysis were allowed to take a compressive load, which represents the mathematical behavior of the stiffness of tensioned members.

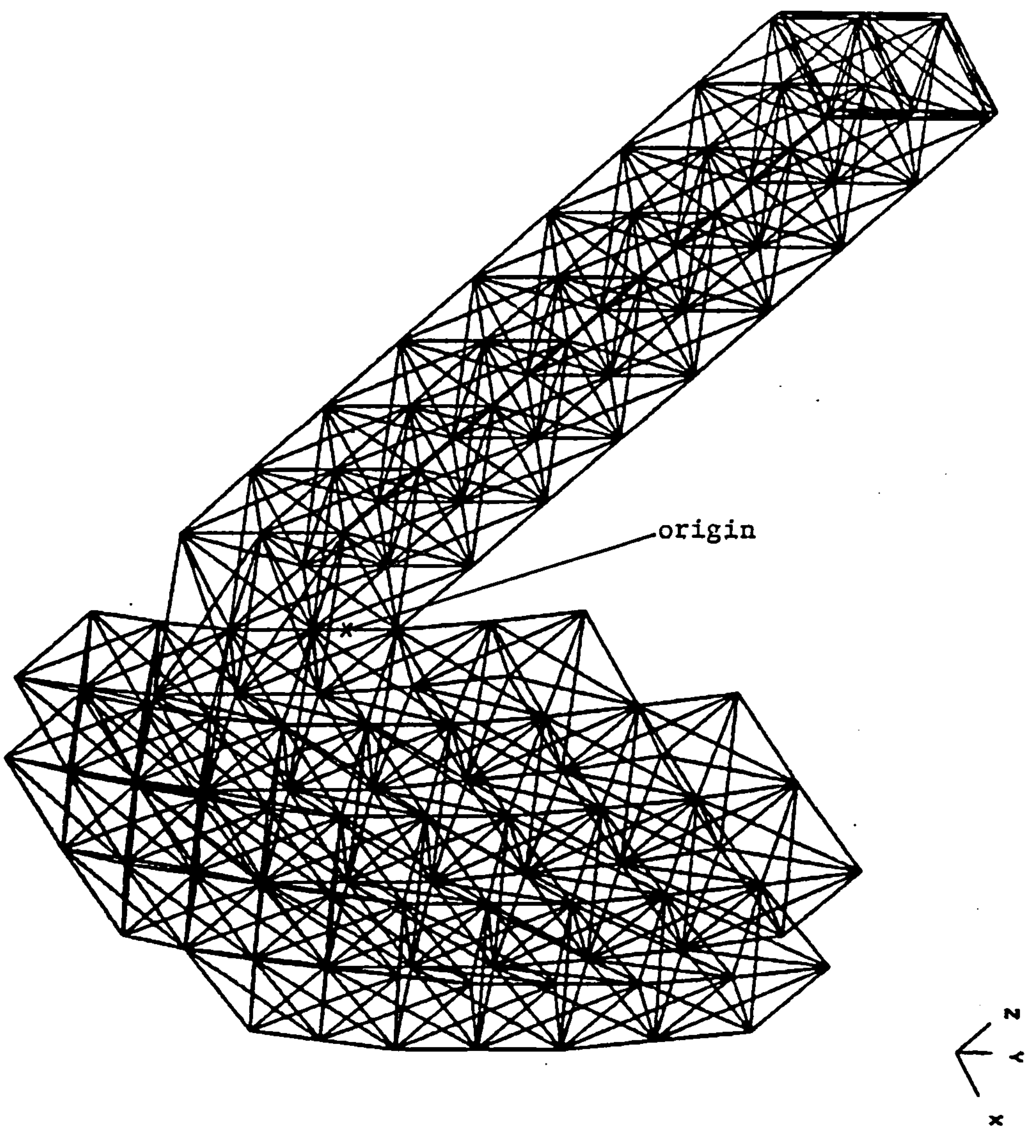

Figure 4 - EOS finite-element model.

A lumped mass was placed at all the nodal locations to simulate the cube-corner fittings, the mesh standoffs, and the RF mesh system. The model's nodal locations are shown in Figure 5 and 6. The midlink hinge's mass was distributed along the length of the surface member because no node existed at that point. The masses of the power system, scientific platform, fuel, electronic housekeeping, and feed beam system were distributed as nonstructural mass.

The modal extraction was performed using the Fast Eigenvalue Extraction Routine (FEER) in COSMIC NASTRAN. The boundary conditions were free, and the model contained 834 degrees of freedom. Mass moments of inertia and the mass center of gravity were calculated by the NASTRAN Grid Point Weight Generator.

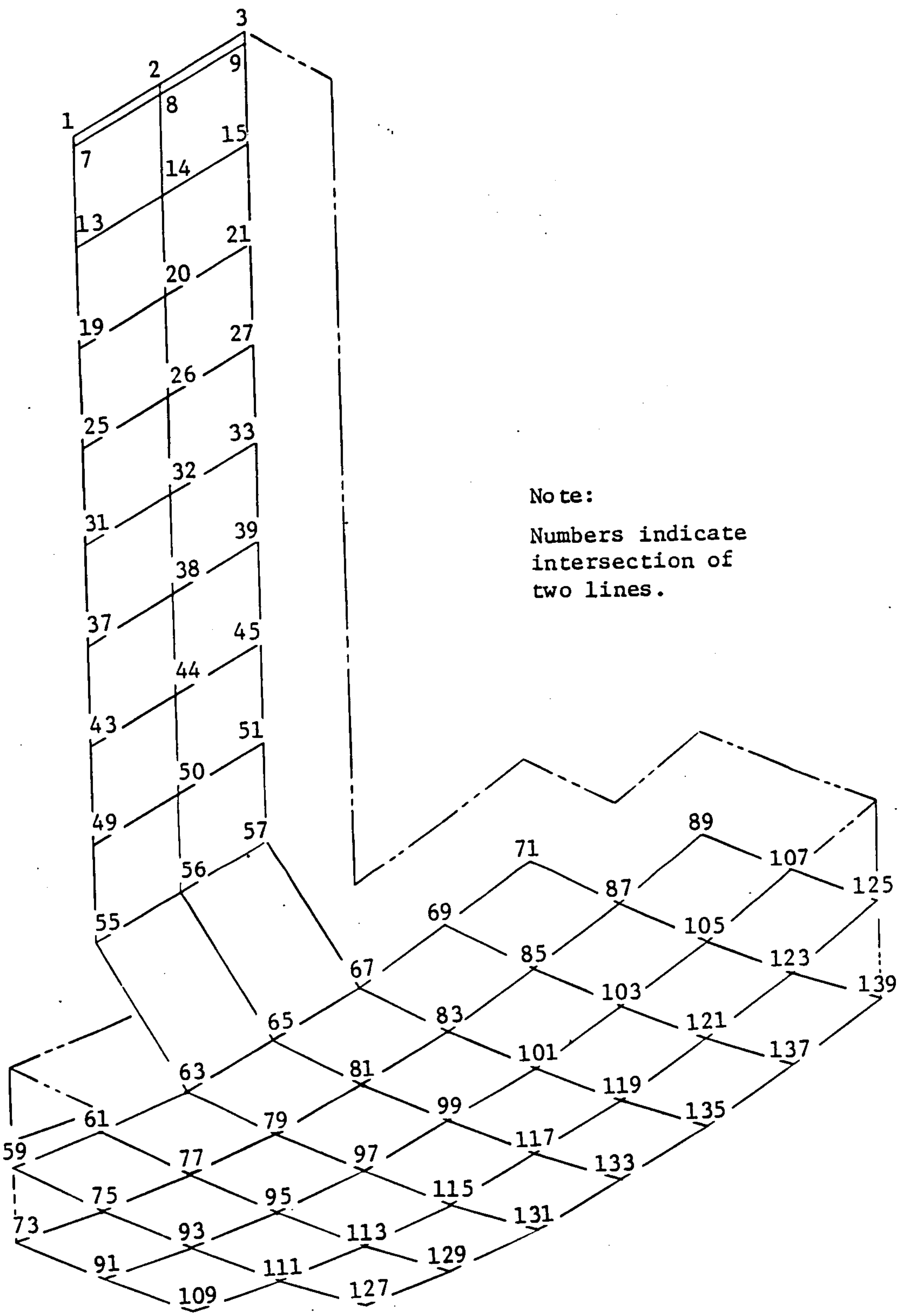

Back Side

Figure 5 - EOS Finite-Element Node Numbers.

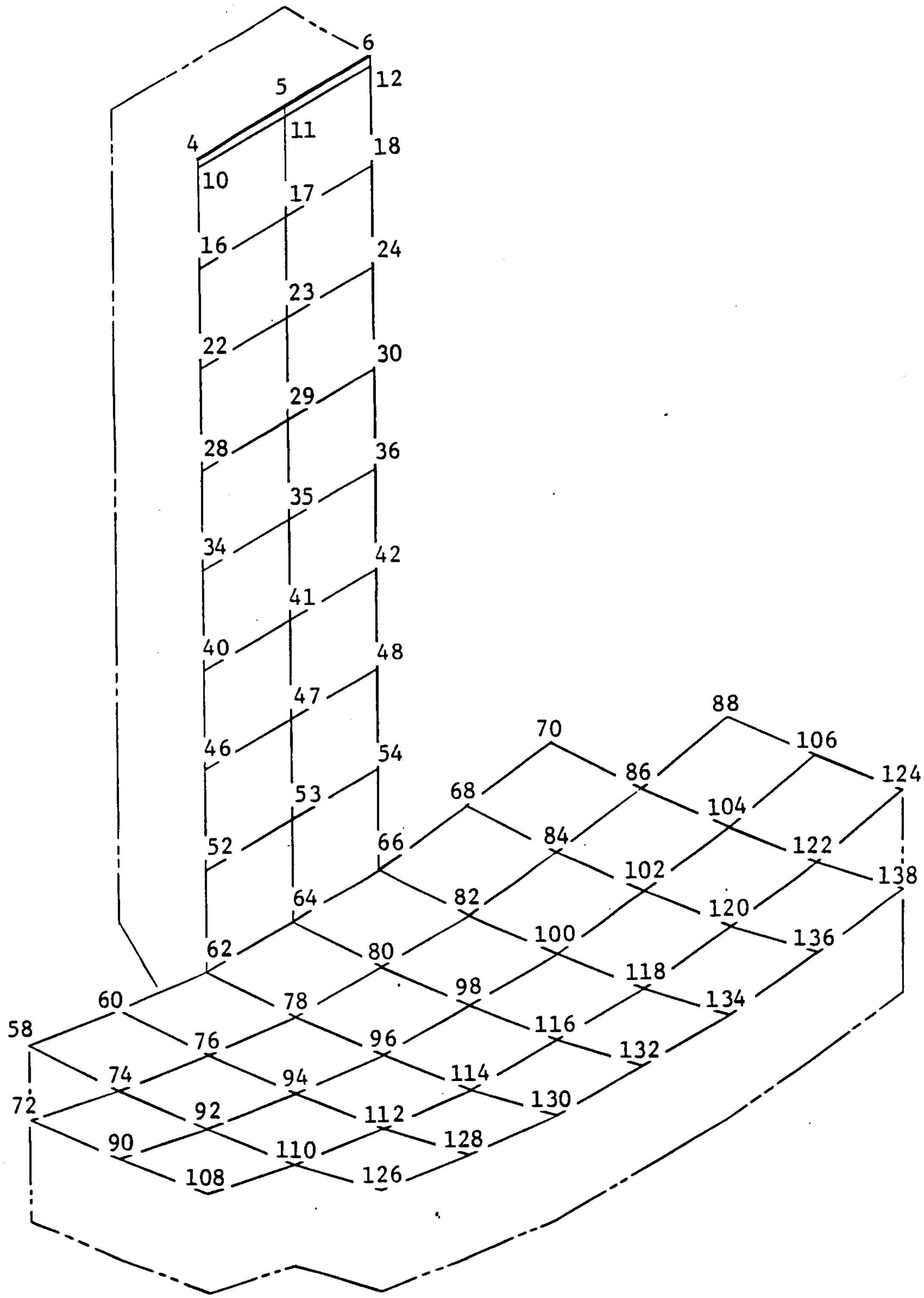

Figure 6 - EOS Finite-Element Node Numbers.

2.2.2 Determination of Slew Times, Thruster Levels, and Maneuver Frequency

This section presents the methodology used to determine the slew times, thruster levels, and fuel requirements per maneuver required to slew the EOS about the Xp-axis, Figure 7. The previous EOS study showed a chemical thruster system was necessary to achieve a reasonable low slew time. Therefore, the specific impulse used for the thruster system equals 225 seconds. Additionally, the thruster system was considered to be a constant thrust step system. Figure 8 shows the torque, rate, and angle profiles assumed for the thruster system.

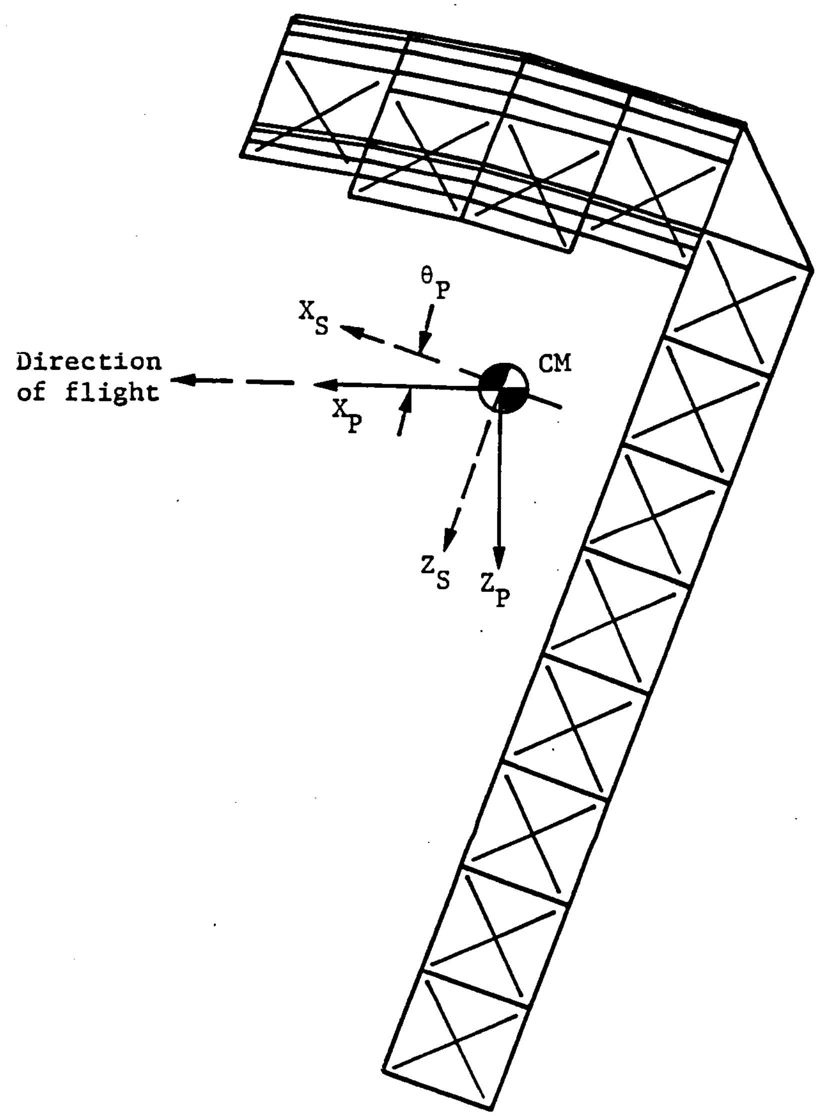

Figure 7 - Flight orientation with respect to principal axis.

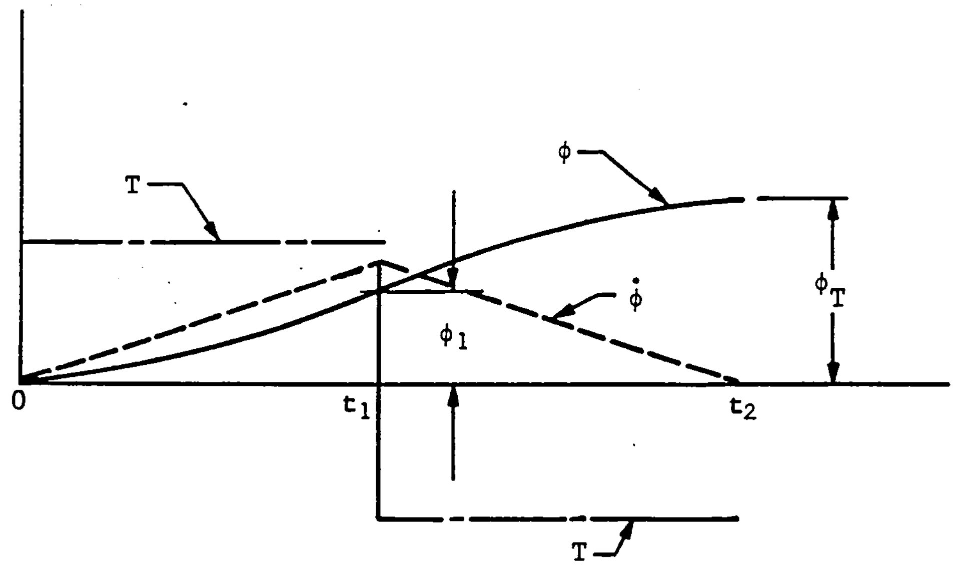

Figure 8 - Torque, rate, and angle profiles.

The total time required for the maneuver is given by

[1] $$t_T = t_1 + t_2 = 2t_1, \; t_1 = t_2$$

and the torque magnitude required is given by

[2] $$T = \frac{2\phi_T I_{xp}}{t_T^2}$$

where

ϕ_T = $2\phi_1$ = 0.2618 radians slew angle (15 degrees)

I_{xp} = mass moment of inertia about the principal X-axis (Kg-m), and

T = thruster level (N) x number of thrusters x moment arm (m)

Therefore, the time required to complete the slew maneuver is determined by solving equation [2] for the total time, t_T.

[3] $$t_T = \sqrt{\frac{2\phi_T I_{xp}}{T}}$$

The mass of fuel required is determined from the following equation:

[4] $$m = \frac{I_t}{I_{sp}\, g}$$

where

I_{sp} = specific impulse, 225 s,
g = acceleration of gravity, 9.81 m/s^2,
I_t = total mass impulse, Ns,
m = mass of fuel, kg.

Knowing the mass of fuel required to slew and the total mass of fuel available, i.e., 1265 kg for the baseline EOS, the number of complete maneuvers before resupply is calculated by:

[5] $$N = \frac{m_T}{2 * m}$$

where

N = number of complete maneuvers,
m_T = total fuel available, 1265 kg,
m = mass of fuel to slew 15 degrees (from equation 4).

(This equation assumes slew thrusters will be used to return EOS to nadir pointing rather than relying on the gravity gradient torque.)

2.2.3 Attitude Hold Requirements

The pointing requirement for EOS about the x-axis is ± 0.08 degree whether in or out of the orbit plane as shown in Figure 9. If no station-keeping thrust is applied to the spacecraft, the length of time the EOS can remain in the out-of-plane position is calculated as follows:

[6] $$t = \sqrt{\frac{2\theta}{\alpha}}$$

where

θ = the angle the spacecraft rotates toward the orbit plane, $\pm$ 0.08 degrees = 1.396×10^{-3} rad
α = angular acceleration determined from the gravity gradient torque

The gravity gradient torque can be determined from the following equation:

[7] $$T_{ggxp} = \frac{3\omega_0^{\ 2}}{2}(I_{zp} - I_{yp})\sin 2\phi$$

where

ω_0 = radial frequency

I_{zp} = mass moment of inertia about the principal z-axis

I_{yp} = mass moment of inertia about the principal y-axis

ϕ = instantaneous slew angle

Therefore, the angular acceleration can be determined from the gravity gradient torque and the length of time the EOS remains in the out-of-plane position if no station keeping thrust is applied. This is determined from equation [6].

If station-keeping thrusters are used to maintain attitude, the total mass of fuel required can be calculated from equation [4]. The thrust level is calculated from the gravity gradient torque as follows:

[8] $$T_H = \frac{T_{ggxp}}{L}$$

where

L = moment arm

Therefore, for a specified impulse, the fuel mass necessary to provide the thrust level determined from equation [8] can be calculated using equation [4].

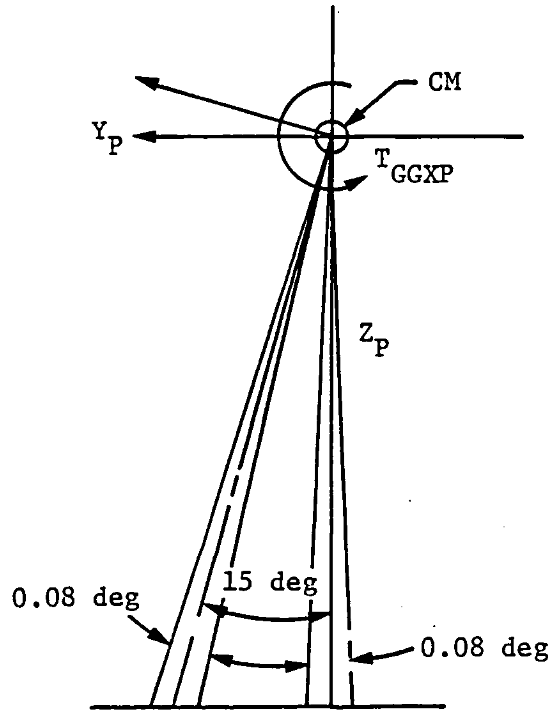

Figure 9 - In and out of orbit plane pointing requirement.

2.3 DYNAMIC TRANSIENT RESPONSE ANALYSIS

A modal transient response analysis was conducted using COSMIC NASTRAN to determine structural deformations of the EOS during the settling time immediately following a 15-degree slew. The finite-element model implemented for the transient analysis was identical to that used for the previously discussed rigid-body analysis. The appendix to this report contains a copy of the COSMIC NASTRAN transient response input deck. The finite-element model was the operational mass case with slewing propellant only. Again, as in the rigid-body analysis, the FEER method was used to accomplish modal extraction in COSMIC NASTRAN.

A realistic range of force amplitudes and time histories necessary to achieve a 15-degree slew angle was applied to the model to identify the sensitivity of EOS performance. Modal damping (0.2, 1, and 5%) was also a parameter considered. A constant thrust was applied for half of the slew time in the positive X-Z direction for two thrusters and in the negative X-Z direction for the two thrusters on the opposite end of the structure. At the halfway point in the slew time, the thrusters were reversed to slow and finally stop the slewing. The amount of thrust applied in the X and Z directions to obtain a desired resultant thrust was geometrically calculated using the principal axis locations calculated in the rigid-body analysis. The thrust levels applied in the transient analysis were so chosen because the resultant slew times are acceptable for projected EOS applications. Figure 10 shows the forcing function profile used in the transient response analysis.

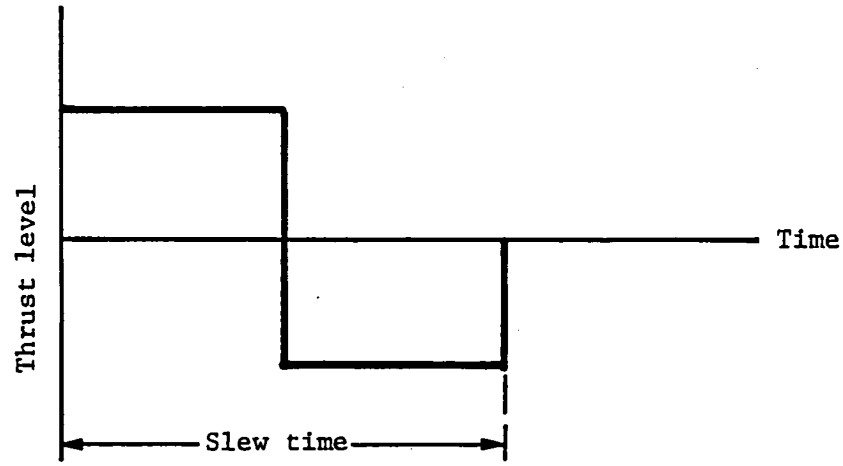

Figure 10 - Forcing function profile.

2.3.1 Linear Model Method of Analysis

Because NASTRAN is strictly a small-displacement analysis and the 15-degree slew maneuver introduces nonlinear rigid-body motion, the rigid-body modes were ignored in analyzing the elastic response of the spacecraft during settling time. This is a valid approach within the linear model assumptions because the rigid-body and elastic effects are uncoupled; i.e., the rigid-body motion has no effect on the elastic response of the system. This approach is proven as follows:

Lagrange's equation of motion is

[1] $$\frac{d}{dt}\frac{\partial T}{\partial q_i} - \frac{\partial T}{\partial q_i} + \frac{\partial D}{\partial q_i} + \frac{\partial U}{\partial q_i} = X(t)$$

where

T = system kinetic energy
D = dissipation function (e.g., structural damping)
U = system potential energy
q_i = generalized displacements in independent coordinates
$X(t)$ = generalized external force

In order to simplify the analysis, assume $D = 0$. If $L = T - U$, then equation [1] becomes

[2] $$\frac{d}{dt}\frac{\partial L}{\partial q_i} - \frac{\partial L}{\partial q_i} = X(t)$$

If $\{x\}$ represents discrete displacements, then

[3] $\{x\} = [\phi]\{q\}$

where

$[\phi]$ = matrix of mode shapes (size of $[\phi]$ is number of DOFs x number of modes)

[4] $T = 1/2 \{\dot{x}\}[m]\{\dot{x}\}$

and

[5] $U = 1/2\{x\}[k]\{x\}$

where

$[m]$ = discrete mass matrix
$[k]$ = discrete stiffness matrix

Substituting equation [3] into equations [4] and [5]

[6] $T = 1/2\{\dot{q}\}[\phi]^T[m][\phi]\{\dot{q}\}$

[7] $U = 1/2\{q\}[\phi]^T[k][\phi]\{q\}$

Thus, since $L = T - U$, then

Thus, since $L = T - U$, then

[8] $\frac{\partial L}{\partial q_i} = (-[\phi]^T[k][\phi])\{q\}$

and

[9] $\frac{d}{dt}\frac{\partial L}{\partial q_i} = ([\phi]^T[m][\phi])\{\ddot{q}\}$

Therefore, equation [2] becomes

[10] $$[\phi]^T[m][\phi]\{\ddot{q}\} + [\phi]^T[k][\phi]\{q\} = X(t)$$

Normalizing the generalized mass matrix, then Lagrange's equation of motion can be written in modal coordinates as

[11] $$\{\ddot{q}\} + \lceil \omega^2 \rfloor\{q\} = [\phi]^T[F]$$

where

$[\omega]$ = diagonal matrix of circular frequencies
$\{\ddot{q}\}$ and $\{q\}$ = vectors of modal accelerations and displacements, respectively
$[\phi]$ = matrix of mode shapes
$[F]$ = vector of applied discrete forces

Partitioning the rigid body and elastic contribution factors in equation [3], then

[12] $$\{x\} = [\phi]\{q\} = [\phi_R | \phi_E] \begin{Bmatrix} q_R \\ q_E \end{Bmatrix}$$

Rewriting equation [11]

[13] $$\begin{Bmatrix} \ddot{q}_R \\ \ddot{q}_E \end{Bmatrix} + \left[\begin{array}{c|c} 0 & 0 \\ \hline 0 & \omega_E^2 \end{array}\right] \begin{Bmatrix} q_R \\ q_E \end{Bmatrix} = \begin{Bmatrix} \phi_R^T F \\ \phi_E^T F \end{Bmatrix}$$

Therefore, it follows that

[14] $$\ddot{q}_R = \phi_R^T F$$

[15] $$\ddot{q}_E + \omega_E^2 q_E = \phi_E^T F$$

Thus, it is shown that elastic and rigid-body effects are totally independent of each other and

[16] $$\{x\} = [\phi_R]\{q_R\} + [\phi_E]\{q_E\}$$

Therefore, the elastic response of the system as determined by COSMIC NASTRAN is the same regardless of whether rigid-body effects are considered.

It should be emphasized the total system energy has been accounted for in equation [1] and therefore it follows the strain energy is considered in the elastic response of the system when the rigid-body effects are ignored. It is also important to note that $[\phi_R]$ represents rigid-body motion for small angular displacements and becomes inaccurate for large angles.

2.4 SYSTEM ERROR ANALYSIS

To determine the settling time for the EOS after slewing had taken place, a system error analysis was performed. The analysis consisted of two sections: (1) determine what errors were present at specific time points after slew using the displacements from the EOS transient response NASTRAN model; and (2) determine the extent these errors effect the system requirements, i.e., resolution, beam efficiency, radiometric resolution, and imaging tolerance.

2.4.1 Determination of System Errors

System errors are defined in three categories: (1) surface roughness, (2) beam scanning, and (3) axial defocusing. Each of these errors is dealt with in accordance to its requirements separately.

2.4.1.1 Surface Roughness - Surface roughness is a random error on the surface. It has contributions from dynamics, pillowing, manufacturing errors, and thermal distortion. The breakdown of this random error is shown in Table 7. Recalling equation [1] from Section 2.1.2 for the determination of beam efficiency, the worst-case random surface error for the system can be determined. Based on the beam efficiency requirement of 90%, the maximum rms of the random surface error is 0.061 cm, for which the proper breakdown is accorded.

The root-sum-squared (rss) requirement of the random surface error is less severe. By again using the 0.061-cm requirement for the rms with the proper percentage breakdowns, the following equation is derived:

[1] $$\text{rss of the rms} = 0.061 = \sqrt{(0.28x)^2 + (0.04x)^2 + (0.28x)^2 + (0.40x)^2}$$

Solving this produces an x of 0.108 cm, to which the percentages are again applied.

TABLE 7 - RANDOM SURFACE ERROR

Surface roughness	%	Worst-case, rms	RSS of RMS
Total[a]	100	0.061	0.061
Dynamics	28	0.0171	0.030
Pillowing	4	0.0024	0.005
Manufacturing	28	0.0171	0.030
Thermal	40	0.0244	0.043

[a]Total is defined as the sum for the worst case rms column, and as the rss for the"RSS of RMS" column.

The random surface error rms used in the analysis is an average of the worst case and the rss, resulting in the following equation, with the error due to dynamics being the sole variable:

[2]

$$rms = \frac{(0.0024 + 0.0171 + 0.0244 + rms_{dyn})}{2} + \frac{\sqrt{(0.005)^2 + (0.030)^2 + (0.043)^2 + (rms_{dyn})^2}}{2}$$

2.4.1.2 Beam Scanning - Motion of the feed and/or the reflector surface will shift the direction of the main beam. This shift can cause the antenna system to scan and look at a wrong target. For this study, three cases were considered. Additional abbrevations such as coma, which accompany these displacements, were not included.

Case 1 - Simple Feed Scanning - A shift in the feed location will displace the main beam in the opposite direction. Figure 11 illustrates the geometry. The ratio between angle θ_1 and θ_2 is known as the beam deviation factor and is approximately 0.992 for the EOS F/D ratio of 2.0.

The equation that describes the case 1 total scan angle is:

[1] $$\theta_T = \theta_1$$

Case 2 - Compound Motion (Additive) - This case includes motion of both feed and reflector as shown in Figure 12. A simple feed displacement with no reflector rotation results in a beam shift as indicated by the arrow. The additional angular displacement caused by rotation of the reflector surface, θ_S, produces a resultant beam shift of $2\theta_S$. The expression that relates the motion of reflector and feed to the total scan angle requirement is given by:

[2] $$\theta_T = 2\theta_S + \theta_1$$

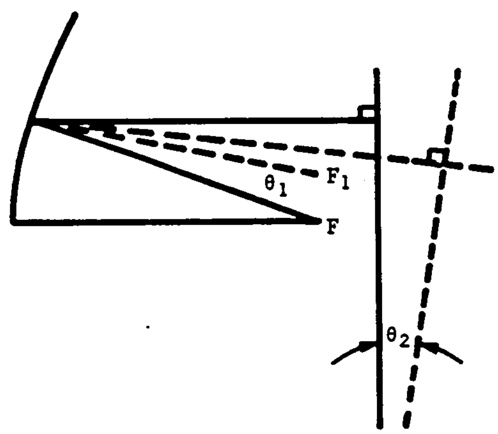

Figure 11 - Case 1, simple feed scanning.

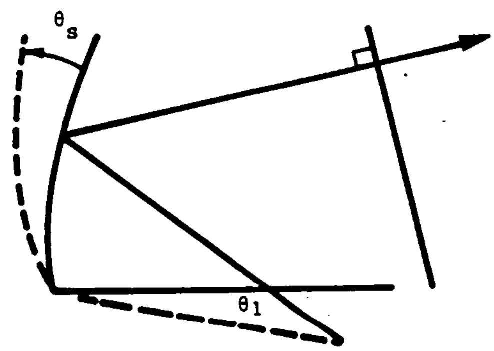

Figure 12 - Case 2, compound motion (additive).

The additive effect of these two motions causes the greatest scanning error.

Case 3 - Compound Motion (Subtractive) - This case also includes motion of both feed and reflector as shown in Figure 13. Consider the simple feed displacement first, with no reflector rotation. The beam shift is the same as case 1 and indicated by the arrow labeled "A." The $2\theta_S$ beam scanning caused by a rotation of θ_S is in the opposite direction to that of arrow "A." It is similar to case 2, and is marked "B."

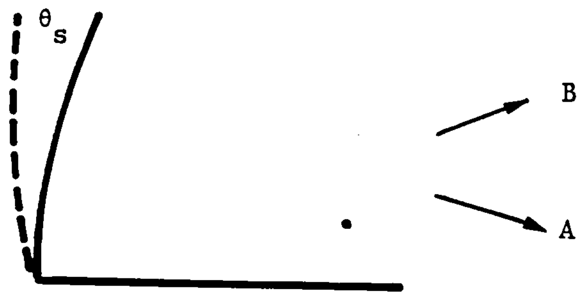

Figure 13 - Case 3, compound motion (subtractive).

The expression that relates the motion of reflector and feed to the total scan angle requirement is given in equation [3].

[3] $$\theta_T = 2\theta_S - \theta_1$$

The effects on beam scanning from these two motions are subtractive. Beam scanning may be reduced to zero when the reflector rotates twice as far and in the opposite direction of the feed.

2.4.1.3 Axial Defocusing - Axial defocusing is brought on by the surface focal point moving off of the feed point. The error is defined as the distance of the new surface focal point location from the distorted feed point location. It can be brought about in any combination of the following three ways:

1) Vertical movement of the feed point;

2) Change in the surface focal length;

3) Vertical movement of the surface.

In Figure 14 the surface opens while the feed point is stationary. The defocusing is shown as ΔF. In Figure 14b, the surface opens while the feed point is also moving up. The upward movement of this feed point negates the effect of the opening to the surface.

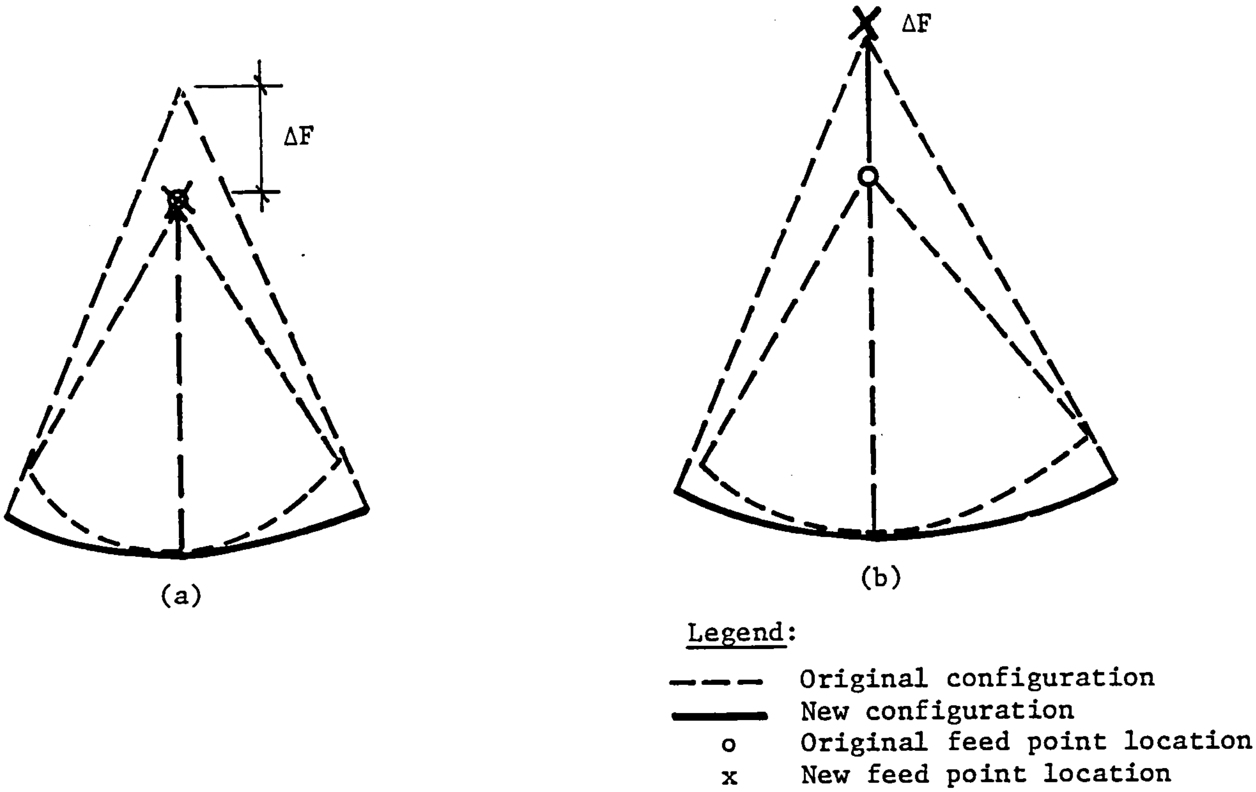

Figure 14 - Examples of axial defocusing.

2.4.2 Creation of Best-Fit Surface

There are 21 standoff points on either side of the EOS surface representing the outer most two contiguous spots. Both during and after slewing, these points will translate in X, Y, and Z directions.

The creation of the best-fit surface involves four variables--three rotations and a change in curvature. The surface rotations are defined as follows: Psi (ψ) is the yaw, theta (θ) is the roll, and beta (β) is the pitch. These are illustrated in Figure 15. The change in curvature is a change in focal length of the surface. Once ψ , θ , β , and F have been established, a new paraboloid surface is generated through equation [1].

[1] $$Zgen = (X^2 + Y^2)/4F$$

The surface roughness is found through an rms technique, using the differences of the Z coordinates between the perfect surface and the actual surface, as shown in equation [2].

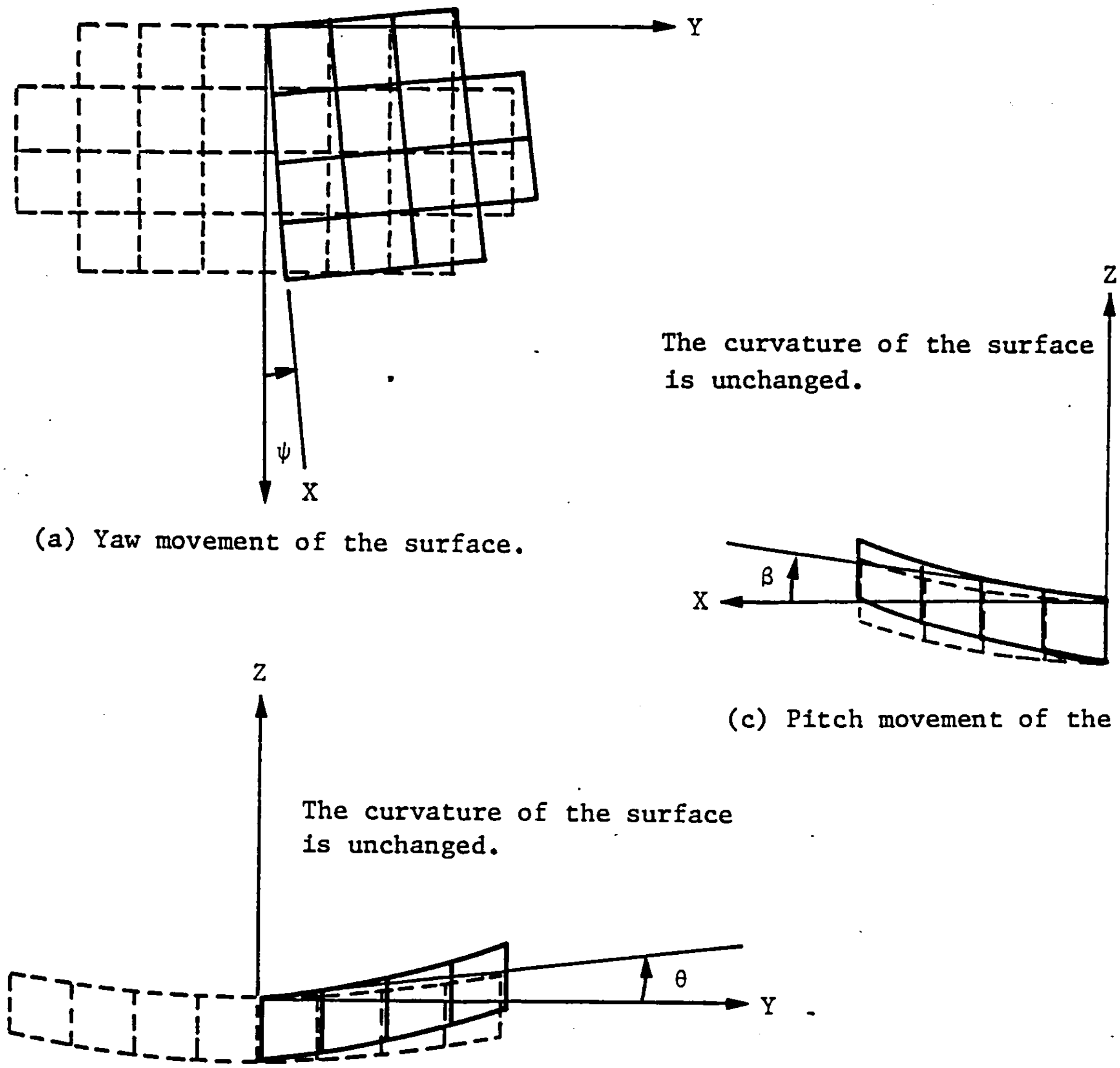

(a) Yaw movement of the surface.

(c) Pitch movement of the surface.

(b) Roll movement of the surface.

Figure 15 - Creation of the Best-Fit Surface.

[2] $$rms_{dyn} = \sqrt{\sum_{n=1}^{21} (Zgen_n - Zact_n)^2 /21}$$

By adjusting these four variables, through orderly iteration, the minimum rms is obtained. Each side of the reflector surface is adjusted separately.

There are two additional node points of interest--the feed points. On the EOS structure, there is actually a line of feeds. However, the outermost two feed points, Figure 16 represent the location of the feeds for the reflector surface areas used in the best-fit surface analysis.

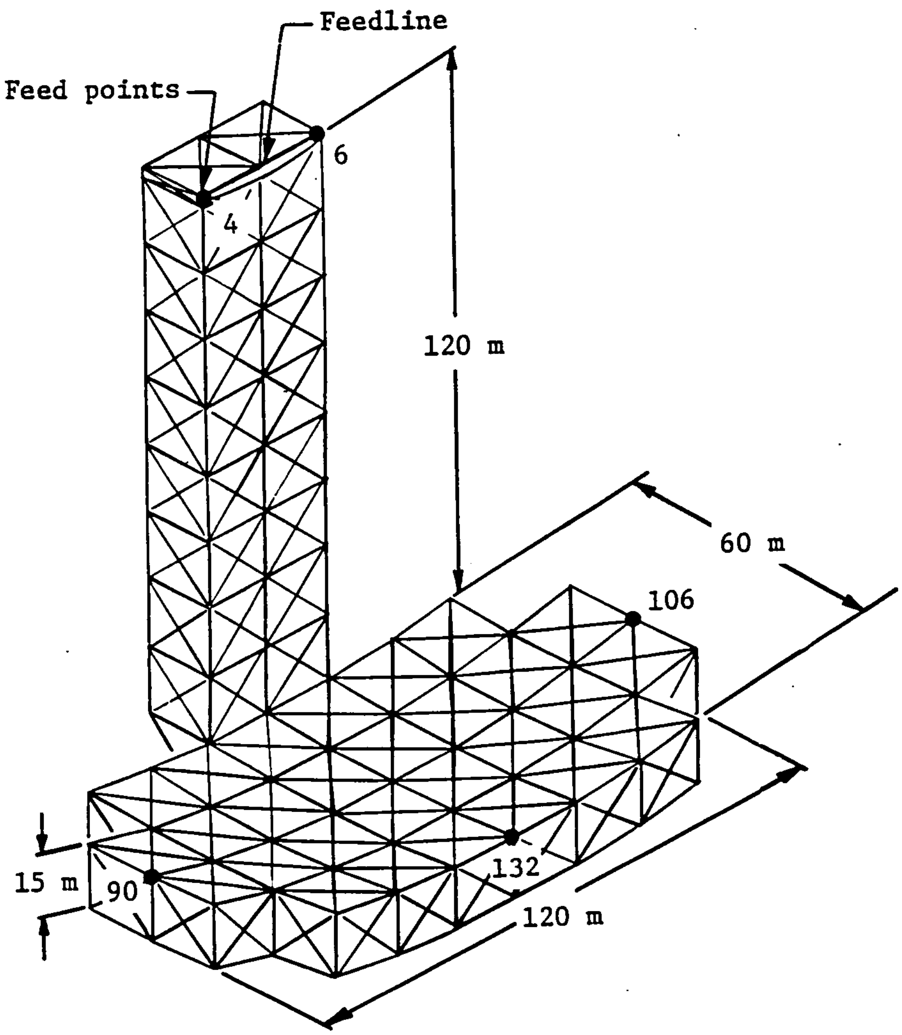

Figure 16 - Critical nodes on EOS structure.

These two points will translate X and Y directions and combining these with the surface rotations, beta and theta, the total scan can be calculated. The Z movement of each of these feed points is used to determine axial defocusing, as described in Section 2.4.1.3.

2.4.3 Use of Best-Fit Analysis

For all slewing cases, the dynamic transient response analysis outputs each of the node points with the corresponding time points and respective translations. Selection of the time points for operational fitness testing now becomes all important. Operational fitness is a function of the deflections of the surface and of the feed points. To choose eligible time points, it is best to look at the critical surface nodes 90, 106, and 132, as well as nodes 4 and 6, shown in Figure 17. The three surface nodes are perimeter nodes and are subject to extreme deflections in the Z direction. It is desirable to choose time points so that their deflections are not exceeded at later times.

These can be chosen from the individual time history curves of each critical node point. These time points will almost always occur at relative peak deflections in the curve, shown in Figure 17.

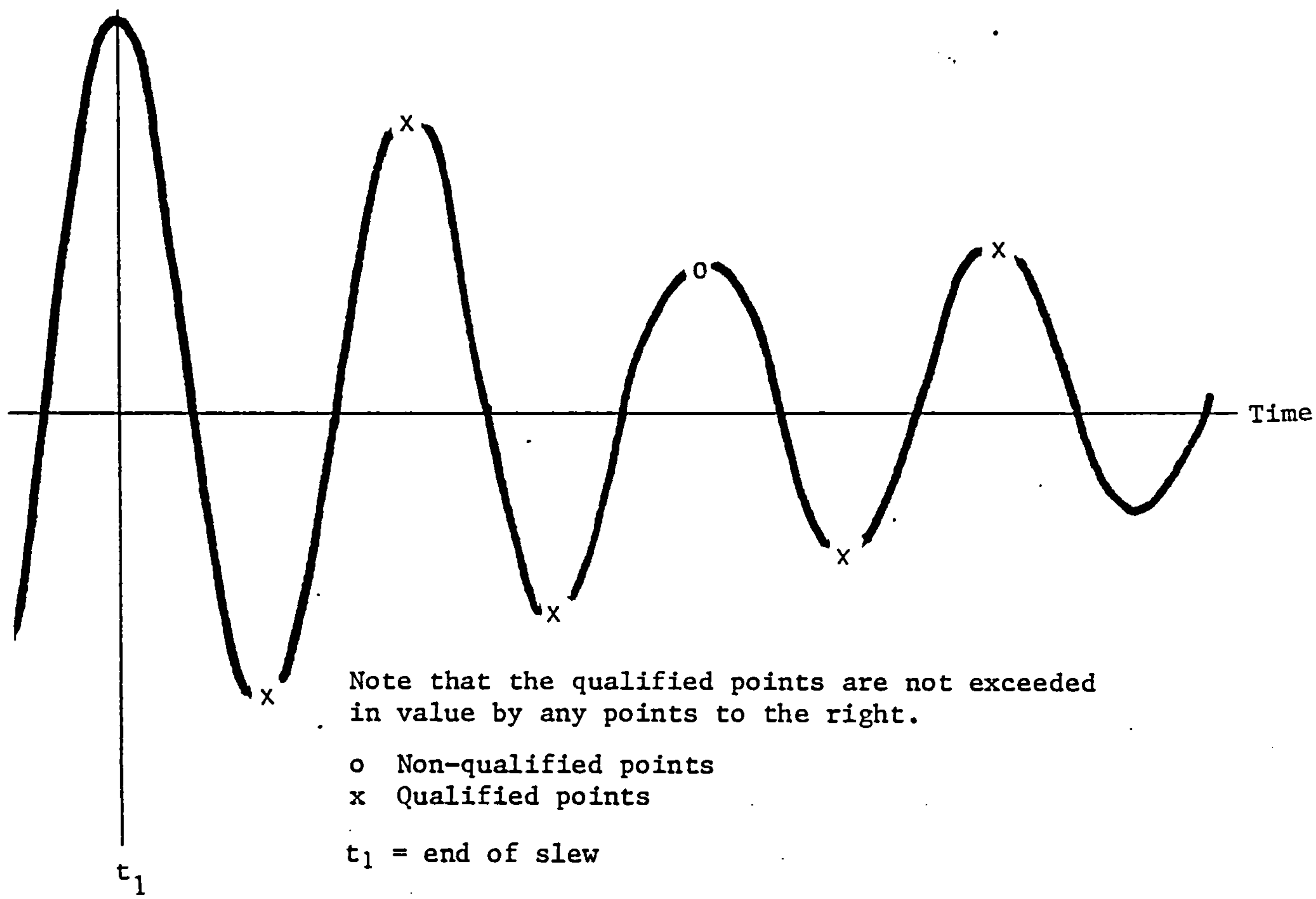

Figure 17 - Typical time history curve.

2.4.4 The Effect of System Errors

Once the error analysis has been concluded, the new best-fit surface must be tested for operational fitness in accordance with the requirements given in Section 2.1.

For each side of the surface, four requirements must be met separately. The time point at which all requirements are first met is the time point at which operation of the radiometer may begin.

If, however, the system does not settle in the time allotted in the transient analysis, the settling time must be estimated. The premise for this estimation is that because displacements decay logarithmically with time, all related parameters must decay in the same fashion. That is, $\Delta G/G$ found in radiometric resolution and Δ BWFN found in resolution must decay logarithmically with respect to time. By plotting either of these two parameters for several time points on semi-log graph paper, a logarithmic decrement can be established, and, with that, an estimate of settling time can be determined. An example of this procedure is shown in Section 3.3.2.

3.0 ANALYSIS RESULTS

The following sections present the results of the various analyses performed and the system impacts caused by adding slew capability to EOS.

3.1 RIGID-BODY ANALYSIS

The mission situation evaluated in the dynamic analysis was a 705-km orbit without orbit transfer fuel but with 1265 kg of slewing propellant. The total mass of the model was 6812 kg. NASTRAN plots of the elastic mode shapes were obtained, and Figures 18 and 19 show the first two elastic modes. Mass moments of inertia and mass center of gravity were calculated by the NASTRAN Grid Point Weight Generator and are listed in Table 8. Using the Grid Point Weight Generator results, the thrust angle, slew time, and attitude hold requirements for the EOS baseline structure being slewed 15 degrees were determined. Figure 20 shows the center-of-gravity thruster locations and thrust angles.

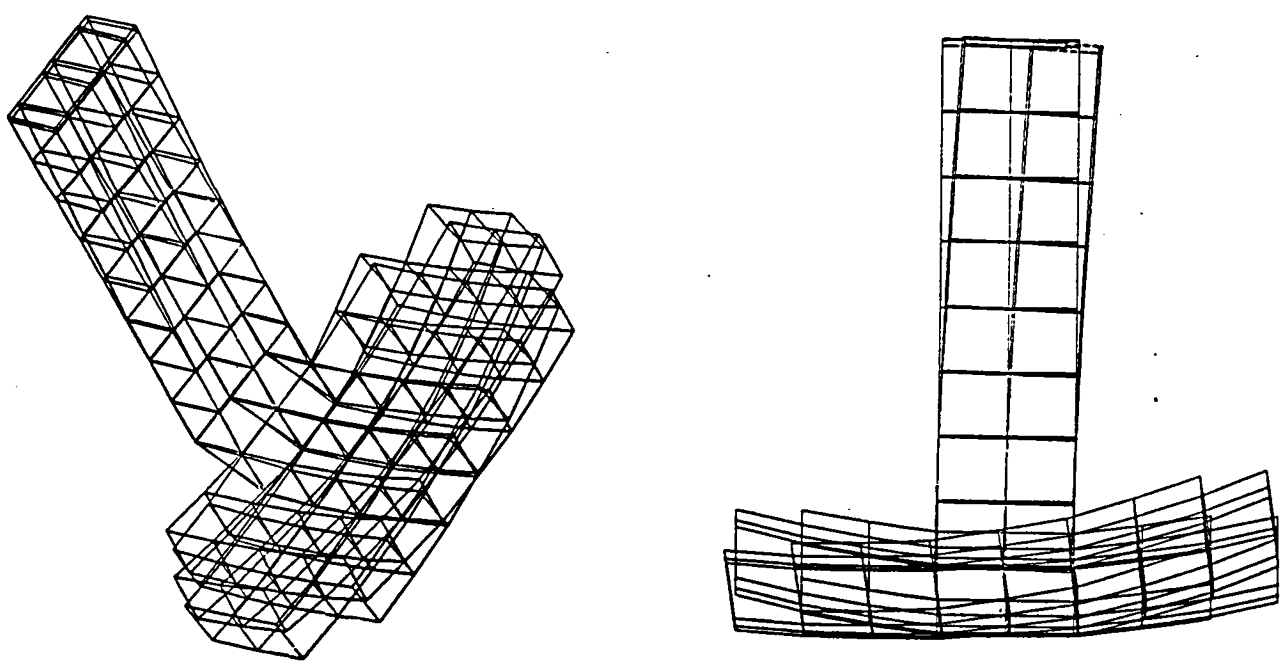

Figure 18 First mode with slewing and without orbit transfer (freq of 0.911 Hz).

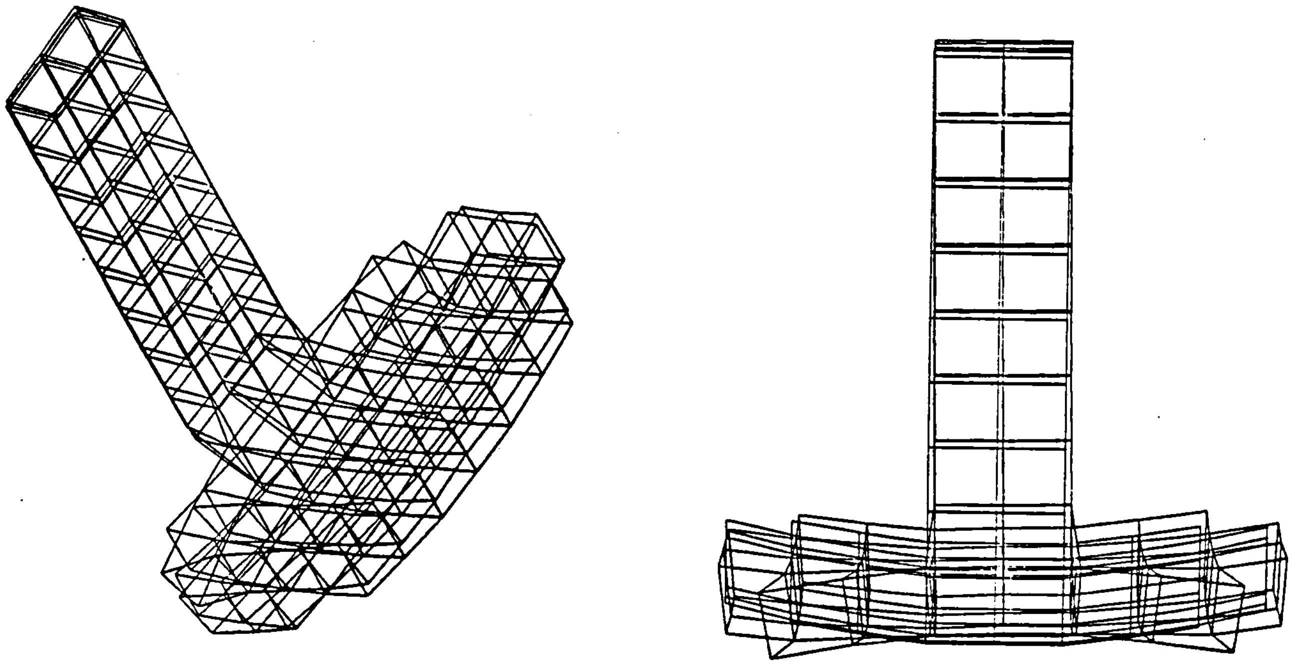

Figure 19 - Second mode with slewing and without orbit transfer (freq of 0.963 Hz).

TABLE 8 - CENTER OF MASS LOCATION AND PRINCIPAL MASS MOMENTS OF INERTIA AS DETERMINED BY NASTRAN GRID POINT WEIGHT GENERATOR

Center of mass location, m[a]		
	X_{cg}	17.13
	Y_{cg}	0.0
	Z_{cg}	31.95
Mass moments of inertia about principal axes, kg-m^2 x 10^7		
	I_{xp}	2.699
	I_{yp}	2.208
	I_{zp}	1.110

[a]Model origin and coordinate system are shown in Figure 20

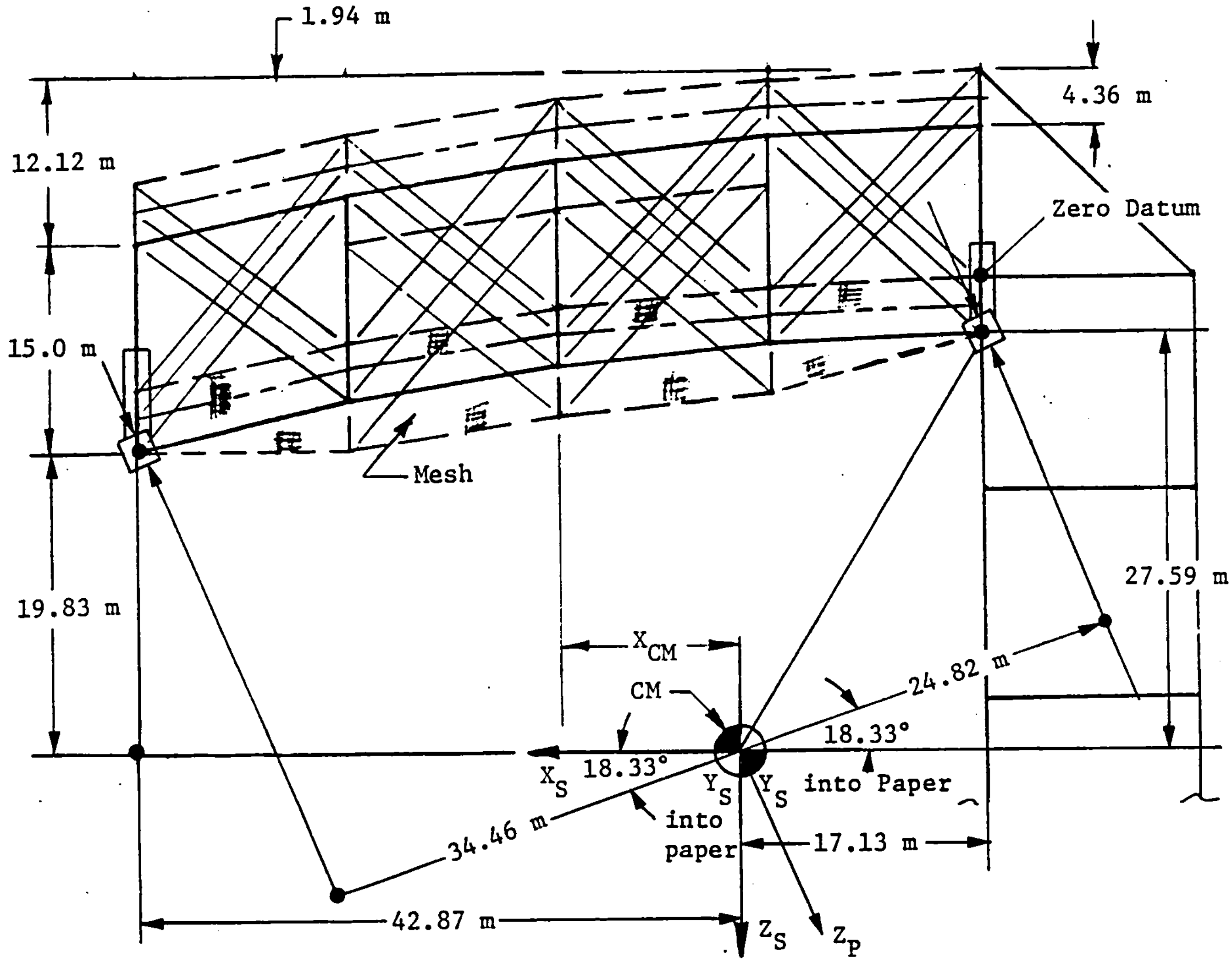

Figure 20 - Thruster system location for slew maneuvers.

3.1.1 Slew Times, Thruster Levels, and Maneuver Frequency

The length of time required for the slew maneuver was calculated using equation [3] in Section 2.2.2. Figure 21 shows the resulting slew time as a function of thrust level using the following:

I_{xp} = 2.69887 x 10^7 kg-m^2 (as determined by the NASTRAN Grid Point Weight Generator)

T_H = Thrust level x 4 thrusters x 45.214 m

Also shown in Figure 21 is the number of slew maneuvers possible before resupply as a function of thruster level. This curve was determined using equations [4] and [5] in Section 2.2.2.

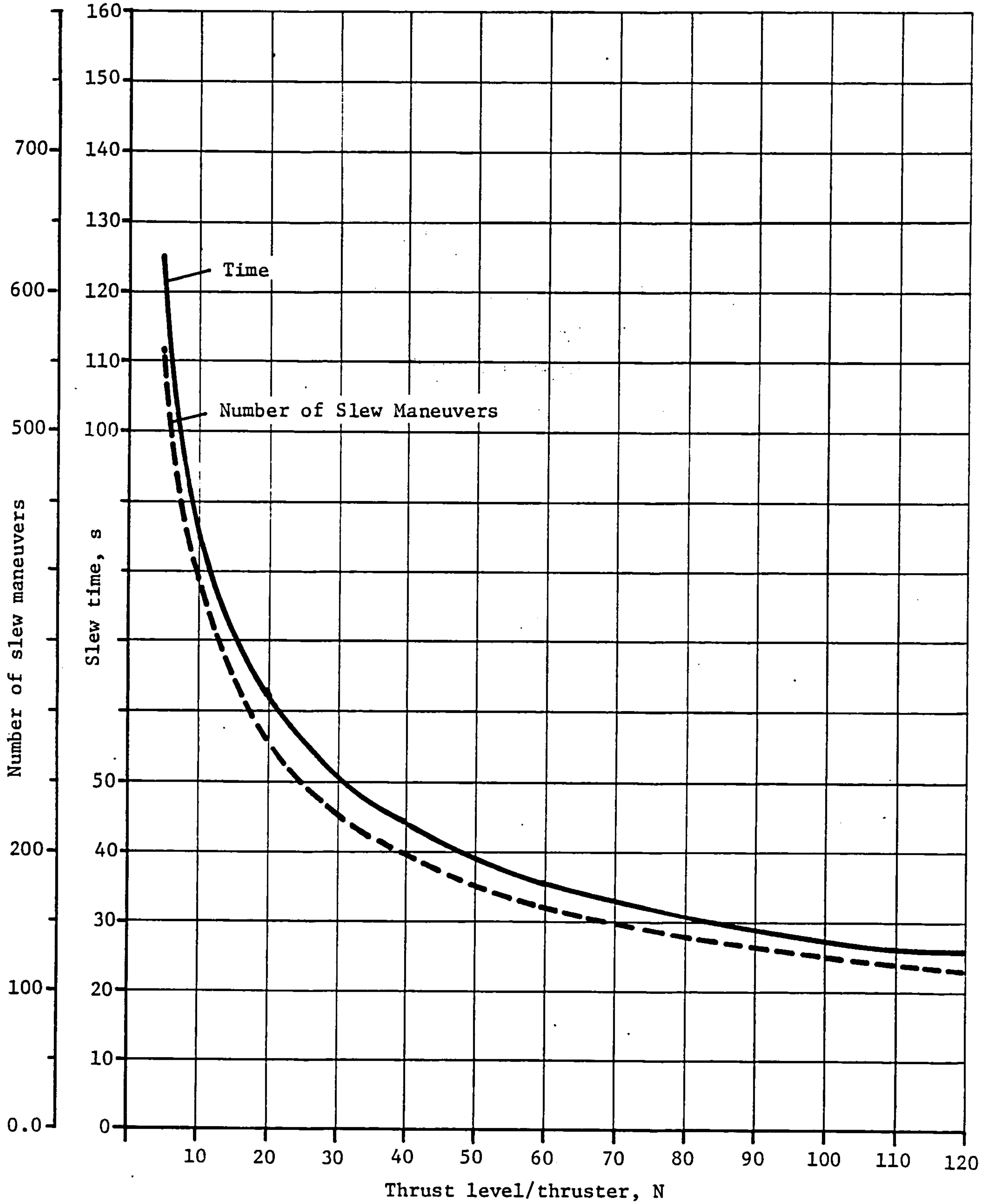

Figure 21 - Slew time and number of slew maneuvers per lifetime.

3.1.2 Attitude Hold Requirements

Because the pointing requirement for EOS about the x-axis is ± 0.08 degrees in or out of the orbit plane, it was possible to determine the length of time the EOS can remain in the out-of-plane position from equations [6] and [7] in Section 2.2.3. The gravity gradient torque was determined from equation [7] in Section 2.2.3 assuming the following:

ω_o^2 = 1.1235×10^{-6} rad/sec^2 (700-km orbit)
I_{zp} = 1.109591×10^7 kg-m^2 (calculated by NASTRAN Grid Point Weight Generator)
I_{yp} = 2.207805×10^7 kg-m^2 (calculated by NASTRAN Grid Point Weight Generator)
ϕ = slew angle = 15 degrees

Therefore,

T_{ggyp} = -9.254 N-m

resulting in an angular acceleration of

$$\alpha = \frac{0.254 \text{ N-m}}{2.699 \times 10^7 \text{ kg-m2}} = 3.43 \times 10^{-7} \text{ rad/sec}^2$$

Thus, the length of time the EOS remains in the out-of-plane position was calculated from equation [6] in Section 2.2.3 to be 90.2 seconds if no station-keeping thrust was applied.

The thrust level necessary to maintain attitude was calculated using equation [8] in Section 2.2.3, using a moment arm length, L, of 45.214 m and the above gravity gradient torque the necessary thrust level was calculated to be 0.20 N. For a 60-second impulse, the fuel mass necessary to provide 0.20 N of thrust is 0.005 kg, from equation [4] Section 2.2.2.

3.2 TRANSIENT ANALYSIS RESULTS

A total of 42 elastic modes were extracted using the FEER method, the highest frequency being 1.94 Hz. It became evident after the first few thrust level-structural damping combinations were investigated, that only the first few structural modes were significantly contributing to the response of the spacecraft. To illustrate, Figure 22a through 22c shows typical displacement curves for each of three thrust levels. As is shown, the highest occurring frequency is 1.1 Hz, indicating that no modes with frequencies greater than 1.1 Hz are significantly contributing to the response of the system. Therefore, only the modes between 0.9 and 1.14 Hz were used to determine the transient response during settling time.

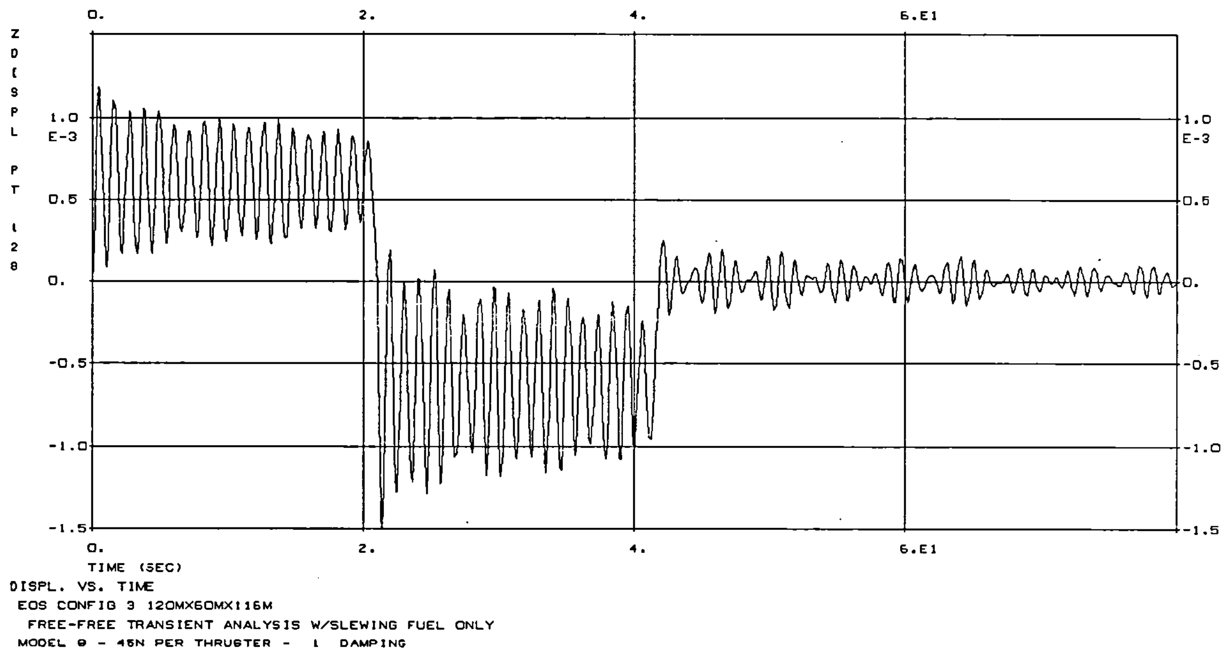

(a) Case 2: node 128, Z-displacement.

Figure 22a - Typical displacement curves.

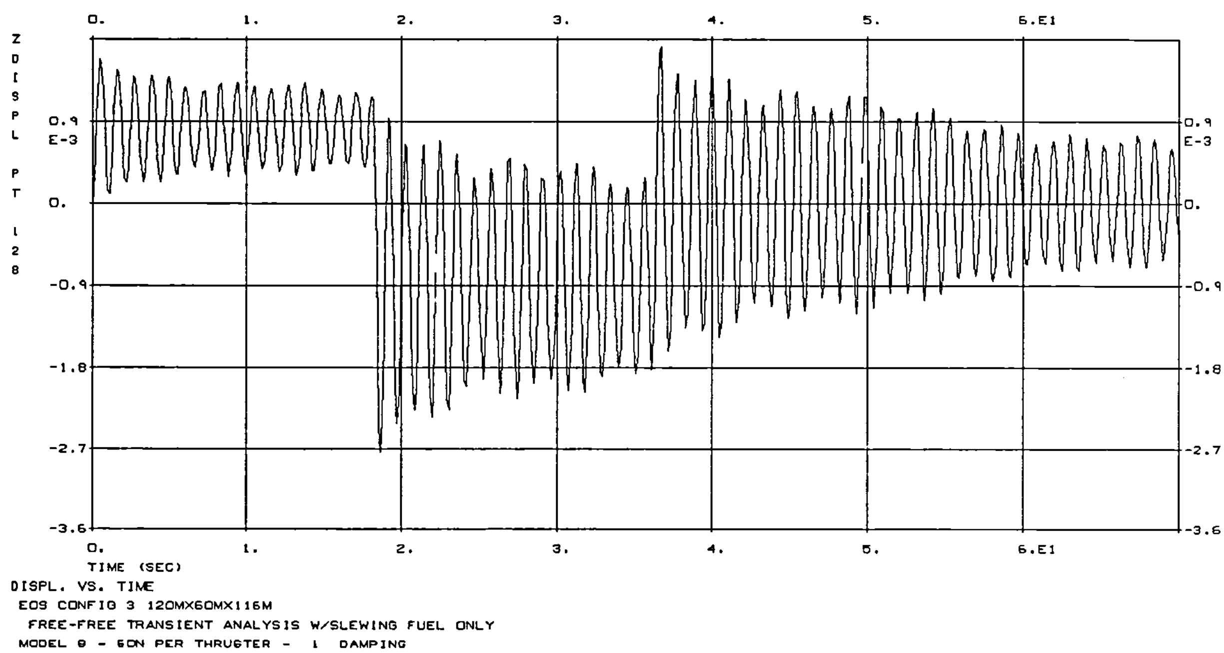

(b) Case 5, node 128, Z-displacement.

Figure 22b - Typical displacement curves.

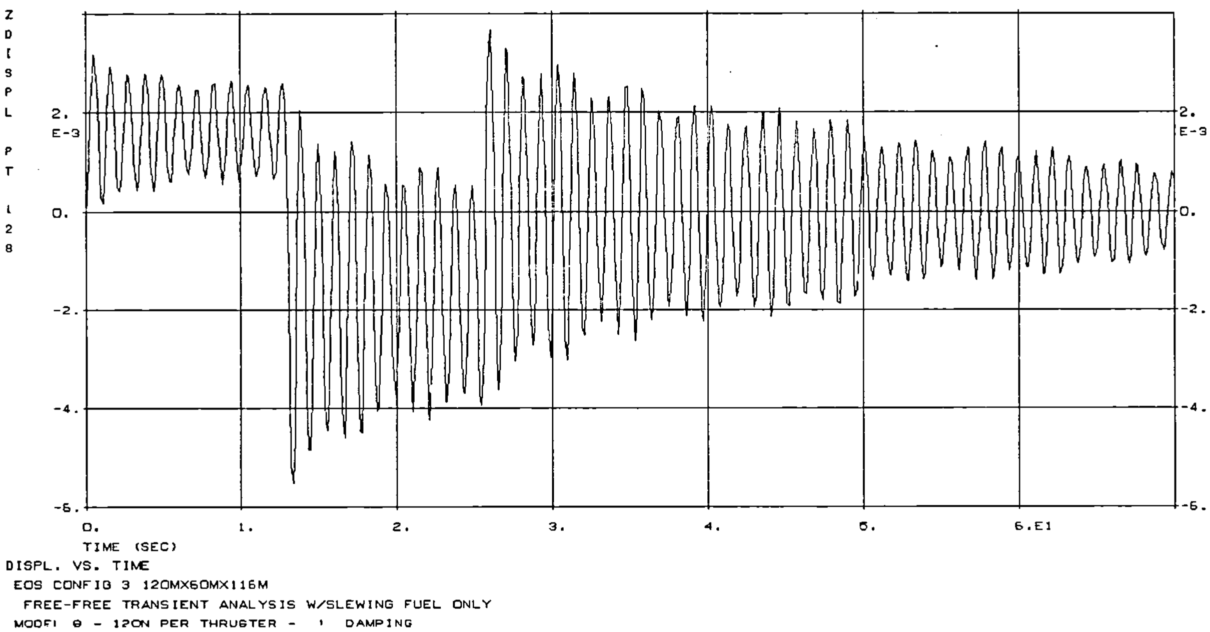

(c) Case 7, node 128, Z-displacement.

Figure 22c - Typical displacement curves.

Table 9 shows the matrix of conditions considered in the transient response analysis. Figure 23 shows the force/time functions for each thrust condition.

TABLE 9 - MATRIX OF ANALYSIS CONDITIONS

Analysis case	Thrust level, N	Structural damping, %	Slew time, s
1	45	0.2	41.7
1′	45	0.2	41.2[a]
2	45	1.0	41.7
2′	45	1.0	41.2[a]
3	50	1.0	39.5
4	60	0.2	36.1
5	60	1.0	36.1
6	60	5.0	36.1
7	120	1.0	25.5
8	120	5.0	25.5

[a]The slew angle achieved for cases 1′ and 2′ is 14.665 deg as opposed to 15 deg for the remaining cases.

The ten thrust/damping conditions shown in Table 9 were input to the COSMIC NASTRAN model transient response analysis, and resulting displacements were tabulated and plotted for use in the system errors analysis to determine at what point in the settling time the system becomes operational.

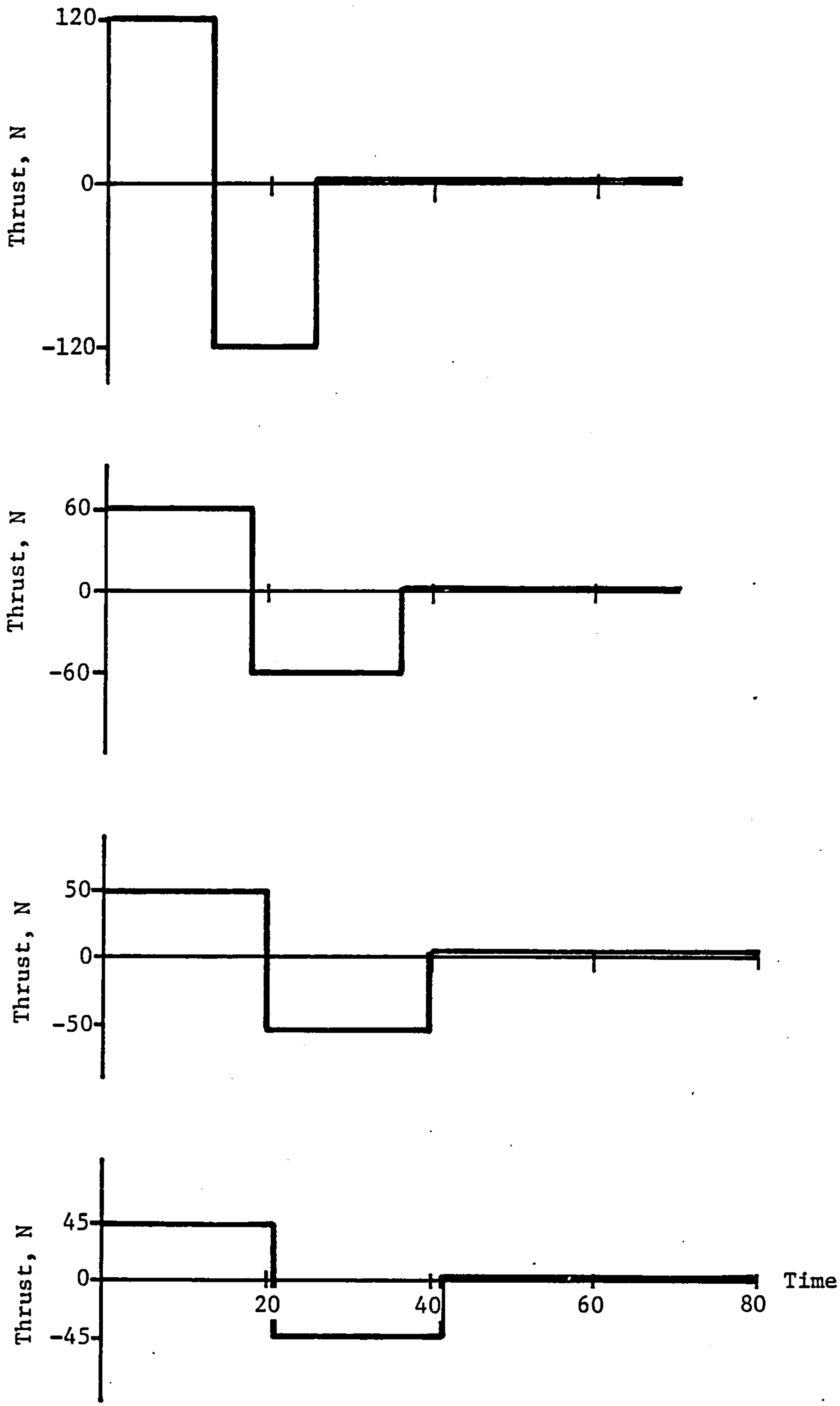

Figure 23 - Forcing functions for analysis thrust conditions.

Figure 24 is a NASTRAN plot of the deformed structure at the beginning of settling time for the 60-N -1% structural damping case. It should be noted that the deformations are not drawn to scale. Because the displacements are very small relative to the size of the structure, they would not be seen in the structural deformation plots if they were drawn to scale. Comparing the deformation plots to the first mode shape shown in Figure 19, it becomes evident that the first mode is primarily contributing to the deformation of the structure. This deformation plot is typical for all thrust level/structural damping conditions investigated that yield a 15-degree slew.

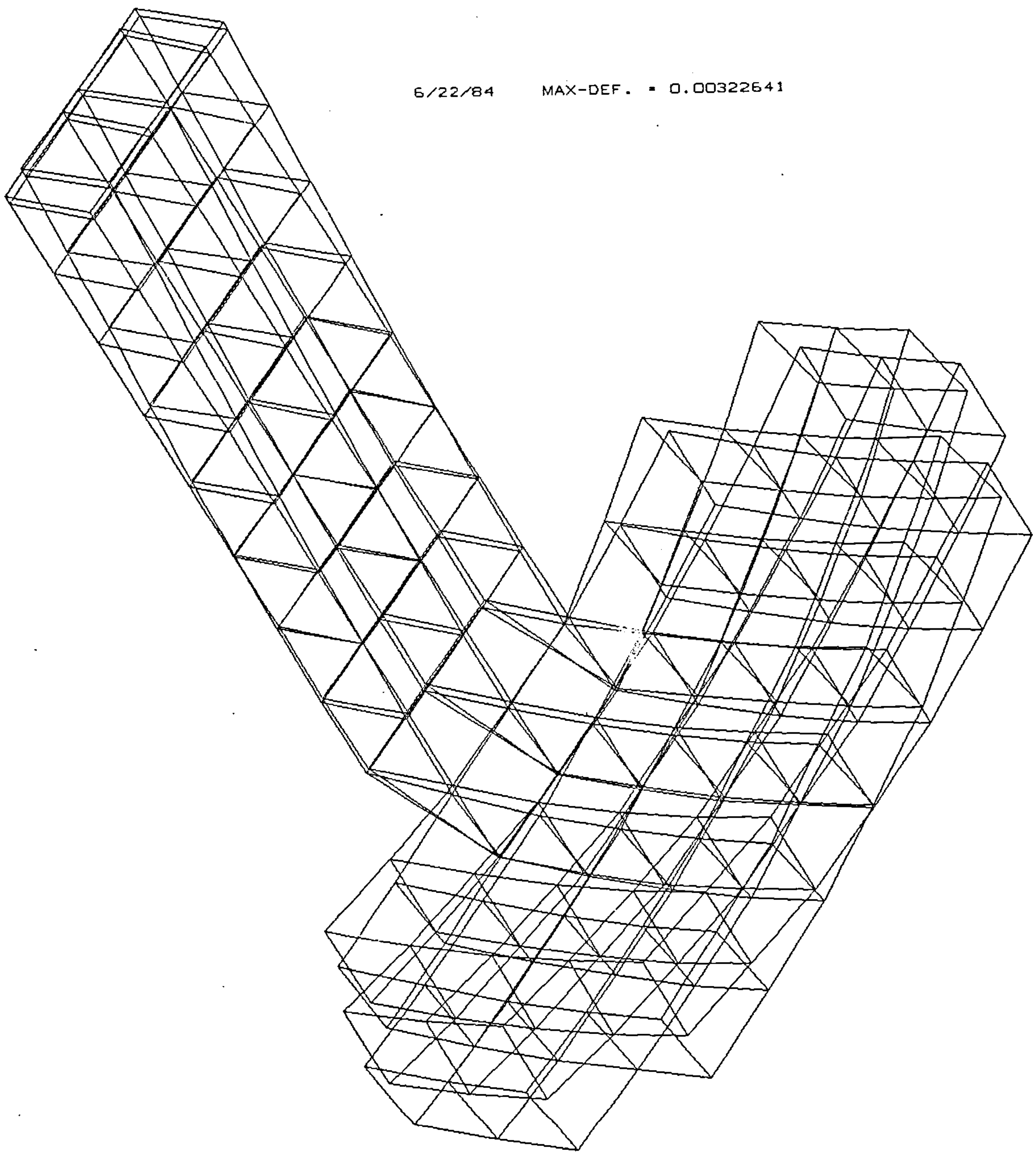

Figure 24 - Case 5, EOS deformed shape at 60N/1% damping.

Displacements were obtained at the node points located on the top surface of the antenna and at two feed points. Figures 25 through 28 show the X and Y-displacement time histories for the two feed points for the 60-N -1% structural damping case. Note that the point numbers on the Y-axis of the curves correspond to the grid points in Figure 6. The displacement axes are the same as those shown in Figure 4. Figures 29 through 31 show the displacements of the reflector surface points 98, 106, and 136 in the Z direction. In general, the plots show the displacements oscillating at the fundamental frequency of approximately 0.9 Hz. However, the plots showing the displacements at the interior points on the surface (e.g., point 98) where the displacements are relative small, display a secondary frequency of approximately 0.05 Hz. This indicates that higher frequency modes are contributing to the deformation of the structure, but to a relatively small degree because this secondary frequency is only apparent when the magnitude of the displacements is small.

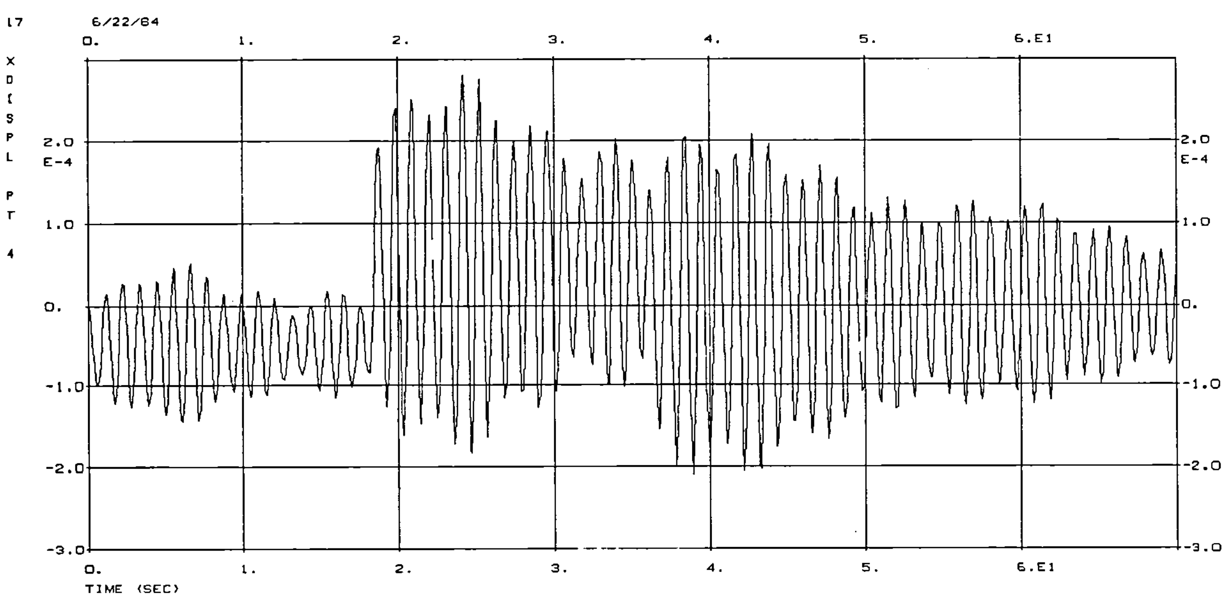

Figure 25 - Case 5, node 4, X-displacement.

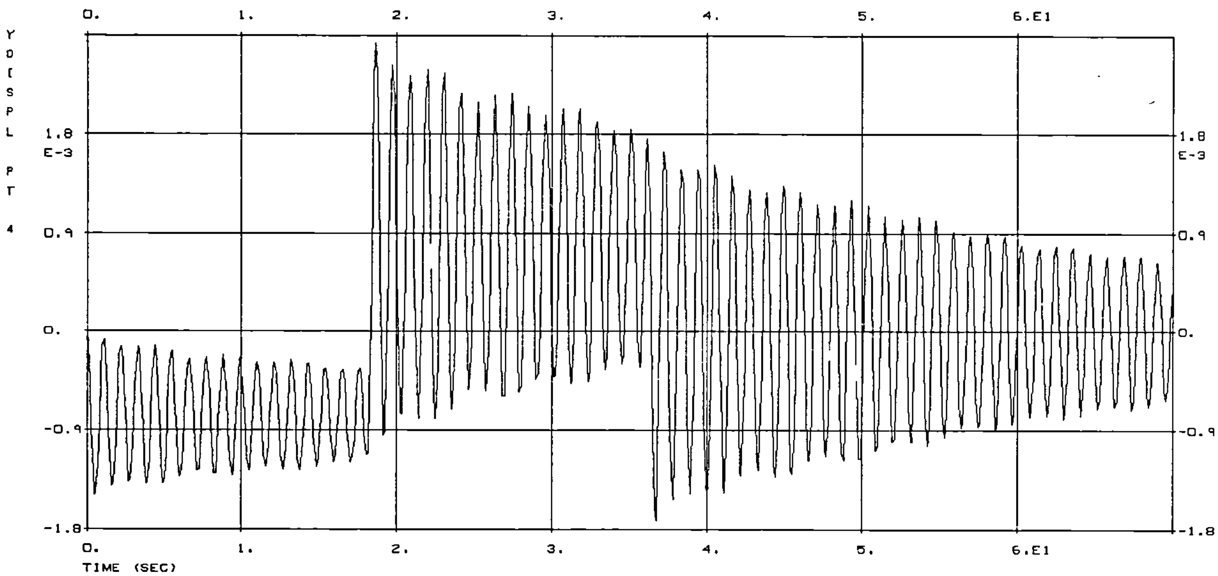

Figure 26 - Case 5, node 4, Y-displacement.

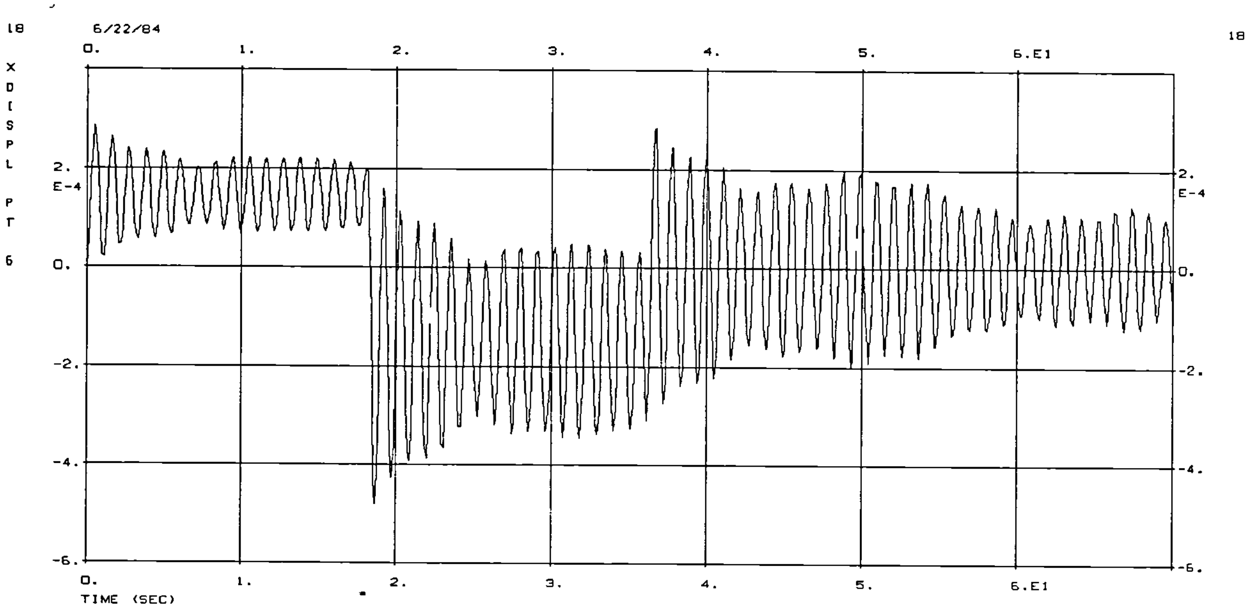

Figure 27 - Case 5, node 6, X-displacement.

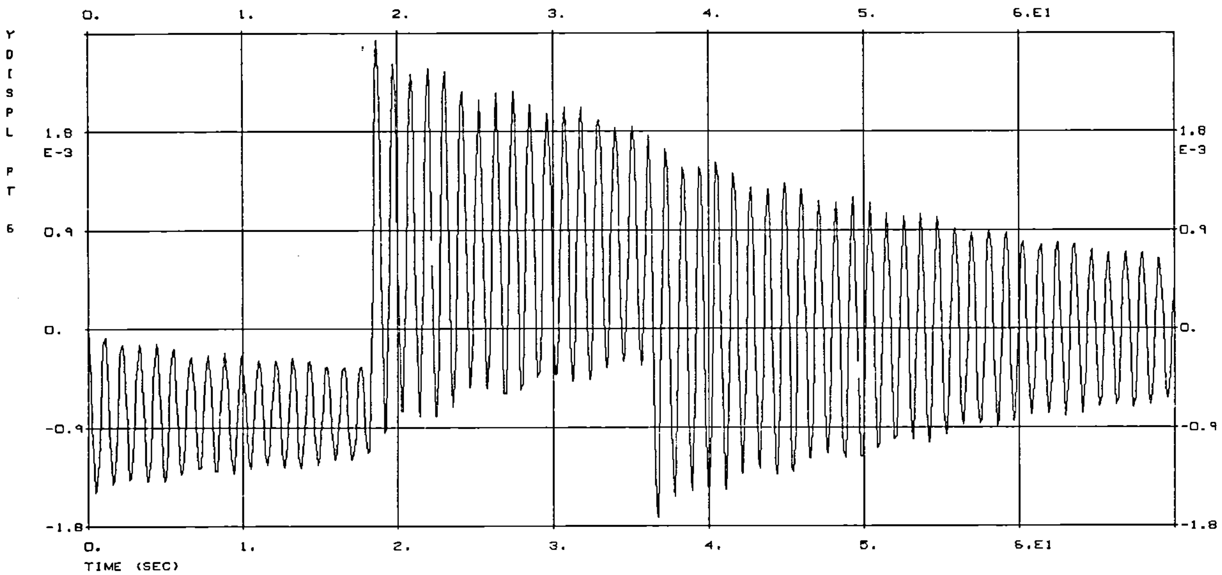

Figure 28 - Case 5, node 6, Y-displacement.

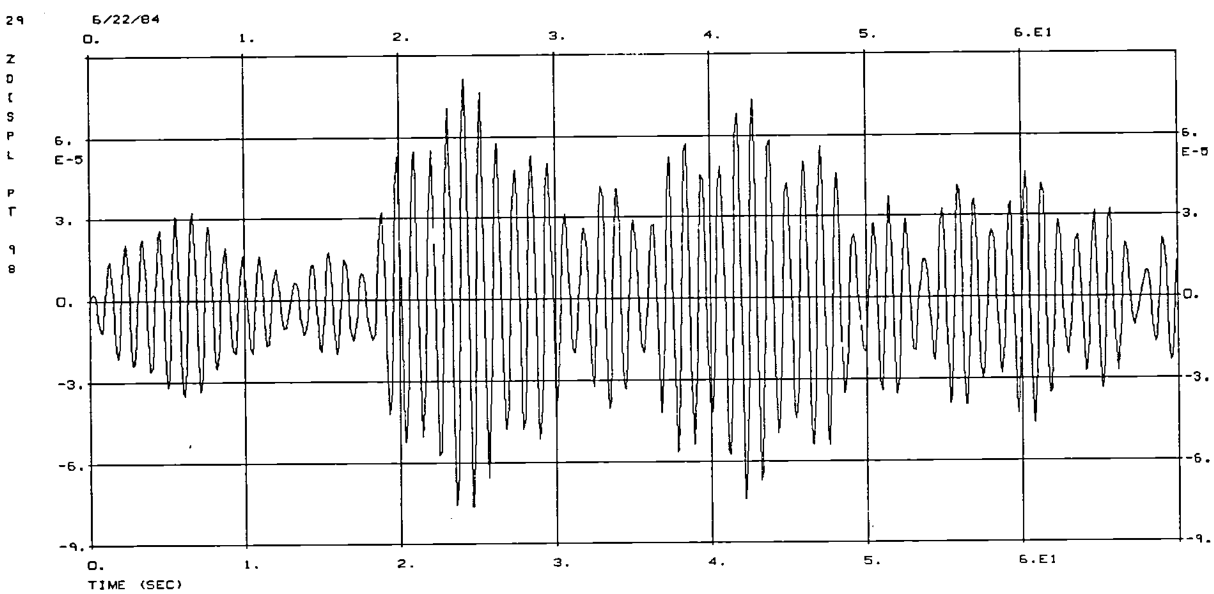

Figure 29 - Case 5, node 98, Z-displacement.

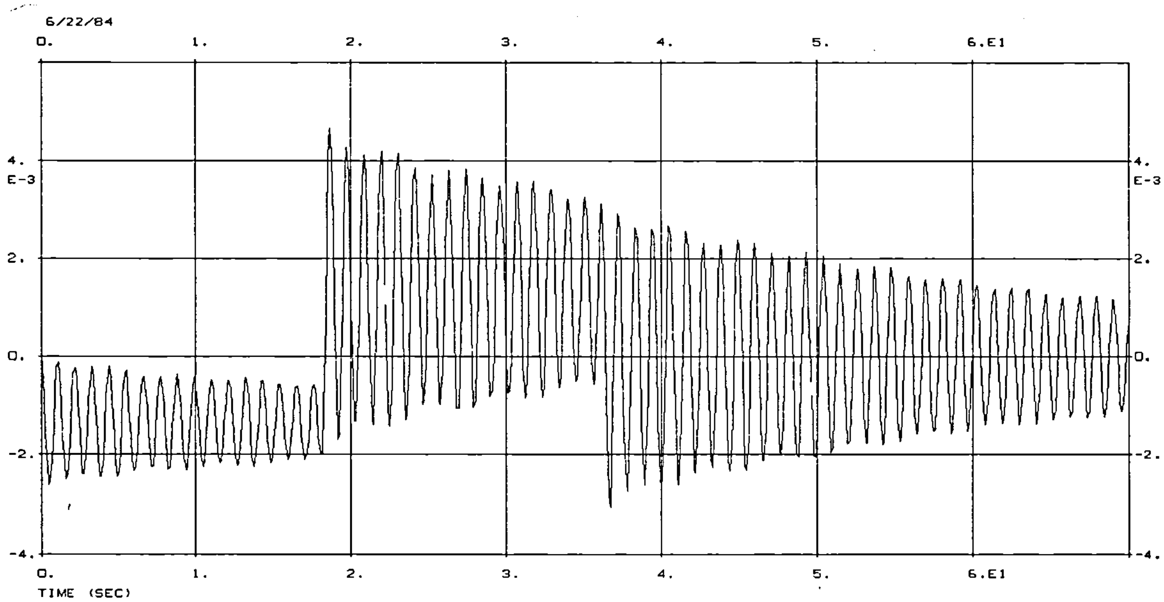

Figure 30 - Case 5, node 106, Z-displacement.

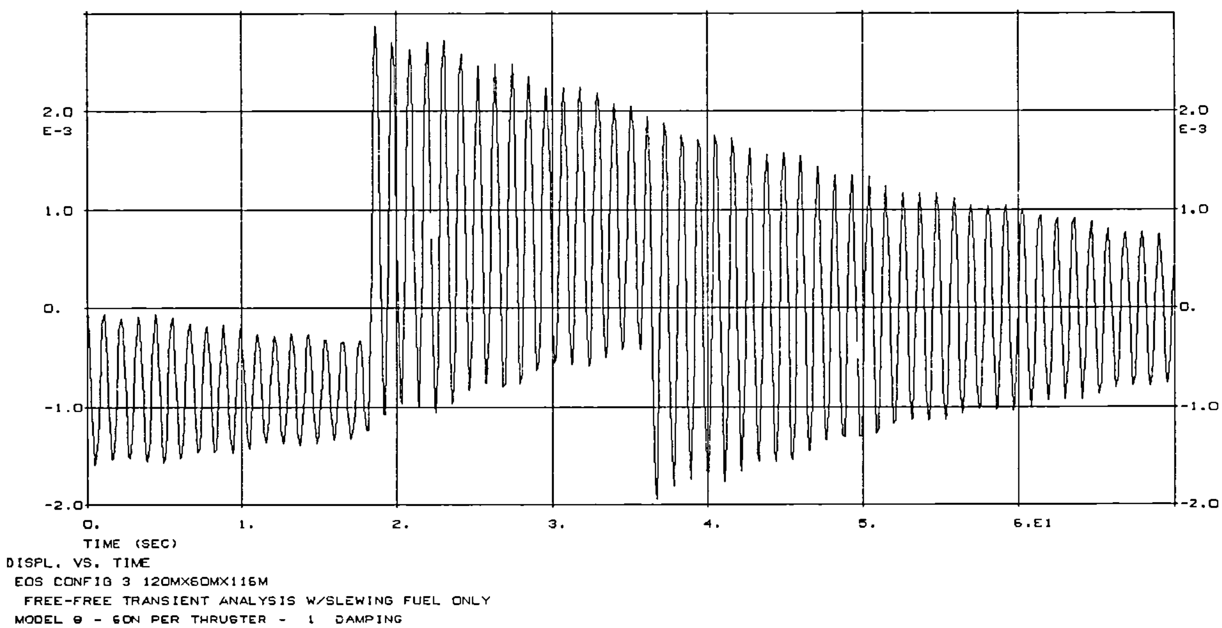

Figure 31 - Case 5, node 136, Z-displacement.

The structural damping effects on the decay rate of the displacements are clearly seen in the plots of the displacement time histories. For the purpose of comparison, Figures 32 and 33 show the Z-displacements of point 106 at 60 N -0.2% structural damping and 60 N -5% structural damping, respectively. As expected, the maximum nodal deflections at the end of slew decreased with increased damping ratios and the decay rate of the displacements followed a logarithmic function.

3.2.1 Impact of Analytically Determined Slew Times

During the transient response analysis, a parallel study was conducted to determine the impact on the settling time when slew times (and, hence, slew angles) were analytically determined. Analysis quickly verified that small variations in the slew angle, at any given thrust level, greatly impact the amount of settling time necessary before the structure again becomes operational.

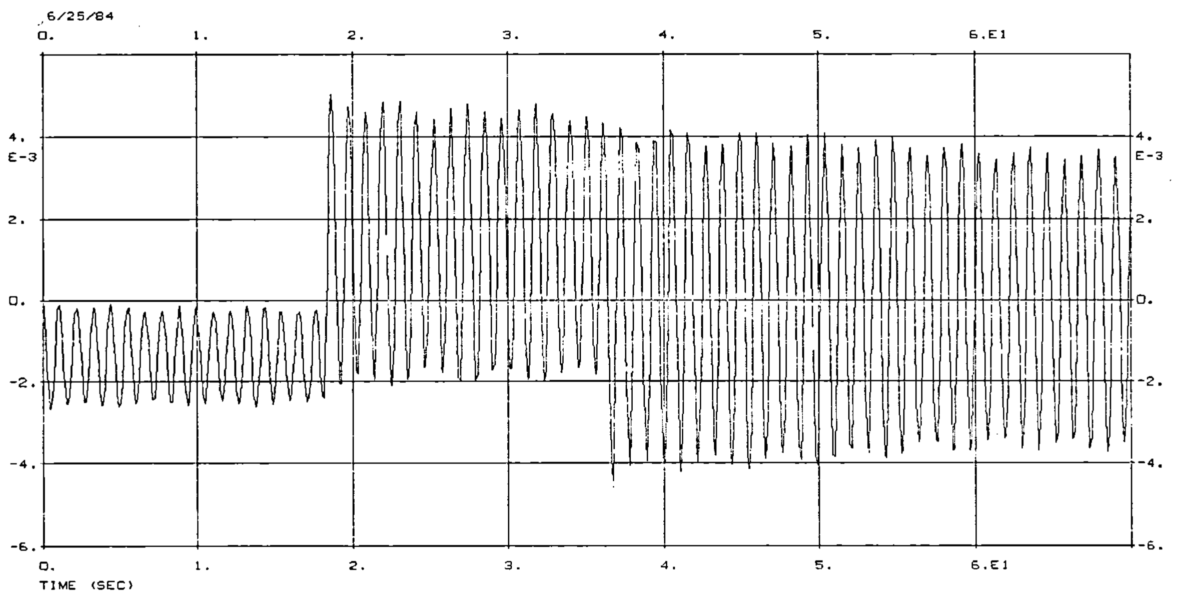

Figure 32 - Case 4, node 106, Z-displacement

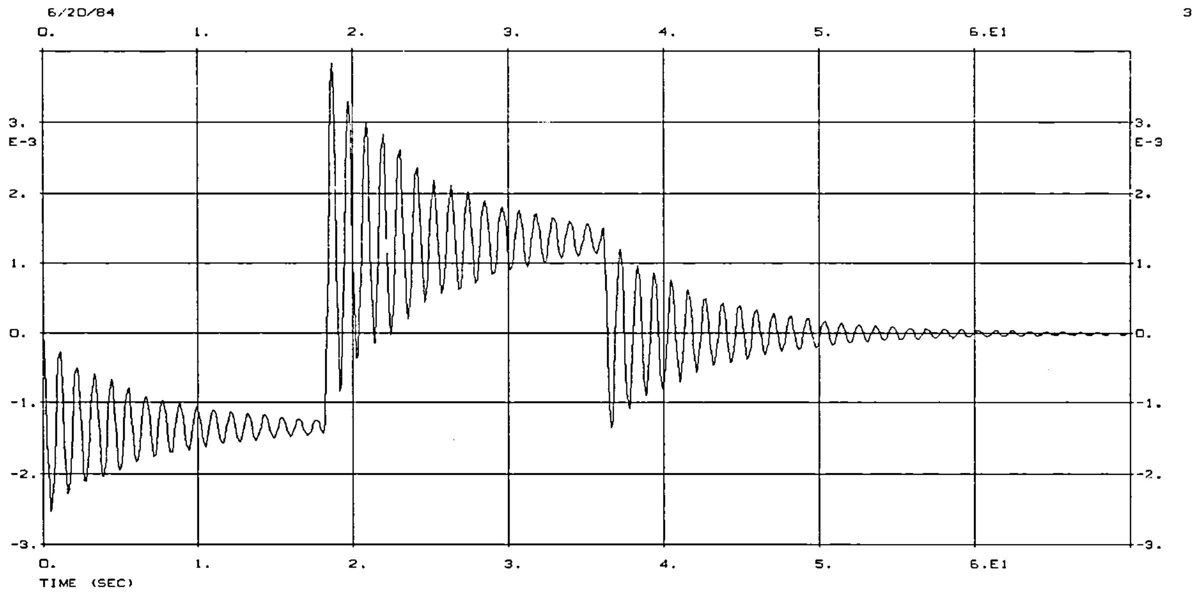

Figure 33 - Case 6, node 106, Z-displacement.

Referring to Table 9, the 45-N thrust with a 0.2 and 1.0% damping cases were each analyzed for two slew times, cases 1, 1', 2, and 2'. Slewing the EOS antenna 15 degrees using 45-N of thrust requires a slew time of 41.7 seconds. However, this slew period resulted in the removal of the thrust force at a time when the elastic displacement of the structure was close to zero. Therefore, the deformation at the start of settling time was very small, and the system error analysis determined the structure to be operational immediately. A transient response analysis was then conducted for the same thrust/ structural damping conditions with the exception that instead of using a slew period of 41.7 seconds, a slew time of 41.2 seconds was implemented. This period was chosen by determining the time nearest 41.7 seconds when the nodal displacements of the structure were at a maximum using the displacement time history curves from the 41.7-second case. The resulting displacements during the settling time were much greater because of the greater displacement at the end of slew time. As a result of the decreased slewing period, the slew angle was reduced to 14.665 degrees.

Figure 34 shows the NASTRAN plot of the deformed structure at the end of slew for the 45-N -0.2% damping case with a slew time of 41.2 seconds (14.665-degree slew). Figure 35 is the NASTRAN deformation plot at the end of slew for the 45-N -0.2% damping case with a slew time of 41.7 seconds (15-degree slew). From these plots it is evident that higher frequency modes are contributing more to the response of the spacecraft when displacements are small than when displacements are relatively large. Figures 36 and 37 show representative displacement time histories for the 45-N -0.2% damping case with a slew period of 41.2 and 41.7 seconds, respectively. Comparing the displacements following the slew maneuver for the 14.665-degree slew and the 15-degree slew, it quickly becomes evident that small adjustments in slew angles result in significant changes in displacements at the end of slew and thus significantly effect settling time.

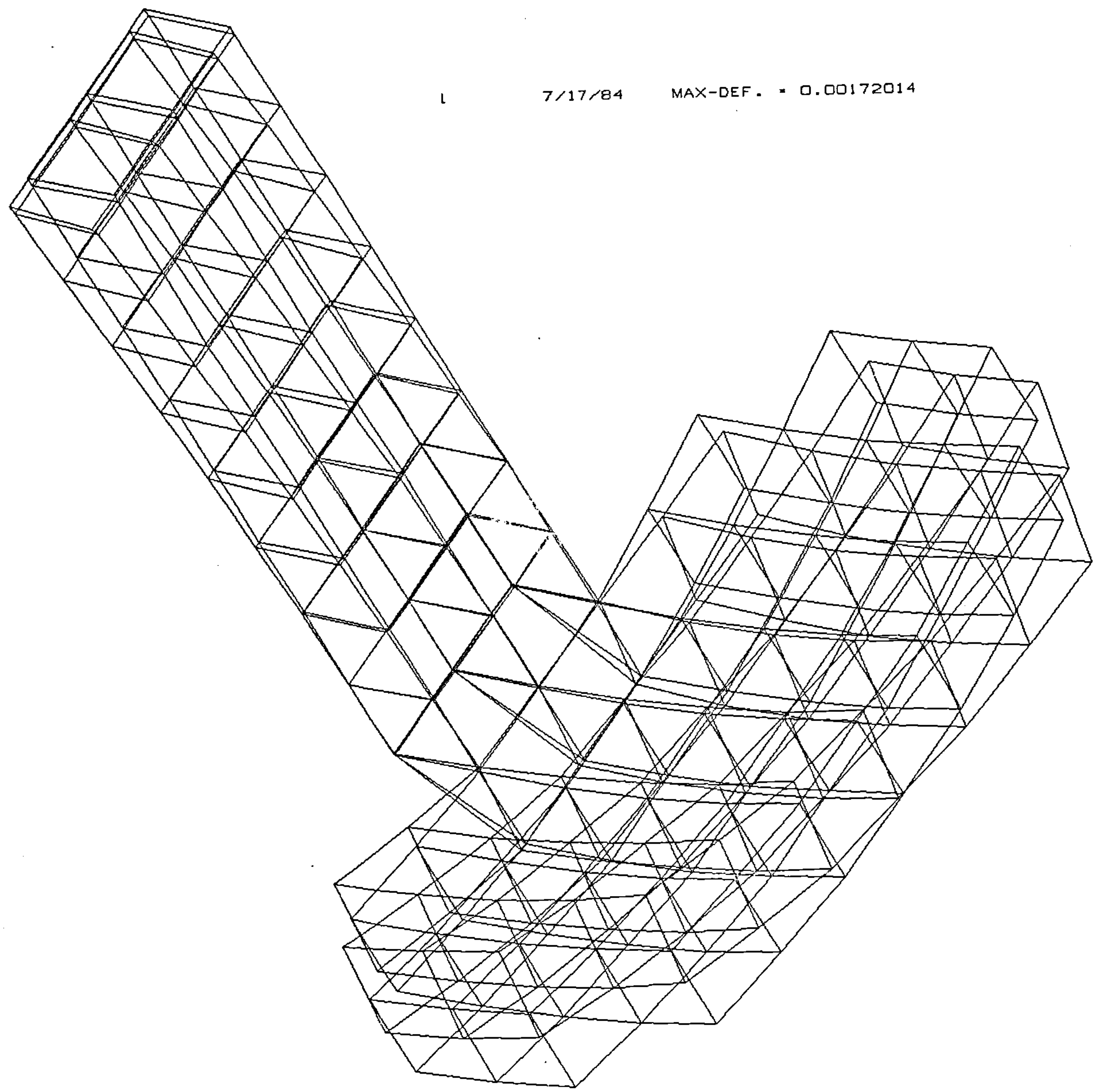

Figure 34 - EOS deformed shape at 45N/0.2% damping, 14.665° slew, case 1'.

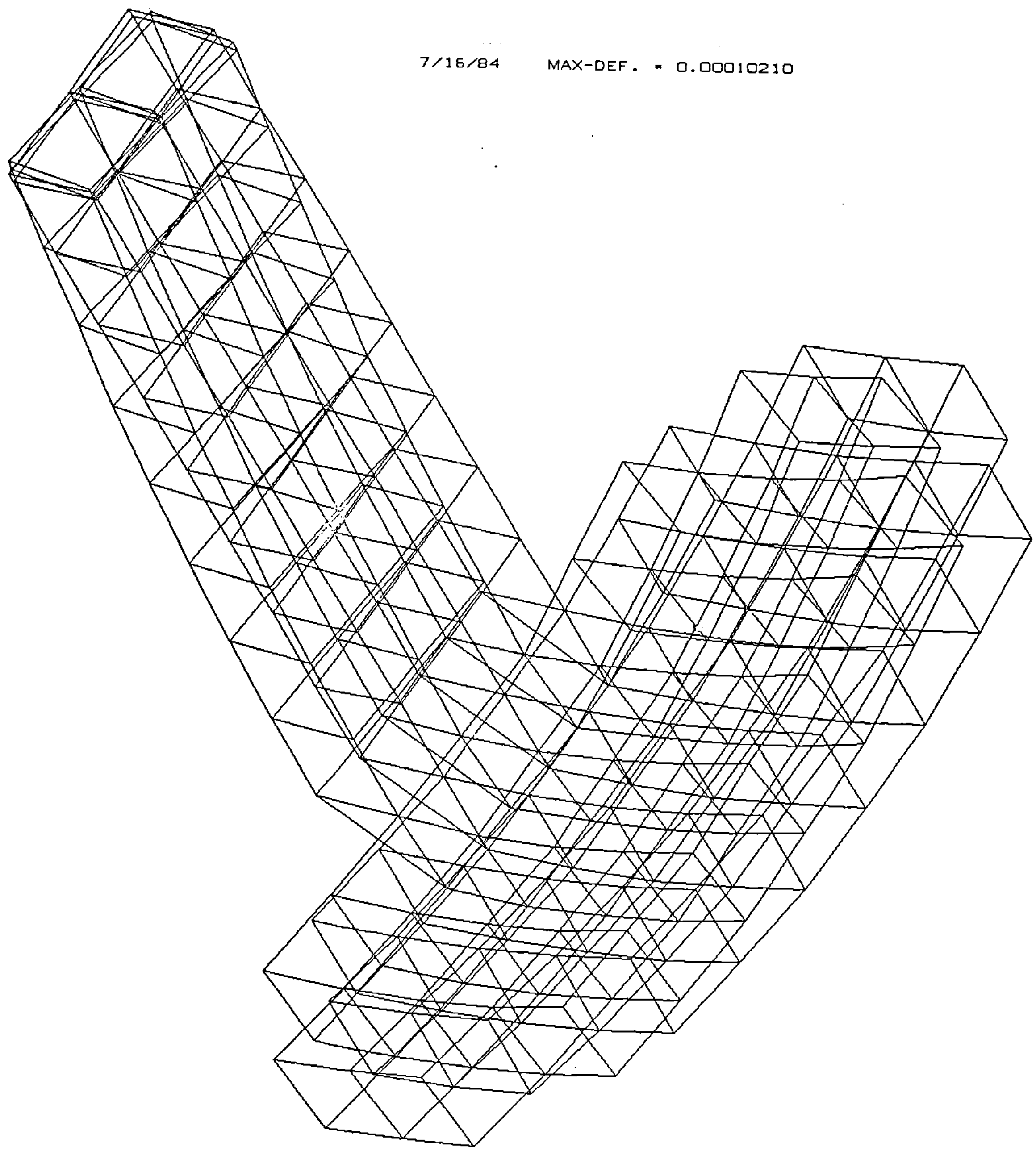

Figure 35 - EOS deformed shape at 45N/0.2% damping, 15° slew, case 1.

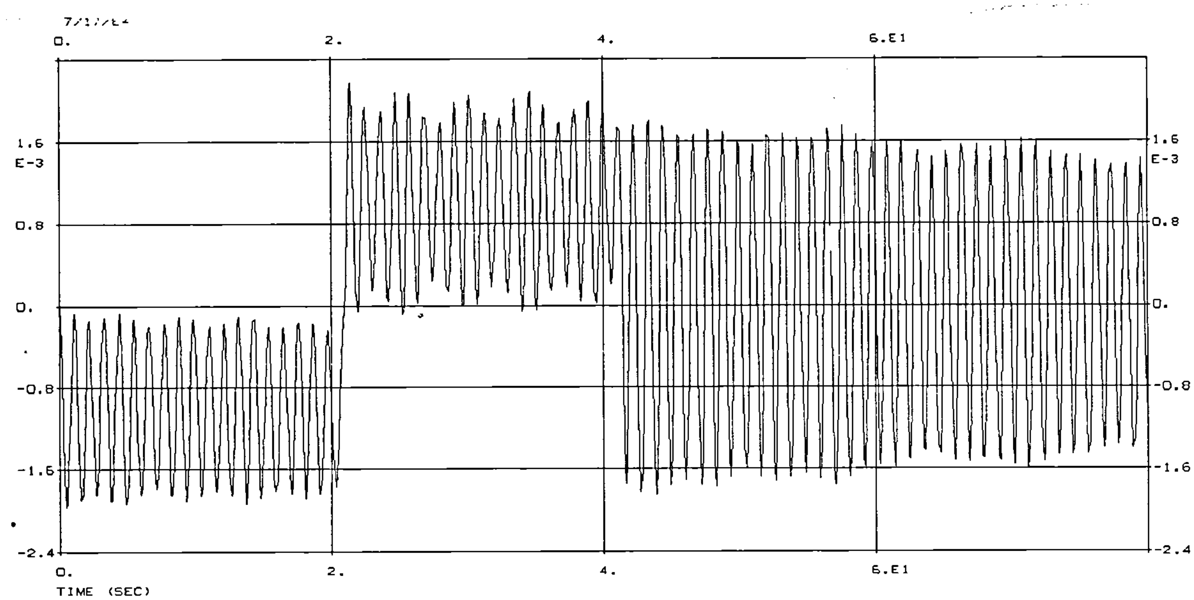

Figure 36 - Case 1´, node 106, Z displacement, 14.665˘ slew.

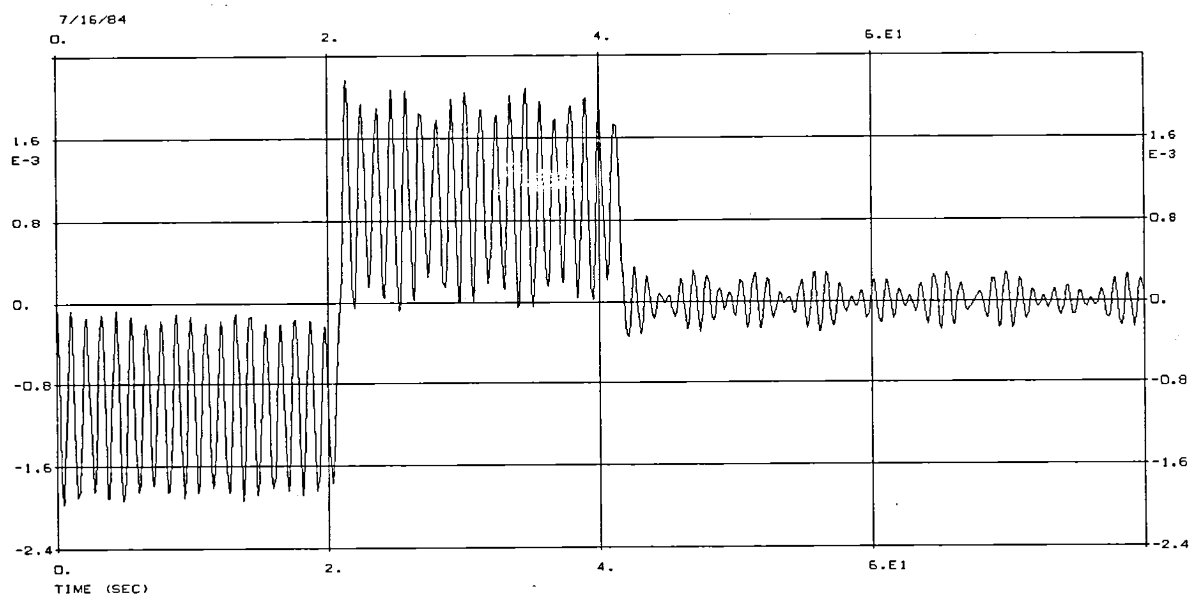

Figure 37 - Case 1, node 106, Z-displacement, 15° slew.

Obviously, the initial conditions at the beginning of settling time are strictly a function of the response frequency and the slewing period. Therefore, at any given thrust level, a slewing period can be determined, which will minimize displacements during settling time, regardless of structural damping considerations.

3.3 SYSTEM ERROR AND OPERATIONAL FITNESS ANALYSIS

The following are representative results of the system error analysis as described in Section 2.4. Table 10 shows the system errors for case 7.

TABLE 10 - SYSTEM ERROR RESULTS OF CASE 7

Case 7 thrust/damping	Time, s	Side	RMS, m	Scan, rad	Defocusing, m
120/1	49.5	1	2.078×10^{-4}	4.673×10^{-5}	-1.786×10^{-2}
		2	2.455×10^{-4}	5.023×10^{-5}	1.691×10^{-2}
	53.4	1	1.937×10^{-4}	-3.929×10^{-5}	1.569×10^{-2}
		2	2.172×10^{-4}	-4.280×10^{-5}	-1.356×10^{-2}
	62.2	1	1.517×10^{-4}	-2.881×10^{-5}	1.178×10^{-2}
		2	1.805×10^{-4}	-2.883×10^{-5}	1.260×10^{-2}
	69.9	1	1.055×10^{-4}	-2.044×10^{-5}	9.327×10^{-3}
		2	1.214×10^{-4}	-2.395×10^{-5}	-8.243×10^{-3}

As expected, the trend is that all three errors decrease with time. Table 11 shows the results of this case from the testing of operational fitness. Again, all facets are moving toward the required values with time. This trend is in concurrence with the premise of logarithmic decay for errors as well as displacements.

TABLE 11 - OPERATIONAL FITNESS RESULTS OF CASE 7

Case 7 thrust/ damping	Time, s	Side	Im tol, rad	Resolution, BWFN	Beam eff'y, %	Radiometric resolution			
						Bm scan, g/g	Ax defoc, g/g	RMS error, g/g	Total, g/g
120/1	49.5	1	4.635E-05	3.385E-03	90.11	4.730E-04	1.332	8.616E-03	1.341
		2	4.983E-05	3.240E-03	89.52	4.730E-04	1.194	1.201E-02	1.206
	53.4	1	3.898E-05	2.564E-03	90.31	4.338E-04	1.028	7.493E-03	1.035
		2	4.246E-05	2.154E-03	89.96	4.337E-01	7.676E-01	9.414E-03	7.775E-01
	62.2	1	2.858E-05	1.432E-03	90.90	3.714E-04	5.796E-01	4.600E-03	5.846E-01
		2	2.860E-05	1.595E-03	90.50	3.714E-04	6.624E-01	6.506E-03	6.693E-01
	69.9	1	2.028E-05	8.553E-04	91.48	3.128E-04	3.632E-01	2.228E-03	3.658E-01
		2	2.375E-05	7.615E-04	91.38	3.128E-04	2.837E-01	2.952E-03	2.869E-01

Table 12 lists results of system errors for all cases and their settling times.

TABLE 12 - SYSTEM ERROR RESULTS

Case	Settling time, s	RMS	Scan	Def
1	0.0	3.269×10^{-5}	$3.653.10^{-6}$	2.809×10^{-3}
1′	Did not settle in allotted time, settle time was extrapolated			
2[a]	0.0	$\sim3.2\times10^{-5}$	$\sim3.6\times10^{-6}$	$\sim2.8\times10^{-3}$
2′	32.3	5.130×10^{-5}	1.143×10^{-5}	-2.739×10^{-3}
3	0.0	3.613×10^{-5}	-8.159×10^{-6}	-1.817×10^{-3}
4	Did not settle in allotted time, settle time was extrapolated			
5	Did not settle in allotted time, settle time was extrapolated			
6	7.7	3.598×10^{-5}	-8.243×10^{-6}	-3.061×10^{-3}
7	Did not settle in allotted time, settle time was extrapolated			
8	13.6	2.842×10^{-5}	-1.138×10^{-5}	-2.314×10^{-3}

[a] System error analysis was not performed on Case 2 since Case 1 settles immediately and it is, therefore, obvious that Case 2 would also settle immediately.

Table 13 lists results of operational fitness testing. These results are derived from the equations in Section 2.1 with the use of the results in Table 12.

TABLE 13 - OPERATIONAL FITNESS RESULTS

Case	Settling time, s	Im tol, rad	Resolution, BWFN	Beam eff'y, %	Radiometric Resolution			
					Bm scan, g/g	Ax defoc, g/g	RMS error, g/g	Total, g/g
1	0.0	3.624E-06	6.553E-05	92.27	1.324E-04	3.295E-02	2.142E-04	3.330E-02
1′			Did not settle in allotted time					
2	0.0		System error analysis not performed					
2′	32.3	1.134E-05	1.038E-04	92.08	2.340E-04	3.132E-02	5.272E-04	3.208E-02
3	0.0	8.094E-06	4.802E-05	92.23	1.983E-04	1.378E-02	2.616E-04	1.424E-02
4			Did not settle in allotted time					
5			Did not settle in allotted time					
6	7.7	8.177E-06	1.008E-04	92.23	1.987E-04	3.911E-02	2.595E-04	3.957E-02
7			Did not settle in allotted time					
8	13.6	1.129E-05	8.217E-05	92.31	2.345E-04	2.236E-02	1.619E-04	2.276E-02

The following are results in tabular and graphic form of the error and operational fitness analysis, along with example calculations and explanation.

Table 14 displays the settling times of each thrust/damping case undertaken for Task 2.

TABLE 14 - VARIANCE OF SETTLING TIME WITH RESPECT TO THRUST LEVELS AND DAMPING

Case	Thrust, N	Damping, %	Settling time, s
1′	45	0.2 (14.665 deg slew)	82.0[a]
1	45	0.2	0.0
2′	45	1.0 (14.665 deg slew)	32.3
2	45	1.0	0.0
3	50	1.0	0.0
4	60	0.2	250.0[a]
5	60	1.0	55.0[a]
6	60	5.0	7.7
7	120	1.0	75.61[a]
8	120	5.0	13.6

[a]Extrapolated settling times.

Readily obvious is the fact that the settling time decreases as damping increases for a particular thrust, an expected result. This trend is graphically depicted in Figure 38.

Note that in the cases involving 50- and 45-N thrust at the normal 15-degree slew angle, regardless of damping, the settling time drops to zero second, that is, the system is operational immediately. This is due to the fact that the system has reached near zero displacement, a phenomenon that is discussed in Section 3.2.1.

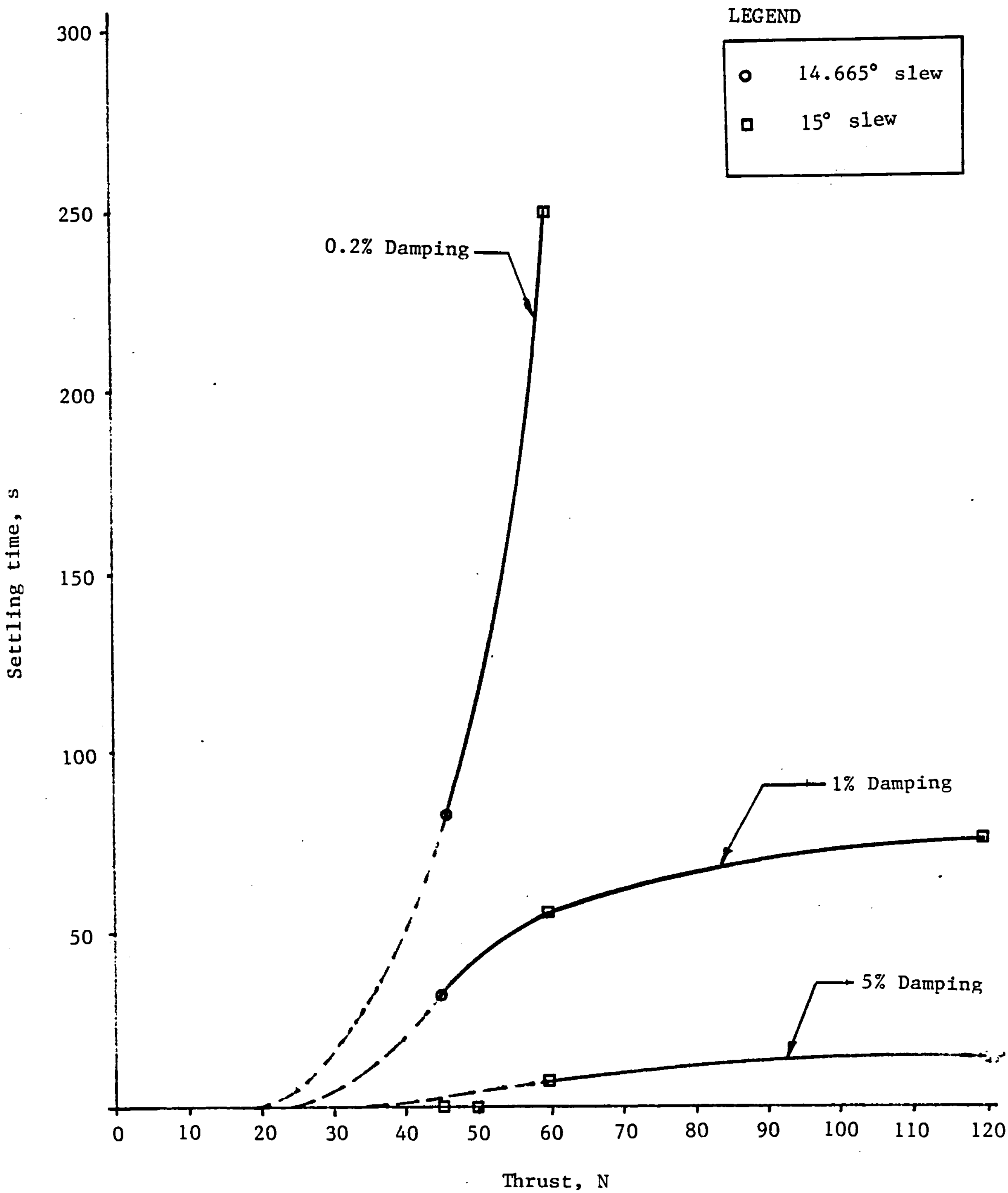

Figure 38 - Variance of settling time with respect to thrust levels and damping

3.3.1 Example Calculations

To illustrate the procedure for the testing of operational fitness, case 8 will be used as an example.

The equations used in operational fitness testing are referenced from Section 2.1. It is important to realize that all four tests on both sides must pass to ensure operational fitness.

Case 8

120 N, 5% damping

$\lambda = 0.02807$ m BDF = 0.992

D = 60 m

Time 39.1 The subscripts 1 and 2 represent sides 1 and 2 of EOS, respectively.

Data from best-fit analysis:

$RMS_1 = 2.45 \times 10^{-5}$ m

$RMS_2 = 2.84 \times 10^{-5}$ m

$\theta_{T1} = -1.149 \times 10^{-5}$ rad

$\theta_{T2} = -1.138 \times 10^{-5}$ rad

$\Delta F_1 = 2.26 \times 10^{-3}$ m

$\Delta F_2 = -2.31 \times 10^{-3}$ m

Test 1: Radiometric Resolution

Beam Scanning

From Equation [2] of Section 2.1.1

$$4.75\ (\Delta G)^4 - 26.75(\Delta G)^2 + \frac{0.992}{1.22(\frac{0.02807}{60})} \times \frac{\theta_T}{0.02807 * 116.1^2} \times \frac{1}{1 + \frac{72}{116.1^2}} = 0$$

The quadratic becomes

$$\Delta G = \sqrt{\frac{5.63157 \pm \sqrt{5.63157^2 - 4(97.189876)\theta_T}}{2}}$$

Take the smallest positive root.

$$\frac{\Delta G}{G} = \frac{1.4 \times 10^{-2}}{59.8} = 2.35 \times 10^{-4}$$

Axial Defocusing

From Equation [1] of Section 2.1.1

$$\frac{\Delta G_1}{G} = \frac{1}{12} \left(\frac{2\pi * 2.257 \times 10^{-3}}{0.02807}\right)^2 = 2.128 \times 10^{-2}$$

$$\frac{\Delta G_2}{G} = \frac{1}{12} \left(\frac{2\pi * -2.314 \times 10^{-3}}{0.02807}\right)^2 = 2.236 \times 10^{-2}$$

Surface Error

From Equation [4] of Section 2.1.1

$$\frac{\Delta G_1}{G} = 1 - e^{-\left(\frac{4\pi * 2.842 \times 10^{-5}}{0.02807}\right)^2} = 1.208 \times 10^{-4}$$

$$\frac{\Delta G_2}{G} = 1 - e^{-\left(\frac{4\pi * 2.842 \times 10^{-5}}{0.02807}\right)^2} = 1.619 \times 10^{-4}$$

Now, in summing up $\Delta G/G$ for each side,

$$\frac{\Delta G_1}{G} = 2.35 \times 10^{-4} + 2.13 \times 10^{-2} + 1.21 \times 10^{-4} = 2.17 \times 10^{-2}$$

$$\frac{\Delta G_2}{G} = 2.35 \times 10^{-4} + 2.24 \times 10^{-2} + 1.62 \times 10^{-4} = 2.28 \times 10^{-2}$$

both of which are less than the limit of 5×10^{-2}.

Test 2: Beam Efficiency

From Equation [1] of Section 2.1.2

where, from Eqn 2 of Section 2.4.1.1

$$rms_{sys} = \frac{(rms_{dyn} + 0.0439) + \sqrt{rms^2_{dyn} + 0.002774}}{2} \text{ with rms in cm.}$$

$$rms_{sys1} = \frac{(2.455 \times 10^{-3} + 0.0439) + \sqrt{(2.455 \times 10^{-3})^2 + 0.002774}}{2}$$

$$= 0.0495 \text{ cm}$$

$$rms_{sys2} = \frac{2.842 \times 10^{-3} + 0.0439 + \sqrt{(2.842 \times 10^{-3})^2 + 0.002774}}{2}$$

$$= 0.0497 \text{ cm}$$

$$BE_{sys1} = 0.97e - (\frac{4\pi * 0.0495}{2.807})^2 = 0.923 > 0.90$$

$$BE_{sys2} = 0.97e - (\frac{4\pi * 0.0497}{2.807})^2 = 0.923 > 0.90$$

Both beam efficiencies are above 90%.

Test 3: Resolution: Equations [1], [2], and [3] of Section 2.1.3

From Equations [1], [2], and [3] of Section 2.1.3

$$\Delta BWFN = \frac{1.650229}{\frac{\pi * 60 * 2}{0.02807}} m^2 = 0.000122873 \text{ m}^2$$

$$m_1 = \frac{2\pi}{0.02807}(2.455 \times 10^{-5} + 2.257 \times 10^{-3} + 1.149 \times 10^{-5} \times 116.1) = 0.80928$$

$$\Delta BWFN_1 = 0.000122873 * 0.80928^2 = 8.000 \times 10^{-5} \text{ rad}$$

$$m_2 = \frac{2\pi}{0.02807}(2.842 \times 10^{-5} + 2.314 \times 10^{-3} + 1.138 \times 10^{-5} \times 116.1) = 0.82007$$

$$\Delta BWFN_1 = 0.000122873 \times 0.82007^2 = 8.217 \times 10^{-5} \text{ rad}$$

Both ΔBWFNs are less than 1.14×10^{-4} rad.

Test 4: Image Tolerance

The image tolerance is the product of the total scan (θ_T) and the beam deviation factor.

$$\text{Im Tol}_1 = 0.992 * 1.149 \times 10^{-5} = 1.139 \times 10^{-5} \text{ rad.}$$

$$\text{Im Tol}_2 = 0.992 * 1.138 \times 10^{-5} = 1.129 \times 10^{-5} \text{ rad.}$$

both of which are less than 0.0014 radians.

It is evident that this example case is operational, because all four tests for either side were passed. It is rather simple to declare that the system becomes operationally fit at or before this chosen time. To determine the time at which system is fit, tests must be conducted on previously occurring times, until such a time is found where the system is not operational.

3.3.2 Extrapolation of Settling Time

There are times when the system does not settle in the time allotted by the transient response analysis, a settling time must be extrapolated. An example of this is case 7.

Using the results in Table 11, it is apparent that this case does not settle in its allotted time. The resolution and radiometric resolution fail to meet their requirements. By plotting ΔBWFN with time as shown in Figure 39, the logarithmic decrement can be found, as can settling time.

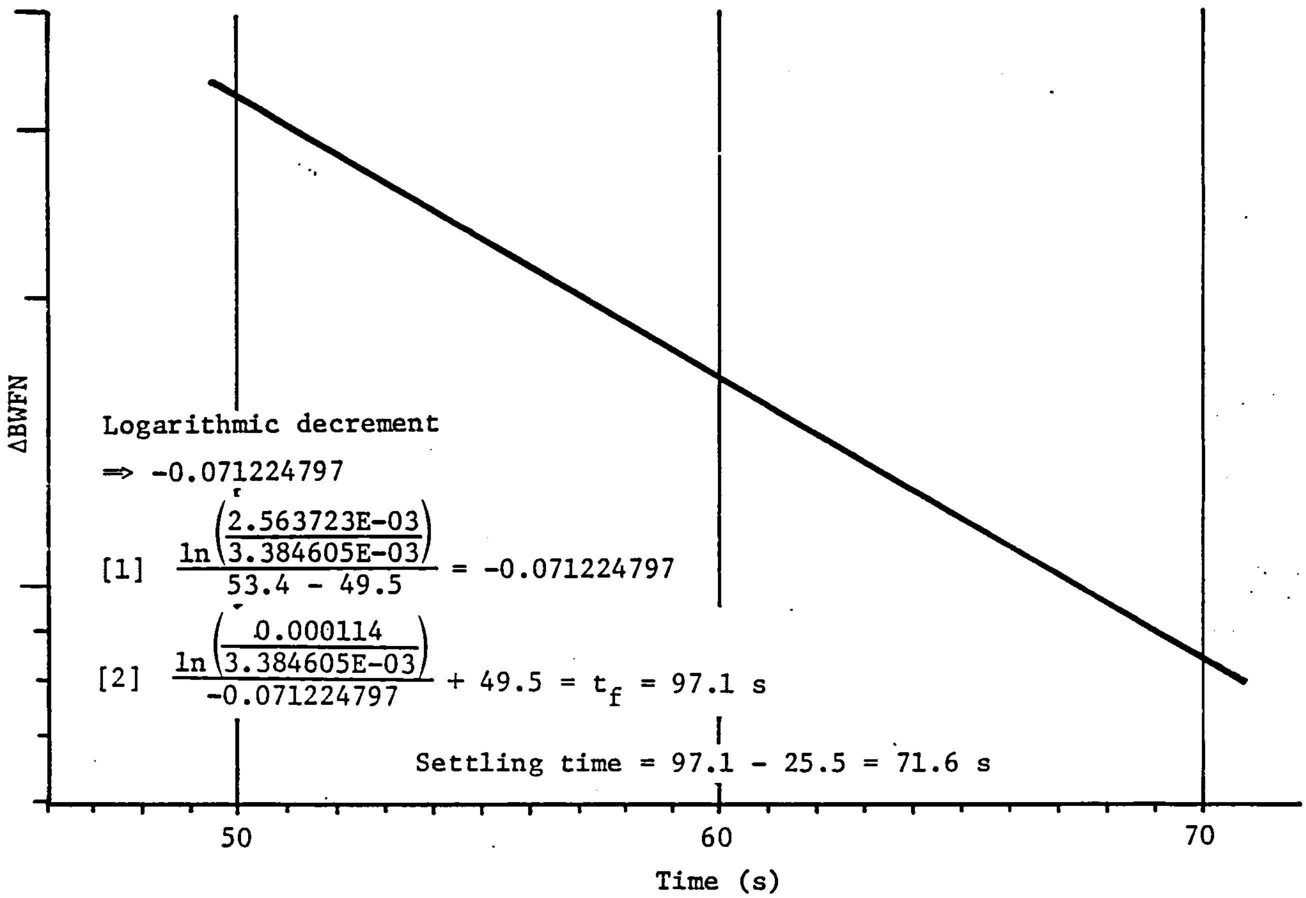

Figure 39 - Extrapolation of settling time, case 7.

3.4 SYSTEM IMPACTS

This section provides the changes to the EOS that would result if slewing capability is incorporated into the design of the spacecraft.

3.4.1 Thruster Systems for Slewing

The present design of the EOS incorporates into the spacecraft two separate thruster systems.

The first system uses monopropellant N_2H_4 for orbit transfer and uses an integral tank and fixed nozzle design located on the perimeter of the reflector structure. The second system is used for the attitude control system and consists of 12 pulsed plasma micro-thrusters. Of the two systems, the orbit transfer thruster system is the best candidate for slew maneuvers. In fact, the propellant tanks were designed to carry 1265 kg of propellant for slew, Figure 40. However, the thrusters that were incorporated into the structure have only a thrust range of 3.1 to 44.5-N. At these thrust levels, slewing would take a significantly longer time than is anticipated as being acceptable. Therefore, to provide adequate slew capability, the thrusters would have to increase in size. Also, the thrusters would have to incorporate a gimbaled nozzle system that would allow positioning of the thrust vectors to be parallel to the principal Z axis, thus eliminating any rotation about the pitch axis during slew.

For station-keeping once EOS has been slewed 15 degrees, a new set of thrusters would be required. Because the pulse plasma thrusters do not produce enough torque, only 2 N-m versus the 9.25 N-m gravity gradient torque, and the orbit transfer thrusters would provide approximately 100 times the torque required. However, this third thruster system could be avoided if the station holding requirement is held under 90 seconds.

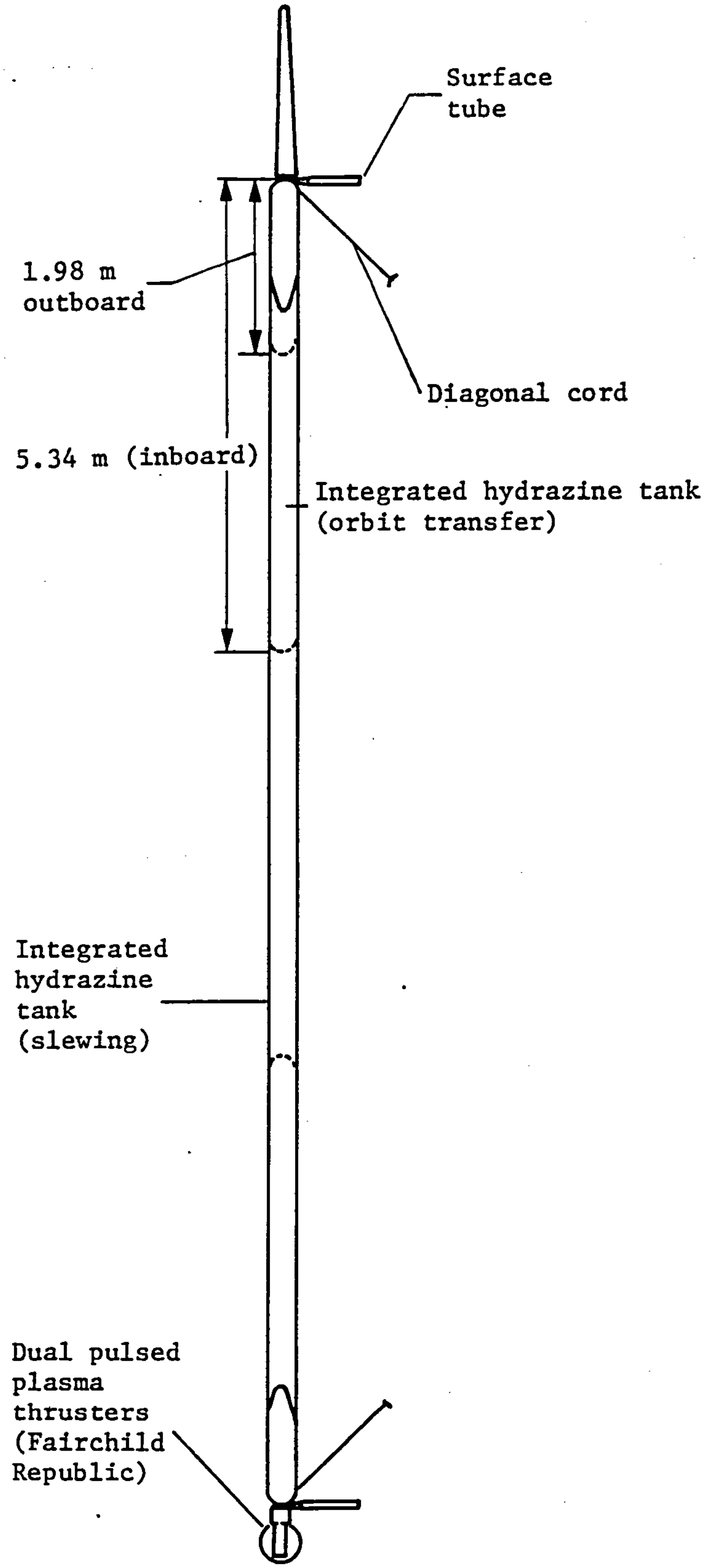

Figure 40 - Integrated hydrazine tanks.

3.4.2 Structural Impacts

Assuming that EOS would be slewed at the fastest rate studied, 15-degree slew in 25.5 seconds using four 120-N thrusters, the resulting g loading on the structure would be approximately 0.004. During the EOS study, orbit transfer requirements produced g loadings of 0.01. Therefore, there would be no significant impacts on a structural basis.

3.4.3 Weight and Complexity Impacts

Assuming the slew requirements would increase the mass of orbit transfer thrusters by approximately 20%. Table 15 shows the subsystem and structural mass summary for the EOS with and without slewing.

TABLE 15 - EOS MASS SUMMARY

Subsystem	Total w/slewing	Total w/o slewing
Feed boom system	717	717
Electronics	110	110
Atmospheric sounding radar	70	70
Mesh and tie system	297	297
Science pallet (SAR & structure)	169	169
Twin PPTs	336	336
Single PPT	176	176
Power		
- Solar panels	300	300
- Battery packs	540	540
Orbit transfer system		
- Inboard propulsion system	660	650
- Outboard propulsion system	256	236
Slewing propulsion system	1265	--
Structural system	2769	2769
Total spacecraft mass	7665	6370

TABLE 16 shows the design changes and complexity impacts on the EOS.

TABLE 16 - DESIGN CHANGES

	w/slewing	w/o slewing
Orbit transfer/slew thrusters	45N to 120N gimbaled $\pm 180°$ thrust direction	3N to 40N nongimbaled single thrust direction
Stationkeeping	Existing PPTs plus additional pair for gravity gradient torque	Existing PPTs

APPENDIX A
NASTRAN TRANSIENT RESPONSE INPUT DECK

```
EOS CONFIG 3 120MX60MX116M
 FREE-FREE TRANSIENT ANALYSIS W/SLEWING FUEL ONLY

 60N PER THRUSTER -  1% DAMPING


ID    EOS MODEL8
CHKPNT  YES
APP    DISP
TIME    500
DIAG    8,9,13,14,21,22
SOL    12,0
CEND
```

CASE CONTROL DECK ECHO

```
CARD
COUNT
  1       TITLE= EOS CONFIG 3 120MX60MX11GM
  2       SUBTITLE=  FREE-FREE TRANSIENT ANALYSIS W/SLEWING FUEL ONLY
  3       LABEL= MODEL 8 - 60N PER THRUSTER -  1% DAMPING
  4       METHOD=  6
  5       SET 1=4,6,58,60,62,64,66,68,70,72,74,76,78,80,82,84,
  6              86,88,90,92,94,96,98,100,102,104,106,108,110,112,
  7              114,116,118,120,122,124,126,128,130,132,134,136,138
 11       DLOAD = 1
 12       DISPLACEMENT = 1
 13       TSTEP = 1
 14       SDAMPING = 1
 15       MAXLINES =  100000
 16       BEGIN BULK
```

S O R T E D   B U L K   D A T A   E C H O

CARD COUNT	. 1 ..	2 ..	3 ..	4 ..	5 ..	6 ..	7 ..	8 ..	9 ..	10 .
1-	CBAR	101	1	72	90	1.0	.0	1.0	1	QC101
2-	+C101	6	6							
3-	CBAR	102	1	90	108	1.0	.0	1.0	1	QC102
4-	+C102	6	6							
5-	CBAR	103	1	88	106	1.0	.0	1.0	1	QC103
6-	+C103	6	6							
7-	CBAR	104	1	106	124	1.0	.0	1.0	1	QC104
8-	+C104	6	6							
9-	CBAR	105	1	58	74	1.0	.0	1.0	1	QC105
10-	+C105	6	6							
11-	CBAR	106	1	74	92	1.0	.0	1.0	1	QC106
12-	+C106	6	6							
13-	CBAR	107	1	92	110	1.0	.0	1.0	1	QC107
14-	+C107	6	6							
15-	CBAR	108	1	110	126	1.0	.0	1.0	1	QC108
16-	+C108	6	6							
17-	CBAR	109	1	60	76	1.0	.0	1.0	1	QC109
18-	+C109	6	6							
19-	CBAR	110	1	76	94	1.0	.0	1.0	1	QC110
20-	+C110	6	6							
21-	CBAR	111	1	94	112	1.0	.0	1.0	1	QC111
22-	+C111	6	6							
23-	CBAR	112	1	112	128	1.0	.0	1.0	1	QC112
24-	+C112	6	6							
25-	CBAR	113	51	62	78	1.0	.0	1.0	1	QC113
26-	+C113	6	6							
27-	CBAR	114	1	78	96	1.0	.0	1.0	1	QC114
28-	+C114	6	6							
29-	CBAR	115	1	96	114	1.0	.0	1.0	1	QC115
30-	+C115	6	6							
31-	CBAR	116	1	114	130	1.0	.0	1.0	1	QC116
32-	+C116	6	6							
33-	CBAR	117	51	64	80	1.0	.0	1.0	1	QC117
34-	+C117	6	6							
35-	CBAR	118	1	80	98	1.0	.0	1.0	1	QC118
36-	+C118	6	6							
37-	CBAR	119	1	98	116	1.0	.0	1.0	1	QC119
38-	+C119	6	6							
39-	CBAR	120	1	116	132	1.0	.0	1.0	1	QC120
40-	+C120	6	6							
41-	CBAR	121	51	66	82	1.0	.0	1.0	1	QC121
42-	+C121	6	6							
43-	CBAR	122	1	82	100	1.0	.0	1.0	1	QC122
44-	+C122	6	6							
45-	CBAR	123	1	100	118	1.0	.0	1.0	1	QC123
46-	+C123	6	6							
47-	CBAR	124	1	118	134	1.0	.0	1.0	1	QC124
48-	+C124	6	6							
49-	CBAR	125	1	68	84	1.0	.0	1.0	1	QC125
50-	+C125	6	6							

S O R T E D   B U L K   D A T A   E C H O

CARD COUNT	. 1 ..	2 ..	3 ..	4 ..	5 ..	6 ..	7 ..	8 ..	9 ..	10 .
51-	CBAR	126	1	84	102	1.0	.0	1.0	1	QC126
52-	+C126	6	6							
53-	CBAR	127	1	102	120	1.0	.0	1.0	1	QC127
54-	+C127	6	6							
55-	CBAR	128	1	120	136	1.0	.0	1.0	1	QC128
56-	+C128	6	6							
57-	CBAR	129	1	70	86	1.0	.0	1.0	1	QC129
58-	+C129	6	6							
59-	CBAR	130	1	86	104	1.0	.0	1.0	1	QC130
60-	+C130	6	6							
61-	CBAR	131	1	104	122	1.0	.0	1.0	1	QC131
62-	+C131	6	6							
63-	CBAR	132	1	122	138	1.0	.0	1.0	1	QC132
64-	+C132	6	6							
65-	CBAR	133	1	58	60	.0	1.0	1.0	1	QC133
66-	+C133	6	6							
67-	CBAR	134	1	60	62	.0	1.0	1.0	1	QC134
68-	+C134	6	6							
69-	CBAR	135	1	62	64	.0	1.0	1.0	1	QC135
70-	+C135	6	6							
71-	CBAR	136	1	64	66	.0	1.0	1.0	1	QC136
72-	+C136	6	6							
73-	CBAR	137	1	66	68	.0	1.0	1.0	1	QC137
74-	+C137	6	6							
75-	CBAR	138	1	68	70	.0	1.0	1.0	1	QC138
76-	+C138	6	6							
77-	CBAR	139	1	126	128	.0	1.0	1.0	1	QC139
78-	+C139	6	6							
79-	CBAR	140	1	128	130	.0	1.0	1.0	1	QC140
80-	+C140	6	6							
81-	CBAR	141	1	130	132	.0	1.0	1.0	1	QC141
82-	+C141	6	6							
83-	CBAR	142	1	132	134	.0	1.0	1.0	1	QC142
84-	+C142	6	6							
85-	CBAR	143	1	134	136	.0	1.0	1.0	1	QC143
86-	+C143	6	6							
87-	CBAR	144	1	136	138	.0	1.0	1.0	1	QC144
88-	+C144	6	6							
89-	CBAR	145	1	74	76	.0	1.0	1.0	1	QC145
90-	+C145	6	6							
91-	CBAR	146	1	76	78	.0	1.0	1.0	1	QC146
92-	+C146	6	6							
93-	CBAR	147	1	78	80	.0	1.0	1.0	1	QC147
94-	+C147	6	6							
95-	CBAR	148	1	80	82	.0	1.0	1.0	1	QC148
96-	+C148	6	6							
97-	CBAR	149	1	82	84	.0	1.0	1.0	1	QC149
98-	+C149	6	6							
99-	CBAR	150	1	84	86	.0	1.0	1.0	1	QC150
100-	+C150	6	6							

S O R T E D   B U L K   D A T A   E C H O

CARD COUNT	. 1 ..	2 ..	3 ..	4 ..	5 ..	6 ..	7 ..	8 ..	9 ..	10 .
101-	CBAR	151	1	92	94	.0	1.0	1.0	1	QC151
102-	+C151	6	6							
103-	CBAR	152	1	94	96	.0	1.0	1.0	1	QC152
104-	+C152	6	6							
105-	CBAR	153	1	96	98	.0	1.0	1.0	1	QC153
106-	+C153	6	6							
107-	CBAR	154	1	98	100	.0	1.0	1.0	1	QC154
108-	+C154	6	6							
109-	CBAR	155	1	100	102	.0	1.0	1.0	1	QC155
110-	+C155	6	6							
111-	CBAR	156	1	102	104	.0	1.0	1.0	1	QC156
112-	+C156	6	6							
113-	CBAR	157	1	110	112	.0	1.0	1.0	1	QC157
114-	+C157	6	6							
115-	CBAR	158	1	112	114	.0	1.0	1.0	1	QC158
116-	+C158	6	6							
117-	CBAR	159	1	114	116	.0	1.0	1.0	1	QC159
118-	+C159	6	6							
119-	CBAR	160	1	116	118	.0	1.0	1.0	1	QC160
120-	+C160	6	6							
121-	CBAR	161	1	118	120	.0	1.0	1.0	1	QC161
122-	+C161	6	6							
123-	CBAR	162	1	120	122	.0	1.0	1.0	1	QC162
124-	+C162	6	6							
125-	CBAR	163	1	72	74	.0	1.0	1.0	1	QC163
126-	+C163	6	6							
127-	CBAR	164	1	90	92	.0	1.0	1.0	1	QC164
128-	+C164	6	6							
129-	CBAR	165	1	108	110	.0	1.0	1.0	1	QC165
130-	+C165	6	6							
131-	CBAR	166	1	86	88	.0	1.0	1.0	1	QC166
132-	+C166	6	6							
133-	CBAR	167	1	104	106	.0	1.0	1.0	1	QC167
134-	+C167	6	6							
135-	CBAR	168	1	122	124	.0	1.0	1.0	1	QC168
136-	+C168	6	6							
137-	CBAR	169	1	73	91	1.0	.0	1.0	1	QC169
138-	+C169	6	6							
139-	CBAR	170	1	91	109	1.0	.0	1.0	1	QC170
140-	+C170	6	6							
141-	CBAR	171	1	89	107	1.0	.0	1.0	1	QC171
142-	+C171	6	6							
143-	CBAR	172	1	107	125	1.0	.0	1.0	1	QC172
144-	+C172	6	6							
145-	CBAR	173	1	59	75	1.0	.0	1.0	1	QC173
146-	+C173	6	6							
147-	CBAR	174	1	75	93	1.0	.0	1.0	1	QC174
148-	+C174	6	6							
149-	CBAR	175	1	93	111	1.0	.0	1.0	1	QC175
150-	+C175	6	6							

S O R T E D   B U L K   D A T A   E C H O

CARD COUNT	. 1 ..	2 ..	3 ..	4 ..	5 ..	6 ..	7 ..	8 ..	9 ..	10 .
151-	CBAR	176	1	111	127	1.0	.0	1.0	1	QC176
152-	+C176	6	6							
153-	CBAR	177	1	61	77	1.0	.0	1.0	1	QC177
154-	+C177	6	6							
155-	CBAR	178	1	77	95	1.0	.0	1.0	1	QC178
156-	+C178	6	6							
157-	CBAR	179	1	95	113	1.0	.0	1.0	1	QC179
158-	+C179	6	6							
159-	CBAR	180	1	113	129	1.0	.0	1.0	1	QC180
160-	+C180	6	6							
161-	CBAR	181	51	63	79	1.0	.0	1.0	1	QC181
162-	+C181	6	6							
163-	CBAR	182	1	79	97	1.0	.0	1.0	1	QC182
164-	+C182	6	6							
165-	CBAR	183	1	97	115	1.0	.0	1.0	1	QC183
166-	+C183	6	6							
167-	CBAR	184	1	115	131	1.0	.0	1.0	1	QC184
168-	+C184	6	6							
169-	CBAR	185	51	65	81	1.0	.0	1.0	1	QC185
170-	+C185	6	6							
171-	CBAR	186	1	81	99	1.0	.0	1.0	1	QC186
172-	+C186	6	6							
173-	CBAR	187	1	99	117	1.0	.0	1.0	1	QC187
174-	+C187	6	6							
175-	CBAR	188	1	117	133	1.0	.0	1.0	1	QC188
176-	+C188	6	6							
177-	CBAR	189	51	67	83	1.0	.0	1.0	1	QC189
178-	+C189	6	6							
179-	CBAR	190	1	83	101	1.0	.0	1.0	1	QC190
180-	+C190	6	6							
181-	CBAR	191	1	101	119	1.0	.0	1.0	1	QC191
182-	+C191	6	6							
183-	CBAR	192	1	119	135	1.0	.0	1.0	1	QC192
184-	+C192	6	6							
185-	CBAR	193	1	69	85	1.0	.0	1.0	1	QC193
186-	+C193	6	6							
187-	CBAR	194	1	85	103	1.0	.0	1.0	1	QC194
188-	+C194	6	6							
189-	CBAR	195	1	103	121	1.0	.0	1.0	1	QC195
190-	+C195	6	6							
191-	CBAR	196	1	121	137	1.0	.0	1.0	1	QC196
192-	+C196	6	6							
193	CBAR	197	1	71	87	1.0	.0	1.0	1	QC197
194-	+C197	6	6							
195-	CBAR	198	1	87	105	1.0	.0	1.0	1	QC198
196-	+C198	6	6							
197-	CBAR	199	1	105	123	1.0	.0	1.0	1	QC199
198-	+C199	6	6							
199-	CBAR	200	1	123	139	1.0	.0	1.0	1	QC200
200-	+C200	6	6							

S O R T E D   B U L K   D A T A   E C H O

CARD COUNT	. 1 ..	2 ..	3 ..	4 ..	5 ..	6 ..	7 ..	8 ..	9 ..	10 .
201-	CBAR	201	1	59	61	.0	1.0	1.0	1	QC201
202-	+C201	6	6							
203-	CBAR	202	1	61	63	.0	1.0	1.0	1	QC202
204-	+C202	6	6							
205-	CBAR	203	1	63	65	.0	1.0	1.0	1	QC203
206-	+C203	6	6							
207-	CBAR	204	1	65	67	.0	1.0	1.0	1	QC204
208-	+C204	6	6							
209-	CBAR	205	1	67	69	.0	1.0	1.0	1	QC205
210-	+C205	6	6							
211-	CBAR	206	1	69	71	.0	1.0	1.0	1	QC206
212-	+C206	6	6							
213-	CBAR	207	1	127	129	.0	1.0	1.0	1	QC207
214-	+C207	6	6							
215-	CBAR	208	1	129	131	.0	1.0	1.0	1	QC208
216-	+C208	6	6							
217-	CBAR	209	1	131	133	.0	1.0	1.0	1	QC209
218-	+C209	6	6							
219-	CBAR	210	1	133	135	.0	1.0	1.0	1	QC210
220-	+C210	6	6							
221-	CBAR	211	1	135	137	.0	1.0	1.0	1	QC211
222-	+C211	6	6							
223-	CBAR	212	1	137	139	.0	1.0	1.0	1	QC212
224-	+C212	6	6							
225-	CBAR	213	1	75	77	.0	1.0	1.0	1	QC213
226-	+C213	6	6							
227-	CBAR	214	1	77	79	.0	1.0	1.0	1	QC214
228-	+C214	6	6							
229-	CBAR	215	1	79	81	.0	1.0	1.0	1	QC215
230-	+C215	6	6							
231-	CBAR	216	1	81	83	.0	1.0	1.0	1	QC216
232-	+C216	6	6							
233-	CBAR	217	1	83	85	.0	1.0	1.0	1	QC217
234-	+C217	6	6							
235-	CBAR	218	1	85	87	.0	1.0	1.0	1	QC218
236-	+C218	6	6							
237-	CBAR	219	1	93	95	.0	1.0	1.0	1	QC219
238-	+C219	6	6							
239-	CBAR	220	1	95	97	.0	1.0	1.0	1	QC220
240-	+C220	6	6							
241-	CBAR	221	1	97	99	.0	1.0	1.0	1	QC221
242-	+C221	6	6							
243-	CBAR	222	1	99	101	.0	1.0	1.0	1	QC222
244-	+C222	6	6							
245-	CBAR	223	1	101	103	.0	1.0	1.0	1	QC223
246-	+C223	6	6							
247-	CBAR	224	1	103	105	.0	1.0	1.0	1	QC224
248-	+C224	6	6							
249-	CBAR	225	1	111	113	.0	1.0	1.0	1	QC225
250-	+C225	6	6							

S O R T E D   B U L K   D A T A   E C H O

CARD COUNT	. 1 ..	2 ..	3 ..	4 ..	5 ..	6 ..	7 ..	8 ..	9 ..	10 .
251-	CBAR	226	1	113	115	.0	1.0	1.0	1	QC226
252-	+C226	6	6							
253-	CBAR	227	1	115	117	.0	1.0	1.0	1	QC227
254-	+C227	6	6							
255-	CBAR	228	1	117	119	.0	1.0	1.0	1	QC228
256-	+C228	6	6							
257-	CBAR	229	1	119	121	.0	1.0	1.0	1	QC229
258-	+C229	6	6							
259-	CBAR	230	1	121	123	.0	1.0	1.0	1	QC230
260-	+C230	6	6							
261-	CBAR	231	1	73	75	.0	1.0	1.0	1	QC231
262-	+C231	6	6							
263-	CBAR	232	1	91	93	.0	1.0	1.0	1	QC232
264-	+C232	6	6							
265-	CBAR	233	1	109	111	.0	1.0	1.0	1	QC233
266-	+C233	6	6							
267-	CBAR	234	1	87	89	.0	1.0	1.0	1	QC234
268-	+C234	6	6							
269-	CBAR	235	1	105	107	.0	1.0	1.0	1	QC235
270-	+C235	6	6							
271-	CBAR	236	1	123	125	.0	1.0	1.0	1	QC236
272-	+C236	6	6							
273-	CBAR	237	51	55	56	1.0	1.0	.0	1	QC237
274-	+C237	6	6							
275-	CBAR	238	51	56	57	1.0	1.0	.0	1	QC238
276-	+C238	6	6							
277-	CBAR	239	51	62	52	-1.0	.0	1.0	1	QC239
278-	+C239	6	6							
279-	CBAR	240	51	64	53	-1.0	.0	1.0	1	QC240
280-	+C240	6	6							
281-	CBAR	241	51	66	54	-1.0	.0	1.0	1	QC241
282-	+C241	6	6							
283-	CBAR	242	51	55	49	-1.0	.0	1.0	1	QC242
284-	+C242	6	6							
285-	CBAR	243	51	56	50	-1.0	.0	1.0	1	QC243
286-	+C243	6	6							
287-	CBAR	244	51	57	51	-1.0	.0	1.0	1	QC244
288-	+C244	6	6							
289-	CBAR	245	51	52	46	-1.0	.0	1.0	1	QC245
290-	+C245	6	6							
291-	CBAR	246	51	53	47	-1.0	.0	1.0	1	QC246
292-	+C246	6	6							
293-	CBAR	247	51	54	48	-1.0	.0	1.0	1	QC247
294-	+C247	6	6							
295-	CBAR	248	51	49	43	-1.0	.0	1.0	1	QC248
296-	+C248	6	6							
297-	CBAR	249	51	50	44	-1.0	.0	1.0	1	QC249
298-	+C249	6	6							
299-	CBAR	250	51	51	45	-1.0	.0	1.0	1	QC250
300-	+C250	6	6							

S O R T E D   B U L K   D A T A   E C H O

CARD COUNT	. 1 ..	2 ..	3 ..	4 ..	5 ..	6 ..	7 ..	8 ..	9 ..	10 .
301-	CBAR	251	1	46	40	-1.0	.0	1.0	1	QC251
302-	+C251	6	6							
303-	CBAR	252	1	47	41	-1.0	.0	1.0	1	QC252
304-	+C252	6	6							
305-	CBAR	253	1	48	42	-1.0	.0	1.0	1	QC253
306-	+C253	6	6							
307-	CBAR	254	1	43	37	-1.0	.0	1.0	1	QC254
308-	+C254	6	6							
309-	CBAR	255	1	44	38	-1.0	.0	1.0	1	QC255
310-	+C255	6	6							
311-	CBAR	256	1	45	39	-1.0	.0	1.0	1	QC256
312-	+C256	6	6							
313-	CBAR	257	1	40	34	-1.0	.0	1.0	1	QC257
314-	+C257	6	6							
315-	CBAR	258	1	41	35	-1.0	.0	1.0	1	QC258
316-	+C258	6	6							
317-	CBAR	259	1	42	36	-1.0	.0	1.0	1	QC259
318-	+C259	6	6							
319-	CBAR	260	1	37	31	-1.0	.0	1.0	1	QC260
320-	+C260	6	6							
321-	CBAR	261	1	38	32	-1.0	.0	1.0	1	QC261
322-	+C261	6	6							
323-	CBAR	262	1	39	33	-1.0	.0	1.0	1	QC262
324-	+C262	6	6							
325-	CBAR	263	1	34	28	-1.0	.0	1.0	1	QC263
326-	+C263	6	6							
327-	CBAR	264	1	35	29	-1.0	.0	1.0	1	QC264
328-	+C264	6	6							
329-	CBAR	265	1	36	30	-1.0	.0	1.0	1	QC265
330-	+C265	6	6							
331-	CBAR	266	1	31	25	-1.0	.0	1.0	1	QC266
332-	+C266	6	6							
333-	CBAR	267	1	32	26	-1.0	.0	1.0	1	QC267
334-	+C267	6	6							
335-	CBAR	268	1	33	27	-1.0	.0	1.0	1	QC268
336-	+C268	6	6							
337-	CBAR	269	1	28	22	-1.0	.0	1.0	1	QC269
338-	+C269	6	6							
339-	CBAR	270	1	29	23	-1.0	.0	1.0	1	QC270
340-	+C270	6	6							
341-	CBAR	271	1	30	24	-1.0	.0	1.0	1	QC271
342-	+C271	6	6							
343-	CBAR	272	1	25	19	-1.0	.0	1.0	1	QC272
344-	+C272	6	6							
345-	CBAR	273	1	26	20	-1.0	.0	1.0	1	QC273
346-	+C273	6	6							
347-	CBAR	274	1	27	21	-1.0	.0	1.0	1	QC274
348-	+C274	6	6							
349-	CBAR	275	1	22	16	-1.0	.0	1.0	1	QC275
350-	+C275	6	6							

S O R T E D   B U L K   D A T A   E C H O

CARD COUNT	. 1 ..	2 ..	3 ..	4 ..	5 ..	6 ..	7 ..	8 ..	9 ..	10 .
351-	CBAR	276	1	23	17	-1.0	.0	1.0	1	QC276
352-	+C276	6	6							
353-	CBAR	277	1	24	18	-1.0	.0	1.0	1	QC277
354-	+C277	6	6							
355-	CBAR	278	1	19	13	-1.0	.0	1.0	1	QC278
356-	+C278	6	6							
357-	CBAR	279	1	20	14	-1.0	.0	1.0	1	QC279
358-	+C279	6	6							
359-	CBAR	280	1	21	15	-1.0	.0	1.0	1	QC280
360-	+C280	6	6							
361-	CBAR	281	1	16	10	-1.0	.0	1.0	1	QC281
362-	+C281	6	6							
363-	CBAR	282	1	17	11	-1.0	.0	1.0	1	QC282
364-	+C282	6	6							
365-	CBAR	283	1	18	12	-1.0	.0	1.0	1	QC283
366-	+C283	6	6							
367-	CBAR	284	1	13	7	-1.0	.0	1.0	1	QC284
368-	+C284	6	6							
369-	CBAR	285	1	14	8	-1.0	.0	1.0	1	QC285
370-	+C285	6	6							
371-	CBAR	286	1	15	9	-1.0	.0	1.0	1	QC286
372-	+C286	6	6							
373-	CBAR	287	1	52	53	1.0	1.0	.0	1	QC287
374-	+C287	6	6							
375-	CBAR	288	1	53	54	1.0	1.0	.0	1	QC288
376-	+C288	6	6							
377-	CBAR	289	1	49	50	1.0	1.0	.0	1	QC289
378-	+C289	6	6							
379-	CBAR	290	1	50	51	1.0	1.0	.0	1	QC290
380-	+C290	6	6							
381-	CBAR	291	1	46	47	1.0	1.0	.0	1	QC291
382-	+C291	6	6							
383-	CBAR	292	1	47	48	1.0	1.0	.0	1	QC292
384-	+C292	6	6							
385-	CBAR	293	1	43	44	1.0	1.0	.0	1	QC293
386-	+C293	6	6							
387-	CBAR	294	1	44	45	1.0	1.0	.0	1	QC294
388-	+C294	6	6							
389-	CBAR	295	1	40	41	1.0	1.0	.0	1	QC295
390-	+C295	6	6							
391-	CBAR	296	1	41	42	1.0	1.0	.0	1	QC296
392-	+C296	6	6							
393-	CBAR	297	1	37	38	1.0	1.0	.0	1	QC297
394-	+C297	6	6							
395-	CBAR	298	1	38	39	1.0	1.0	.0	1	QC298
396-	+C298	6	6							
397-	CBAR	299	1	34	35	1.0	1.0	.0	1	QC299
398-	+C299	6	6							
399-	CBAR	300	1	35	36	1.0	1.0	.0	1	QC300
400-	+C300	6	6							

S O R T E D   B U L K   D A T A   E C H O

CARD COUNT	. 1 ..	2 ..	3 ..	4 ..	5 ..	6 ..	7 ..	8 ..	9 ..	10 .
401-	CBAR	301	1	31	32	1.0	1.0	.0	1	QC301
402-	+C301	6	6							
403-	CBAR	302	1	32	33	1.0	1.0	.0	1	QC302
404-	+C302	6	6							
405-	CBAR	303	1	28	29	1.0	1.0	.0	1	QC303
406-	+C303	6	6							
407-	CBAR	304	1	29	30	1.0	1.0	.0	1	QC304
408-	+C304	6	6							
409-	CBAR	305	1	25	26	1.0	1.0	.0	1	QC305
410-	+C305	6	6							
411-	CBAR	306	1	26	27	1.0	1.0	.0	1	QC306
412-	+C306	6	6							
413-	CBAR	307	1	22	23	1.0	1.0	.0	1	QC307
414-	+C307	6	6							
415-	CBAR	308	1	23	24	1.0	1.0	.0	1	QC308
416-	+C308	6	6							
417-	CBAR	309	1	19	20	1.0	1.0	.0	1	QC309
418-	+C309	6	6							
419-	CBAR	310	1	20	21	1.0	1.0	.0	1	QC310
420-	+C310	6	6							
421-	CBAR	311	1	16	17	1.0	1.0	.0	1	QC311
422-	+C311	6	6							
423-	CBAR	312	1	17	18	1.0	1.0	.0	1	QC312
424-	+C312	6	6							
425-	CBAR	313	1	13	14	1.0	1.0	.0	1	QC313
426-	+C313	6	6							
427-	CBAR	314	1	14	15	1.0	1.0	.0	1	QC314
428-	+C314	6	6							
429-	CBAR	315	21	10	11	1.0	1.0	.0	1	QC315
430-	+C315	6	6							
431-	CBAR	316	21	11	12	1.0	1.0	.0	1	QC316
432-	+C316	6	6							
433-	CBAR	317	1	7	8	1.0	1.0	.0	1	QC317
434-	+C317	6	6							
435-	CBAR	318	1	8	9	1.0	1.0	.0	1	QC318
436-	+C318	6	6							
437-	CBAR	319	1	10	4	-1.0	.0	1.0	1	QC319
438-	+C319	6	6							
439-	CBAR	320	1	11	5	-1.0	.0	1.0	1	QC320
440-	+C320	6	6							
441-	CBAR	321	1	12	6	-1.0	.0	1.0	1	QC321
442-	+C321	6	6							
443-	CBAR	322	1	7	1	-1.0	.0	1.0	1	QC322
444-	+C322	6	6							
445-	CBAR	323	1	8	2	-1.0	.0	1.0	1	QC323
446-	+C323	6	6							
447-	CBAR	324	1	9	3	-1.0	.0	1.0	1	QC324
448-	+C324	6	6							
449-	CBAR	325	21	4	5	1.0	1.0	.0	1	QC325
450-	+C325	6	6							

SORTED BULK DATA ECHO

CARD COUNT	. 1 ..	2 ..	3 ..	4 ..	5 ..	6 ..	7 ..	8 ..	9 ..	10 .
451-	CBAR	326	21	5	6	1.0	1.0	.0	1	QC326
452-	+C326	6	6							
453-	CBAR	327	1	1	2	1.0	1.0	.0	1	QC327
454-	+C327	6	6							
455-	CBAR	328	1	2	3	1.0	1.0	.0	1	QC328
456-	+C328	6	6							
457-	CBAR	401	20	72	73	1.0	.0	-1.0	1	
458-	CBAR	402	2	90	91	1.0	.0	-1.0	1	
459-	CBAR	403	20	108	109	1.0	.0	-1.0	1	
460-	CBAR	404	20	88	89	1.0	.0	-1.0	1	
461-	CBAR	405	2	106	107	1.0	.0	-1.0	1	
462-	CBAR	406	20	124	125	1.0	.0	-1.0	1	
463-	CBAR	407	2	74	75	1.0	.0	-1.0	1	
464-	CBAR	408	2	76	77	1.0	.0	-1.0	1	
465-	CBAR	409	2	78	79	1.0	.0	-1.0	1	
466-	CBAR	410	2	80	81	1.0	.0	-1.0	1	
467-	CBAR	411	2	82	83	1.0	.0	-1.0	1	
468-	CBAR	412	2	84	85	1.0	.0	-1.0	1	
469-	CBAR	413	2	86	87	1.0	.0	-1.0	1	
470-	CBAR	414	2	92	93	1.0	.0	-1.0	1	
471-	CBAR	415	2	94	95	1.0	.0	-1.0	1	
472-	CBAR	416	2	96	97	1.0	.0	-1.0	1	
473-	CBAR	417	2	98	99	1.0	.0	-1.0	1	
474-	CBAR	418	2	100	101	1.0	.0	-1.0	1	
475-	CBAR	419	2	102	103	1.0	.0	-1.0	1	
476-	CBAR	420	2	104	105	1.0	.0	-1.0	1	
477-	CBAR	421	2	110	111	1.0	.0	-1.0	1	
478-	CBAR	422	2	112	113	1.0	.0	-1.0	1	
479-	CBAR	423	2	114	115	1.0	.0	-1.0	1	
480-	CBAR	424	2	116	117	1.0	.0	-1.0	1	
481-	CBAR	425	2	118	119	1.0	.0	-1.0	1	
482-	CBAR	426	2	120	121	1.0	.0	-1.0	1	
483-	CBAR	427	2	122	123	1.0	.0	-1.0	1	
484-	CBAR	428	25	126	127	1.0	.0	-1.0	1	
485-	CBAR	429	2	128	129	1.0	.0	-1.0	1	
486-	CBAR	430	2	130	131	1.0	.0	-1.0	1	
487-	CBAR	431	2	132	133	1.0	.0	-1.0	1	
488-	CBAR	432	2	134	135	1.0	.0	-1.0	1	
489-	CBAR	433	2	136	137	1.0	.0	-1.0	1	
490-	CBAR	434	25	138	139	1.0	.0	-1.0	1	
491-	CBAR	435	29	58	59	1.0	.0	-1.0	1	
492-	CBAR	436	2	60	61	1.0	.0	-1.0	1	
493-	CBAR	437	2	68	69	1.0	.0	-1.0	1	
494-	CBAR	438	29	70	71	1.0	.0	-1.0	1	
495-	CBAR	439	2	52	49	-1.0	.0	1.0	1	
496-	CBAR	440	2	53	50	-1.0	.0	1.0	1	
497-	CBAR	441	2	54	51	-1.0	.0	1.0	1	
498-	CBAR	442	2	46	43	-1.0	.0	1.0	1	
499-	CBAR	443	2	47	44	-1.0	.0	1.0	1	
500-	CBAR	444	2	48	45	-1.0	.0	1.0	1	

SORTED BULK DATA ECHO

CARD COUNT	. 1 ..	2 ..	3 ..	4 ..	5 ..	6 ..	7 ..	8 ..	9 ..	10 .
501-	CBAR	445	2	40	37	-1.0	.0	1.0	1	
502-	CBAR	446	2	41	38	-1.0	.0	1.0	1	
503-	CBAR	447	2	42	39	-1.0	.0	1.0	1	
504-	CBAR	448	2	34	31	-1.0	.0	1.0	1	
505-	CBAR	449	2	35	32	-1.0	.0	1.0	1	
506-	CBAR	450	2	36	33	-1.0	.0	1.0	1	
507-	CBAR	451	2	28	25	-1.0	.0	1.0	1	
508-	CBAR	452	2	29	26	-1.0	.0	1.0	1	
509-	CBAR	453	2	30	27	-1.0	.0	1.0	1	
510-	CBAR	454	2	22	19	-1.0	.0	1.0	1	
511-	CBAR	455	2	23	20	-1.0	.0	1.0	1	
512-	CBAR	456	2	24	21	-1.0	.0	1.0	1	
513-	CBAR	457	2	16	13	-1.0	.0	1.0	1	
514-	CBAR	458	2	17	14	-1.0	.0	1.0	1	
515-	CBAR	459	2	18	15	-1.0	.0	1.0	1	
516-	CBAR	460	20	10	7	-1.0	.0	1.0	1	
517-	CBAR	461	2	11	8	-1.0	.0	1.0	1	
518-	CBAR	462	20	12	9	-1.0	.0	1.0	1	
519-	CBAR	463	2	4	1	-1.0	.0	1.0	1	
520-	CBAR	464	22	5	2	-1.0	.0	1.0	1	
521-	CBAR	465	2	6	3	-1.0	.0	1.0	1	
522-	CBAR	501	54	62	55	-1.0	.0	1.0	1	QC501
523-	+C501	6								
524-	CBAR	502	54	64	56	-1.0	.0	1.0	1	QC502
525-	+C502	6								
526-	CBAR	503	54	66	57	-1.0	.0	1.0	1	QC503
527-	+C503	6								
528-	CBAR	504	53	62	63	1.0	.0	1.0	1	
529-	CBAR	505	53	64	65	1.0	.0	1.0	1	
530-	CBAR	506	53	66	67	1.0	.0	1.0	1	
531-	CBAR	551	58	63	55	-.5	.0	1.0	1	QC551
532-	+C551	6	6							
533-	CBAR	552	58	65	56	-.5	.0	1.0	1	QC552
534-	+C552	6	6							
535-	CBAR	553	58	67	57	-.5	.0	1.0	1	QC553
536-	+C553	6	6							
537-	CONM2	2001	1	0	44.223					
538-	CONM2	2002	2	0	.332					
539-	CONM2	2003	3	0	44.223					
540-	CONM2	2004	4	0	44.223					
541-	CONM2	2005	5	0	70.332					
542-	CONM2	2006	6	0	44.223					
543-	CONM2	2007	7	0	.332					
544-	CONM2	2008	8	0	.479					
545-	CONM2	2009	9	0	.332					
546-	CONM2	2010	10	0	.332					
547-	CONM2	2011	11	0	.479					
548-	CONM2	2012	12	0	.332					
549-	CONM2	2013	13	0	.332					
550-	CONM2	2014	14	0	.479					

SORTED BULK DATA ECHO

CARD COUNT	1	2	3	4	5	6	7	8	9	10
551-	CONM2	2015	15	0	.332					
552-	CONM2	2016	16	0	.332					
553-	CONM2	2017	17	0	.479					
554-	CONM2	2018	18	0	.332					
555-	CONM2	2019	19	0	.332					
556-	CONM2	2020	20	0	.479					
557-	CONM2	2021	21	0	.332					
558-	CONM2	2022	22	0	.332					
559-	CONM2	2023	23	0	.479					
560-	CONM2	2024	24	0	.332					
561-	CONM2	2025	25	0	.332					
562-	CONM2	2026	26	0	.479					
563-	CONM2	2027	27	0	.332					
564-	CONM2	2028	28	0	.332					
565-	CONM2	2029	29	0	.479					
566-	CONM2	2030	30	0	.332					
567-	CONM2	2031	31	0	.332					
568-	CONM2	2032	32	0	.479					
569-	CONM2	2033	33	0	.332					
570-	CONM2	2034	34	0	.332					
571-	CONM2	2035	35	0	.479					
572-	CONM2	2036	36	0	.332					
573-	CONM2	2037	37	0	.332					
574-	CONM2	2038	38	0	.479					
575-	CONM2	2039	39	0	.332					
576-	CONM2	2040	40	0	.332					
577-	CONM2	2041	41	0	.479					
578-	CONM2	2042	42	0	.332					
579-	CONM2	2043	43	0	.332					
580-	CONM2	2044	44	0	.479					
581-	CONM2	2045	45	0	.332					
582-	CONM2	2046	46	0	.332					
583-	CONM2	2047	47	0	.479					
584-	CONM2	2048	48	0	.332					
585-	CONM2	2049	49	0	.332					
586-	CONM2	2050	50	0	.479					
587-	CONM2	2051	51	0	.332					
588-	CONM2	2052	52	0	.332					
589-	CONM2	2053	53	0	.479					
590-	CONM2	2054	54	0	.332					
591-	CONM2	2055	55	0	.332					
592-	CONM2	2056	56	0	.479					
593-	CONM2	2057	57	0	.332					
594-	CONM2	2058	58	0	4.810					
595-	CONM2	2059	59	0	84.223					
596-	CONM2	2060	60	0	6.170					
597-	CONM2	2061	61	0	.332					
598-	CONM2	2062	62	0	6.317					
599-	CONM2	2063	63	0	.706					
600-	CONM2	2064	64	0	6.317					

S O R T E D   B U L K   D A T A   E C H O

CARD COUNT	1	2	3	4	5	6	7	8	9	10
601-	CONM2	2065	65	0	.706					
602-	CONM2	2066	66	0	6.317					
603-	CONM2	2067	67	0	.706					
604-	CONM2	2068	68	0	6.170					
605-	CONM2	2069	69	0	.332					
606-	CONM2	2070	70	0	4.810					
607-	CONM2	2071	71	0	84.223					
608-	CONM2	2072	72	0	4.810					
609-	CONM2	2073	73	0	1.130					
610-	CONM2	2074	74	0	11.317					
611-	CONM2	2075	75	0	.479					
612-	CONM2	2076	76	0	11.317					
613-	CONM2	2077	77	0	.479					
614-	CONM2	2078	78	0	11.317					
615-	CONM2	2079	79	0	.479					
616-	CONM2	2080	80	0	11.317					
617-	CONM2	2081	81	0	.479					
618-	CONM2	2082	82	0	11.317					
619-	CONM2	2083	83	0	.479					
620-	CONM2	2084	84	0	11.317					
621-	CONM2	2085	85	0	.479					
622-	CONM2	2086	86	0	11.317					
623-	CONM2	2087	87	0	.479					
624-	CONM2	2088	88	0	4.810					
625-	CONM2	2089	89	0	1.130					
626-	CONM2	2090	90	0	6.170					
627-	CONM2	2091	91	0	1.700					
628-	CONM2	2092	92	0	11.317					
629-	CONM2	2093	93	0	.479					
630-	CONM2	2094	94	0	11.317					
631-	CONM2	2095	95	0	.479					
632-	CONM2	2096	96	0	11.317					
633-	CONM2	2097	97	0	.479					
634-	CONM2	2098	98	0	11.317					
635-	CONM2	2099	99	0	.479					
636-	CONM2	2100	100	0	11.317					
638-	CONM2	2102	102	0	11.317					
639-	CONM2	2103	103	0	.479					
640-	CONM2	2104	104	0	11.317					
641-	CONM2	2105	105	0	.479					
642-	CONM2	2106	106	0	6.170					
643-	CONM2	2107	107	0	1.700					
644-	CONM2	2108	108	0	4.810					
645-	CONM2	2109	109	0	1.130					
646-	CONM2	2110	110	0	11.317					
647-	CONM2	2111	111	0	.479					
648-	CONM2	2112	112	0	11.317					
649-	CONM2	2113	113	0	.479					
650-	CONM2	2114	114	0	11.317					

SORTED BULK DATA ECHO

CARD COUNT	. 1 ..	2 ..	3 ..	4 ..	5 ..	6 ..	7 ..	8 ..	9 ..	10 .
651-	CONM2	2115	115	0	.479					
652-	CONM2	2116	116	0	11.317					
653-	CONM2	2117	117	0	.479					
654-	CONM2	2118	118	0	11.317					
655-	CONM2	2119	119	0	.479					
656-	CONM2	2120	120	0	11.317					
657-	CONM2	2121	121	0	.479					
658-	CONM2	2122	122	0	11.317					
659-	CONM2	2123	123	0	.479					
660-	CONM2	2124	124	0	4.810					
661-	CONM2	2125	125	0	1.130					
662-	CONM2	2126	126	0	4.810					
663-	CONM2	2127	127	0	84.223					
664-	CONM2	2128	128	0	6.170					
665-	CONM2	2129	129	0	.332					
666-	CONM2	2130	130	0	6.170					
667-	CONM2	2131	131	0	.332					
668-	CONM2	2132	132	0	175.317					
669-	CONM2	2133	133	0	.332					
670-	CONM2	2134	134	0	6.170					
671-	CONM2	2135	135	0	.332					
672-	CONM2	2136	136	0	6.170					
673-	CONM2	2137	137	0	.332					
674-	CONM2	2138	138	0	4.810					
675-	CONM2	2139	139	0	84.223					
676-	CROD	601	5	72	91					
677-	CROD	602	5	73	90					
678-	CROD	603	5	90	109					
679-	CROD	604	5	91	108					
680-	CROD	605	5	88	107					
681-	CROD	606	5	89	106					
682-	CROD	607	5	106	125					
683-	CROD	608	5	107	124					
684-	CROD	609	5	58	75					
685-	CROD	610	5	59	74					
686-	CROD	611	5	74	93					
687-	CROD	612	5	75	92					
688-	CROD	613	5	92	111					
689-	CROD	614	5	93	110					
690-	CROD	615	5	110	127					
691-	CROD	616	5	111	126					
692-	CROD	617	5	60	77					
693-	CROD	618	5	61	76					
694-	CROD	619	5	76	95					
695-	CROD	620	5	77	94					
696-	CROD	621	5	94	113					
697-	CROD	622	5	95	112					
698-	CROD	623	5	112	129					
699-	CROD	624	5	113	128					
700-	CROD	625	5	62	79					

SORTED BULK DATA ECHO

CARD COUNT	. 1 ..	2 ..	3 ..	4 ..	5 ..	6 ..	7 ..	8 ..	9 ..	10 .
701-	CROD	626	5	63	78					
702-	CROD	627	5	78	97					
703-	CROD	628	5	79	96					
704-	CROD	629	5	96	115					
705-	CROD	630	5	97	114					
706-	CROD	631	5	114	131					
707-	CROD	632	5	115	130					
708-	CROD	633	5	64	81					
709-	CROD	634	5	65	80					
710-	CROD	635	5	80	99					
711-	CROD	636	5	81	98					
712-	CROD	637	5	98	117					
713-	CROD	638	5	99	116					
714-	CROD	639	5	116	133					
715-	CROD	640	5	117	132					
716-	CROD	641	5	66	83					
717-	CROD	642	5	67	82					
718-	CROD	643	5	82	101					
719-	CROD	644	5	83	100					
720-	CROD	645	5	100	119					
721-	CROD	646	5	101	118					
722-	CROD	647	5	118	135					
723-	CROD	648	5	119	134					
724-	CROD	649	5	68	85					
725-	CROD	650	5	69	84					
726-	CROD	651	5	84	103					
727-	CROD	652	5	85	102					
728-	CROD	653	5	102	121					
729-	CROD	654	5	103	120					
730-	CROD	655	5	120	137					
731-	CROD	656	5	121	136					
732-	CROD	657	5	70	87					
733-	CROD	658	5	71	86					
734-	CROD	659	5	86	105					
735-	CROD	660	5	87	104					
736-	CROD	661	5	104	123					
737-	CROD	662	5	105	122					
738-	CROD	663	5	122	139					
739-	CROD	664	5	123	138					
740-	CROD	665	5	72	75					
741-	CROD	666	5	73	74					
742-	CROD	667	5	90	93					
743-	CROD	668	5	91	92					
744-	CROD	669	5	108	111					
745-	CROD	670	5	109	110					
746-	CROD	671	5	86	89					
747-	CROD	672	5	87	88					
748-	CROD	673	5	104	107					
749-	CROD	674	5	105	106					
750-	CROD	675	5	122	125					

SORTED BULK DATA ECHO

CARD COUNT	. 1 ..	2 ..	3 ..	4 ..	5 ..	6 ..	7 ..	8 ..	9 ..	10 .
751-	CROD	676	5	123	124					
752-	CROD	677	5	58	61					
753-	CROD	678	5	59	60					
754-	CROD	679	5	60	63					
755-	CROD	680	5	61	62					
756-	CROD	681	5	62	65					
757-	CROD	682	5	63	64					
758-	CROD	683	5	64	67					
759-	CROD	684	5	65	66					
760-	CROD	685	5	66	69					
761-	CROD	686	5	67	68					
762-	CROD	687	5	68	70					
763-	CROD	688	5	69	70					
764-	CROD	689	5	74	77					
765-	CROD	690	5	75	76					
766-	CROD	691	5	76	79					
767-	CROD	692	5	77	78					
768-	CROD	693	5	78	81					
769-	CROD	694	5	79	80					
770-	CROD	695	5	80	83					
771-	CROD	696	5	81	82					
772-	CROD	697	5	82	85					
773-	CROD	698	5	83	84					
774-	CROD	699	5	84	87					
775-	CROD	700	5	85	86					
776-	CROD	701	5	92	95					
777-	CROD	702	5	93	94					
778-	CROD	703	5	94	97					
779-	CROD	704	5	95	96					
780-	CROD	705	5	96	99					
781-	CROD	706	5	97	98					
782-	CROD	707	5	98	101					
783-	CROD	708	5	99	100					
784-	CROD	709	5	100	103					
785-	CROD	710	5	101	102					
786-	CROD	711	5	102	105					
787-	CROD	712	5	103	104					
788-	CROD	713	5	110	113					
789-	CROD	714	5	111	112					
790-	CROD	715	5	112	115					
791-	CROD	716	5	113	114					
792-	CROD	717	5	114	117					
793-	CROD	718	5	115	116					
794-	CROD	719	5	116	119					
795-	CROD	720	5	117	118					
796-	CROD	721	5	118	121					
797-	CROD	722	5	119	120					
798-	CROD	723	5	120	123					
799-	CROD	724	5	121	122					
800-	CROD	725	5	126	129					

SORTED BULK DATA ECHO

CARD COUNT	. 1 ..	2 ..	3 ..	4 ..	5 ..	6 ..	7 ..	8 ..	9 ..	10 .
801-	CROD	726	5	127	128					
802-	CROD	727	5	128	131					
803-	CROD	728	5	129	130					
804-	CROD	729	5	130	133					
805-	CROD	730	5	131	132					
806-	CROD	731	5	132	135					
807-	CROD	732	5	133	134					
808-	CROD	733	5	134	137					
809-	CROD	734	5	135	136					
810-	CROD	735	5	136	139					
811-	CROD	736	5	137	138					
812-	CROD	737	5	62	49					
813-	CROD	738	5	55	52					
814-	CROD	739	5	64	50					
815-	CROD	740	5	56	53					
816-	CROD	741	5	66	51					
817-	CROD	742	5	57	54					
818-	CROD	743	5	49	46					
819-	CROD	744	5	52	43					
820-	CROD	745	5	50	47					
821-	CROD	746	5	53	44					
822-	CROD	747	5	51	48					
823-	CROD	748	5	54	45					
824-	CROD	749	5	43	40					
825-	CROD	750	5	46	37					
826-	CROD	751	5	44	41					
827-	CROD	752	5	47	38					
828-	CROD	753	5	45	42					
829-	CROD	754	5	48	39					
830-	CROD	755	5	37	34					
831-	CROD	756	5	40	31					
832-	CROD	757	5	38	35					
833-	CROD	758	5	41	32					
834-	CROD	759	5	39	36					
835-	CROD	760	5	42	33					
836-	CROD	761	5	31	28					
837-	CROD	762	5	34	25					
838-	CROD	763	5	32	29					
839-	CROD	764	5	35	26					
840-	CROD	765	5	33	30					
841-	CROD	766	5	36	27					
842-	CROD	767	5	25	22					
843-	CROD	768	5	28	19					
844-	CROD	769	5	26	23					
845-	CROD	770	5	29	20					
846-	CROD	771	5	27	24					
847-	CROD	772	5	30	21					
848-	CROD	773	5	19	16					
849-	CROD	774	5	22	13					
850-	CROD	775	5	20	17					

SORTED BULK DATA ECHO

CARD COUNT	. 1 ..	2 ..	3 ..	4 ..	5 ..	6 ..	7 ..	8 ..	9 ..	10 .
851-	CROD	776	5	23	14					
852-	CROD	777	5	21	18					
853-	CROD	778	5	24	15					
854-	CROD	779	5	13	10					
855-	CROD	780	5	16	7					
856-	CROD	781	5	14	11					
857-	CROD	782	5	17	8					
858-	CROD	783	5	15	12					
859-	CROD	784	5	18	9					
860-	CROD	785	5	55	64					
861-	CROD	786	5	62	56					
862-	CROD	787	5	64	57					
863-	CROD	788	5	56	66					
864-	CROD	789	5	52	50					
865-	CROD	790	5	49	53					
866-	CROD	791	5	53	51					
867-	CROD	792	5	50	54					
868-	CROD	793	5	46	44					
869-	CROD	794	5	43	47					
870-	CROD	795	5	47	45					
871-	CROD	796	5	44	48					
872-	CROD	797	5	40	38					
873-	CROD	798	5	37	41					
874-	CROD	799	5	41	39					
875-	CROD	800	5	38	42					
876-	CROD	801	5	34	32					
877-	CROD	802	5	31	35					
878-	CROD	803	5	35	33					
879-	CROD	804	5	32	36					
880-	CROD	805	5	28	26					
881-	CROD	806	5	25	29					
882-	CROD	807	5	29	27					
883-	CROD	808	5	26	30					
884-	CROD	809	5	22	20					
885-	CROD	810	5	19	23					
886-	CROD	811	5	23	21					
887-	CROD	812	5	20	24					
888-	CROD	813	5	16	14					
889-	CROD	814	5	13	17					
890-	CROD	815	5	17	15					
891-	CROD	816	5	14	18					
892-	CROD	817	5	10	8					
893-	CROD	818	5	7	11					
894-	CROD	819	5	11	9					
895-	CROD	820	5	8	12					
896-	CROD	821	5	63	56					
897-	CROD	822	5	55	65					
898-	CROD	823	5	65	57					
899-	CROD	824	5	56	67					
900-	CROD	825	5	7	4					

S O R T E D   B U L K   D A T A   E C H O

CARD COUNT	. 1 ..	2 ..	3 ..	4 ..	5 ..	6 ..	7 ..	8 ..	9 ..	10 .
901-	CROD	826	5	10	1					
902-	CROD	827	5	8	5					
903-	CROD	828	5	11	2					
904-	CROD	829	5	9	6					
905-	CROD	830	5	12	3					
906-	CROD	831	5	4	2					
907-	CROD	832	5	1	5					
908-	CROD	833	5	5	3					
909-	CROD	834	5	2	6					
910-	CROD	1001	6	72	92					
911-	CROD	1002	6	90	74					
912-	CROD	1003	6	108	92					
913-	CROD	1004	6	90	110					
914-	CROD	1005	6	86	106					
915-	CROD	1006	6	104	88					
916-	CROD	1007	6	122	106					
917-	CROD	1008	6	104	124					
918-	CROD	1009	6	58	76					
919-	CROD	1010	6	74	60					
920-	CROD	1011	6	60	78					
921-	CROD	1012	6	76	62					
922-	CROD	1013	6	62	80					
923-	CROD	1014	6	78	64					
924-	CROD	1015	6	64	82					
925-	CROD	1016	6	80	66					
926-	CROD	1017	6	66	84					
927-	CROD	1018	6	82	68					
928-	CROD	1019	6	68	86					
929-	CROD	1020	6	84	70					
930-	CROD	1021	6	74	94					
931-	CROD	1022	6	92	76					
932-	CROD	1023	6	76	96					
933-	CROD	1024	6	94	78					
934-	CROD	1025	6	78	98					
935-	CROD	1026	6	96	80					
936-	CROD	1027	6	80	100					
937-	CROD	1028	6	98	82					
938-	CROD	1029	6	82	102					
939-	CROD	1030	6	100	84					
940-	CROD	1031	6	84	104					
941-	CROD	1032	6	102	86					
942-	CROD	1033	6	92	112					
943-	CROD	1034	6	110	94					
944-	CROD	1035	6	94	114					
945-	CROD	1036	6	112	96					
946-	CROD	1037	6	96	116					
947-	CROD	1038	6	114	98					
948-	CROD	1039	6	98	118					
949-	CROD	1040	6	116	100					
950-	CROD	1041	6	100	120					

S O R T E D   B U L K   D A T A   E C H O

CARD COUNT	1	2	3	4	5	6	7	8	9	10
951-	CROD	1042	6	118	102					
952-	CROD	1043	6	102	122					
953-	CROD	1044	6	120	104					
954-	CROD	1045	6	110	128					
955-	CROD	1046	6	126	112					
956-	CROD	1047	6	112	130					
957-	CROD	1048	6	128	114					
958-	CROD	1049	6	114	132					
959-	CROD	1050	6	130	116					
960-	CROD	1051	6	116	134					
961-	CROD	1052	6	132	118					
962-	CROD	1053	6	118	136					
963-	CROD	1054	6	134	120					
964-	CROD	1055	6	120	138					
965-	CROD	1056	6	136	122					
966-	CROD	1057	6	73	93					
967-	CROD	1058	6	91	75					
968-	CROD	1059	6	109	93					
969-	CROD	1060	6	91	111					
970-	CROD	1061	6	87	107					
971-	CROD	1062	6	105	89					
972-	CROD	1063	6	123	107					
973-	CROD	1064	6	105	125					
974-	CROD	1065	6	59	77					
975-	CROD	1066	6	75	61					
976-	CROD	1067	6	61	79					
977-	CROD	1068	6	77	63					
978-	CROD	1069	6	63	81					
979-	CROD	1070	6	79	65					
980-	CROD	1071	6	65	83					
981-	CROD	1072	6	81	67					
982-	CROD	1073	6	67	85					
983-	CROD	1074	6	83	69					
984-	CROD	1075	6	69	87					
985-	CROD	1076	6	85	71					
986-	CROD	1077	6	75	95					
987-	CROD	1078	6	93	77					
988-	CROD	1079	6	77	97					
989-	CROD	1080	6	95	79					
990-	CROD	1081	6	79	99					
991-	CROD	1082	6	97	81					
992-	CROD	1083	6	81	101					
993-	CROD	1084	6	99	83					
994-	CROD	1085	6	83	103					
995-	CROD	1086	6	101	85					
996-	CROD	1087	6	85	105					
997-	CROD	1088	6	103	87					
998-	CROD	1089	6	93	113					
999-	CROD	1090	6	111	95					
1000-	CROD	1091	6	95	115					

S O R T E D   B U L K   D A T A   E C H O

CARD COUNT	. 1 ..	2 ..	3 ..	4 ..	5 ..	6 ..	7 ..	8 ..	9 ..	10 .
1001-	CROD	1092	6	113	97					
1002-	CROD	1093	6	97	117					
1003-	CROD	1094	6	115	99					
1004-	CROD	1095	6	99	119					
1005-	CROD	1096	6	117	101					
1006-	CROD	1097	6	101	121					
1007-	CROD	1098	6	119	103					
1008-	CROD	1099	6	103	123					
1009-	CROD	1100	6	121	105					
1010-	CROD	1101	6	111	129					
1011-	CROD	1102	6	127	113					
1012-	CROD	1103	6	113	131					
1013-	CROD	1104	6	129	115					
1014-	CROD	1105	6	115	133					
1015-	CROD	1106	6	131	117					
1016-	CROD	1107	6	117	135					
1017-	CROD	1108	6	133	119					
1018-	CROD	1109	6	119	137					
1019-	CROD	1110	6	135	121					
1020-	CROD	1111	6	121	139					
1021-	CROD	1112	6	137	123					
1022-	CROD	1113	6	62	53					
1023-	CROD	1114	6	64	52					
1024-	CROD	1115	6	53	66					
1025-	CROD	1116	6	64	54					
1026-	CROD	1117	6	55	50					
1027-	CROD	1118	6	49	56					
1028-	CROD	1119	6	56	51					
1029-	CROD	1120	6	50	57					
1030-	CROD	1121	6	52	47					
1031-	CROD	1122	6	46	53					
1032-	CROD	1123	6	53	48					
1033-	CROD	1124	6	47	54					
1034-	CROD	1125	6	49	44					
1035-	CROD	1126	6	43	50					
1036-	CROD	1127	6	50	45					
1037-	CROD	1128	6	44	51					
1038-	CROD	1129	6	46	41					
1039-	CROD	1130	6	40	47					
1040-	CROD	1131	6	47	42					
1041-	CROD	1132	6	41	48					
1042-	CROD	1133	6	43	38					
1043-	CROD	1134	6	37	44					
1044-	CROD	1135	6	44	39					
1045-	CROD	1136	6	38	45					
1046-	CROD	1137	6	40	35					
1047-	CROD	1138	6	34	41					
1048-	CROD	1139	6	41	36					
1049-	CROD	1140	6	35	42					
1050-	CROD	1141	6	37	32					

S O R T E D   B U L K   D A T A   E C H O

CARD COUNT	. 1 ..	2 ..	3 ..	4 ..	5 ..	6 ..	7 ..	8 ..	9 ..	10 .
1051-	CROD	1142	6	31	38					
1052-	CROD	1143	6	38	33					
1053-	CROD	1144	6	32	39					
1054-	CROD	1145	6	34	29					
1055-	CROD	1146	6	28	35					
1056-	CROD	1147	6	35	30					
1057-	CROD	1148	6	29	36					
1058-	CROD	1149	6	31	26					
1059-	CROD	1150	6	25	32					
1060-	CROD	1151	6	32	27					
1061-	CROD	1152	6	26	33					
1062-	CROD	1153	6	28	23					
1063-	CROD	1154	6	22	29					
1064-	CROD	1155	6	29	24					
1065-	CROD	1156	6	23	30					
1066-	CROD	1157	6	25	20					
1067-	CROD	1158	6	19	26					
1068-	CROD	1159	6	26	21					
1069-	CROD	1160	6	20	27					
1070-	CROD	1161	6	22	17					
1071-	CROD	1162	6	16	23					
1072-	CROD	1163	6	23	18					
1073-	CROD	1164	6	17	24					
1074-	CROD	1165	6	19	14					
1075-	CROD	1166	6	13	20					
1076-	CROD	1167	6	20	15					
1077-	CROD	1168	6	14	21					
1078-	CROD	1169	6	16	11					
1079-	CROD	1170	6	10	17					
1080-	CROD	1171	6	17	12					
1081-	CROD	1172	6	11	18					
1082-	CROD	1173	6	13	8					
1083-	CROD	1174	6	7	14					
1084-	CROD	1175	6	14	9					
1085-	CROD	1176	6	8	15					
1086-	CROD	1177	6	10	5					
1087-	CROD	1178	6	4	11					
1088-	CROD	1179	6	11	6					
1089-	CROD	1180	6	5	12					
1090-	CROD	1181	6	7	2					
1091-	CROD	1182	6	1	8					
1092-	CROD	1183	6	8	3					
1093-	CROD	1184	6	2	9					
1094-	DAREA	1	58	3	56.96	58	1	18.87		
1095-	DAREA	1	70	3	-56.96	70	1	-18.87		
1096-	DAREA	1	126	3	56.96	126	1	18.87		
1097-	DAREA	1	138	3	-56.96	138	1	-18.87		
1098-	EIGR	6	FEER	1.0			42			+ABC
1099-	+ABC	MASS								
1100-	GRAV	3	0	.98066	0.0	0.0	-1.			

SORTED BULK DATA ECHO

CARD COUNT	. 1 ..	2 ..	3 ..	4 ..	5 ..	6 ..	7 ..	8 ..	9 ..	10 .
1101-	GRID	1	0	-16.190	-15.160	117.040				
1102-	GRID	2	0	-16.190	0.000	117:040				
1103-	GRID	3	0	-16.190	15.160	117.040				
1104-	GRID	4	0	-1.160	-15.160	117.190				
1105-	GRID	5	0	-1.160	0.000	117.190				
1106-	GRID	6	0	-1.160	15.160	117.190				
1107-	GRID	7	0	-16.180	-15.160	115.540				
1108-	GRID	8	0	-16.180	0.000	115.540				
1109-	GRID	9	0	-16.180	15.160	115.540				
1110-	GRID	10	0	-1.140	-15.160	115.680				
1111-	GRID	11	0	-1.140	0.000	115.680				
1112-	GRID	12	0	-1.140	15.160	115.680				
1113-	GRID	13	0	-16.030	-15.160	100.940				
1114-	GRID	14	0	-16.030	0.000	100.950				
1115-	GRID	15	0	-16.030	15.160	100.950				
1116-	GRID	16	0	-1.000	-15.160	101.090				
1117-	GRID	17	0	-1.000	0.000	101.090				
1118-	GRID	18	0	-1.000	15.160	101.090				
1119-	GRID	19	0	-15.890	-15.160	86.350				
1120-	GRID	20	0	-15.890	0.000	86.360				
1121-	GRID	21	0	-15.890	15.160	86.360				
1122-	GRID	22	0	-.860	-15.160	86.500				
1123-	GRID	23	0	-.860	0.000	86.500				
1124-	GRID	24	0	-.860	15.160	86.500				
1125-	GRID	25	0	-15.750	-15.160	71.760				
1126-	GRID	26	0	-15.750	0.000	71.760				
1127-	GRID	27	0	-15.750	15.160	71.760				
1128-	GRID	28	0	-.710	-15.160	71.910				
1129-	GRID	29	0	-.710	0.000	71.910				
1130-	GRID	30	0	-.710	15.160	71.910				
1131-	GRID	31	0	-15.610	-15.160	57.170				
1132-	GRID	32	0	-15.610	0.000	57.170				
1133-	GRID	33	0	-15.610	15.160	57.170				
1134-	GRID	34	0	-.570	-15.160	57.320				
1135-	GRID	35	0	-.570	0.000	57.320				
1136-	GRID	36	0	-.570	15.160	57.320				
1137-	GRID	37	0	-15.460	-15.160	42.580				
1138-	GRID	38	0	-15.460	0.000	42.580				
1139-	GRID,	39	0	-15.460	15.160	42.580				
1140-	GRID	40	0	-.430	-15.160	42.720				
1141-	GRID	41	0	-.430	0.000	42.720				
1142-	GRID	42	0	-.430	15.160	42.720				
1143-	GRID	43	0	-15.320	-15.160	27.980				
1144-	GRID	44	0	-15.320	0.000	27.990				
1145-	GRID	45	0	-15.320	15.160	27.990				
1146-	GRID	46	0	-.290	-15.160	28.130				
1147-	GRID	47	0	-.290	0.000	28.130				
1148-	GRID	48	0	-.290	15.160	28.130				
1149-	GRID	49	0	-15.180	-15.160	13.390				
1150-	GRID	50	0	-15.180	0.000	13.390				

S O R T E D   B U L K   D A T A   E C H O

CARD COUNT	. 1 ..	2 ..	3 ..	4 ..	5 ..	6 ..	7 ..	8 ..	9 ..	10 .
1151-	GRID	51	0	-15.180	15.160	13.390				
1152-	GRID	52	0	-.140	-15.160	13.540				
1153-	GRID	53	0	-.140	0.000	13.540				
1154-	GRID	54	0	-.140	15.160	13.540				
1155-	GRID	55	0	-15.040	-15.160	-1.200				
1156-	GRID	56	0	-15.040	0.000	-1.200				
1157-	GRID	57	0	-15.040	15.160	-1.200				
1158-	GRID	58	0	0.000	-45.214	3.353				
1159-	GRID	59	0	0.000	-45.214	-11.685				
1160-	GRID	60	0	0.000	-30.250	.919				
1161-	GRID	61	0	0.000	-30.250	-14.119				
1162-	GRID	62	0	0.000	-15.161	-1.053				
1163-	GRID	63	0	0.000	-15.161	-16.091				
1164-	GRID	64	0	0.000	0.000	-1.053				
1165-	GRID	65	0	0.000	0.000	-16.091				
1166-	GRID	66	0	0.000	15.161	-1.053				
1167-	GRID	67	0	0.000	15.161	-16.091				
1168-	GRID	68	0	0.000	30.250	.919				
1169-	GRID	69	0	0.000	30.250	-14.119				
1170-	GRID	70	0	0.000	45.214	3.353				
1171-	GRID	71	0	0.000	45.214	-11.685				
1172-	GRID	72	0	15.161	-60.000	7.197				
1173-	GRID	73	0	15.161	-60.000	-7.833				
1174-	GRID	74	0	15.161	-45.214	3.845				
1175-	GRID	75	0	15.161	-45.214	-11.186				
1176-	GRID	76	0	15.161	-30.250	1.411				
1177-	GRID	77	0	15.161	-30.250	-13.620				
1178-	GRID	78	0	15.161	-15.161	-.561				
1179-	GRID	79	0	15.161	-15.161	-15.592				
1180-	GRID	80	0	15.161	0.000	-.561				
1181-	GRID	81	0	15.161	0.000	-15.592				
1182-	GRID	82	0	15.161	15.161	-.561				
1183-	GRID	83	0	15.161	15.161	-15.592				
1184-	GRID	84	0	15.161	30.250	1.411				
1185-	GRID	85	0	15.161	30.250	-13.620				
1186-	GRID	86	0	15.161	45.214	3.845				
1187-	GRID	87	0	15.161	45.214	-11.186				
1188-	GRID	88	0	15.161	60.000	7.197				
1189-	GRID	89	0	15.161	60.000	-7.833				
1190-	GRID	90	0	30.250	-60.000	8.670				
1191-	GRID	91	0	30.250	-60.000	-6.353				
1192-	GRID	92	0	30.250	-45.214	5.317				
1193-	GRID	93	0	30.250	-45.214	-9.705				
1194-	GRID	94	0	30.250	-30.250	2.884				
1195-	GRID	95	0	30.250	-30.250	-12.139				
1196-	GRID	96	0	30.250	-15.161	.912				
1197-	GRID	97	0	30.250	-15.161	-14.111				
1198-	GRID	98	0	30.250	0.000	.912				
1199-	GRID	99	0	30.250	0.000	-14.111				
1200-	GRID	100	0	30.250	15.161	.912				

S O R T E D   B U L K   D A T A   E C H O

```
CARD
COUNT          .   1  ..   2  ..   3  ..   4  ..   5  ..   6  ..   7  ..   8  ..   9  ..  10  .
1201-          GRID    101     0       30.250  15.161  -14.111
1202-          GRID    102     0       30.250  30.250  2.884
1203-          GRID    103     0       30.250  30.250  -12.139
1204-          GRID    104     0       30.250  45.214  5.317
1205-          GRID    105     0       30.250  45.214  -9.705
1206-          GRID    106     0       30.250  60.000  8.670
1207-          GRID    107     0       30.250  60.000  -6.353
1208-          GRID    108     0       45.214  -60.000 11.100
1209-          GRID    109     0       45.214  -60.000 -3.915
1210-          GRID    110     0       45.214  -45.214 7.747
1211-          GRID    111     0       45.214  -45.214 -7.268
1212-          GRID    112     0       45.214  -30.250 5.313
1213-          GRID    113     0       45.214  -30.250 -9.701
1214-          GRID    114     0       45.214  -15.161 3.341
1215-          GRID    115     0       45.214  -15.161 -11.673
1216-          GRID    116     0       45.214  0.000   3.341
1217-          GRID    117     0       45.214  0.000   -11.673
1218-          GRID    118     0       45.214  15.161  3.341
1219-          GRID    119     0       45.214  15.161  -11.673
1220-          GRID    120     0       45.214  30.250  5.313
1221-          GRID    121     0       45.214  30.250  -9.701
1222-          GRID    122     0       45.214  45.214  7.747
1223-          GRID    123     0       45.214  45.214  -7.268
1224-          GRID    124     0       45.214  60.000  11.100
1225-          GRID    125     0       45.214  60.000  -3.915
1226-          GRID    126     0       60.000  -45.214 11.128
1227-          GRID    127     0       60.000  -45.214 -3.911
1228-          GRID    128     0       60.000  -30.250 8.694
1229-          GRID    129     0       60.000  -30.250 -6.345
1230-          GRID    130     0       60.000  -15.161 6.722
1231-          GRID    131     0       60.000  -15.161 -8.317
1232-          GRID    132     0       60.000  0.000   6.722
1233-          GRID    133     0       60.000  0.000   -8.317
1234-          GRID    134     0       60.000  15.161  6.722
1235-          GRID    135     0       60.000  15.161  -8.317
1236-          GRID    136     0       60.000  30.250  8.694
1237-          GRID    137     0       60.000  30.250  -6.345
1238-          GRID    138     0       60.000  45.214  11.128
1239-          GRID    139     0       60.000  45.214  -3.911
1240-          MAT1    1       1.66E11 1.31E10 .193    1605.43 -.252E-672.
1241           MAT1    2       1.82E11 1.43E10 .35     1716.15 -.522E-672.
1242           MAT1    11      2.34E11 0.0     0.0     1662.28 -.396E-60.0
1243-          MAT1    51      1.879E111.055E10.154    1605.43 -.19E-6
1244-          MAT1    53      1.866E111.150E10.198    1716.15 -.21E-6
1245-          MAT1    54      1.889E111.170E10.225    1716.15 -.23E-6
1246-          MAT1    58      1.956E119.585E9 .136    1716.15 -.20E-6
1247-          PARAM   COUPMASS1
1248-          PARAM   GRDPNT  0
1249-          PARAM   HFREQ   1.14
1250-          PARAM   LFREQ   .9
```

```
                                S O R T E D   B U L K   D A T A   E C H O
CARD
COUNT        .   1  ..   2  ..   3  ..   4  ..   5  ..   6  ..   7  ..   8  ..   9  ..  10  .
1251-        PBAR    1       1       1.715E-41.471E-71.471E-72.941E-7.03
1252-        PBAR    2       2       3.806E-42.753E-72.753E-75.506E-7
1253-        PBAR    20      2       7.000E-42.081E-62.081E-65.506E-79.333
1254-        PBAR    21      1       7.000E-42.081E-62.081E-62.941E-711.492
1255-        PBAR    22      2       7.000E-42.081E-62.081E-65.506E-77.333
1256-        PBAR    25      2       7.000E-42.081E-62.081E-65.506E-721.306
1257-        PBAR    29      2       7.000E-42.081E-62.081E-65.506E-722.96U
1258-        PBAR    51      51      3.271E-42.755E-72.755E-75.509E-7
1259-        PBAR    53      53      1.353E-34.880E-71.120E-62.568E-8
1260-        PBAR    54      54      4.238E-42.230E-72.528E-73.00E-10
1261-        PBAR    58      58      5.340E-42.060E-72.060E-73.080E-7
1262-        PROD    5       11      3.486E-50.0      0.0
1263-        PROD    6       11      5.230E-50.0      0.0
1264-        SPC     1       58      123     0.0
1265-        SPC     1       70      123     0.0
1266-        SPC     1       126     123     0.0
1267-        SPC     1       138     123     0.0
1268-        TABDMP1 1                                                                +TD1
1269-        +TD1    .9      .010    1.14    .010    ENDT
1270-        TABLED1 1                                                                +TF1
1271-        +TF1    0.0     1.0     18.049  1.0     18.051  -1.0    36.099  -1.0     +TF11
1272-        +TF11   36.1    0.0     40.0    0.0     ENDT
1273-        TLOAD1  1       1                       1
1274-        TSTEP   1       1400 .  .05     2
             ENDDATA
```

1. Report No.	2. Government Accession No.	3. Recipient's Catalog No.
NASA CR-172470		

4. Title and Subtitle	5. Report Date
OPERATIONAL FITNESS OF BOX TRUSS ANTENNAS IN RESPONSE TO DYNAMIC SLEWING	January 1985
	6. Performing Organization Code

7. Author(s)	8. Performing Organization Report No.
E. E. Bachtell, S. S. Bettadapur, W. A. Schartel, L. A. Karanian	MCR-84-594
9. Performing Organization Name and Address	10. Work Unit No.
Martin Marietta Corporation Denver Aerospace P.O. Box 179 Denver, Colorado 80201	11. Contract or Grant No. NAS1-17551

12. Sponsoring Agency Name and Address	13. Type of Report and Period Covered
National Aeronautics and Space Administration Washington, D. C. 20546	Contractor Report
	14. Sponsoring Agency Code

15. Supplementary Notes

Langley technical monitor: Uriel M. Lovelace
Final Report -- Task 2

16. Abstract

A parametric study was performed to define slewing capability of large satellites along with associated system changes or subsystem weight and complexity impacts. The satellite configuration and structural arrangement from the Earth Observation Spacecraft(EOS) study was used as the baseline spacecraft. Varying slew rates, settling times, damping, maneuver frequencies, and attitude hold times provided the data required to establish applicability to a wide range of potential missions. The key elements of the study are as follows:

1) determine the dynamic transient response of the antenna system;
2) calculate the system errors produced by the dynamic response;
3) determine if the antenna has exceeded operational requirements at completion of the slew, and if so;
4) determine when the antenna has settled to the operational requirements.

The slew event is not considered complete until the antenna is within operational limits.

17. Key Words (Suggested by Author(s))	18. Distribution Statement
Large Space Structures Radiometers Dynamics Slewing Spacecraft Transient Response	Unclassified - Unlimited Subject Category 18

19. Security Classif. (of this report)	20. Security Classif. (of this page)	21. No. of Pages	22. Price
Unclassified	Unclassified	97	